Titre: Title:	Etude de l'optimisation énergétique d'un procédé de séchage de boues agricoles en lit à jet
Auteur: Author:	Arturo Macchi
Date:	1997
Type:	Mémoire ou thèse / Dissertation or Thesis
Référence: Citation:	Macchi, A. (1997). Etude de l'optimisation énergétique d'un procédé de séchage de boues agricoles en lit à jet [Mémoire de maîtrise, École Polytechnique de Montréal]. PolyPublie. https://publications.polymtl.ca/6680/

UNIVERSITÉ DE MONTRÉAL

ÉTUDE DE L'OPTIMISATION ÉNERGÉTIQUE D'UN PROCÉDÉ DE SÉCHAGE DE BOUES AGRICOLES EN LIT À JET

ARTURO MACCHI
DÉPARTEMENT DE GÉNIE CHIMIQUE
ÉCOLE POLYTECHNIQUE DE MONTRÉAL

MÉMOIRE PRÉSENTÉ EN VUE DE L'OBTENTION
DU DIPLÔME DE MAÎTRISE ÈS SCIENCES APPLIQUÉES
(GÉNIE CHIMIQUE)
JUIN 1997

UNIVERSITÉ DE MONTRÉAL

ÉCOLE POLYTECHNIQUE DE MONTRÉAL

Ce mémoire intitulé :

ÉTUDE DE L'OPTIMISATION ÉNERGÉTIQUE D'UN PROCÉDÉ DE SÉCHAGE DE BOUES AGRICOLES EN LIT À JET

présenté par : MACCHI Arturo

en vue de l'obtention du diplôme de : Maîtrise ès sciences appliquées

à été dûment accepté par le jury d'examen constitué de:

M. KLVANA Danilo, Ph.D., président

M. LEGROS Robert, Ph.D., membre et directeur de recherche

M. CHAOUKI Jamal, Ph.D., membre et codirecteur de recherche

M. BRUNET Stéphane, M.Sc.A., membre

DÉDICACE

.....

À mes parents : Zigrida Bems Macchi et Domenico Macchi

À mes frères : Paolo, Carlo et Domenico jr.

À Christine

.....À ma famille.....

REMERCIEMENTS

Je tiens tout d'abord à exprimer mes sincères remerciements à mon directeur de recherche Monsieur Robert Legros et Monsieur Jamal Chaouki qui a codirigé ce travail. Leur confiance, leurs conseils et leurs critiques m'ont toujours été d'un grand recours.

Je voudrais également remercier Monsieur Xiatao Bi pour son amitié, son aide et son implication soutenue dans cette étude.

Je remercie également Messieurs Daniel Dumas, Robert Delisle, Carol Painchaud et Jean Huard pour leur aide et support technique.

J'exprime ma gratitude à Stéphane Brunet ingénieur de recherche chez Gaz Métropolitain et au professeur Danilo Klvana pour l'honneur qu'ils m'ont fait de participer au jury de cette thèse. Je leur adresse ici mes remerciements pour leurs critiques et conseils.

Je tiens également à remercier le CRSNG, le FCAR du Quebec et Gaz Métropolitain inc. pour leur soutien financier.

RÉSUMÉ

La gestion des boues des procédés d'assainissement, qu'elles proviennent de l'épuration des eaux usées domestiques, de sources industrielles (e.g. du secteur des pâtes et papier) ou de sources agricoles (e.g. l'élevage de porcs), devient un problème incontournable au Québec. Depuis quelques années, une technologie de séchage des boues basée sur le lit à jet est à l'étude au centre Biopro de l'École Polytechnique de Montréal. Le système s'est avéré très performant pour le séchage des boues d'épuration des eaux usées ainsi que pour des boues de désencrage. Cependant, le système de séchage de boues n'a pas été optimisé en fonction de la production des gaz chauds ni des émissions de polluants et d'odeurs.

Un nouveau concept de séchage à haut rendement énergétique qui consiste à acheminer les gaz de séchage qui sortent du séchoir en lit à jet vers une chambre de combustion a été mis au point. Cette chambre de combustion utilise un brûleur au gaz naturel afin de procurer un environnement de destruction efficace des composés organiques volatiles et des odeurs présents dans les gaz de séchage. Les gaz de combustion sont ensuite utilisés comme source d'énergie pour le séchage par contact direct et indirect avec les boues.

L'objectif principal de ce projet est d'améliorer le rendement énergétique du système de séchage au centre Biopro par l'ajout de surfaces d'échange de chaleur indirect dans le lit à jet.

Afin d'accomplir cet objectif, il est initialement nécessaire d'effectuer une étude sur le transfert de chaleur indirect en lit à jet. Une sonde thermique permettant de mesurer les coefficients de transfert de chaleur indirect à différentes positions radiales et axiales dans le lit à jet a été développée. Les coefficients de transfert de chaleur (h_s) obtenus varient

entre 95 et 230 W/m^2°C et sont de 0 à 30 % plus faibles dans l'anneau qu'au centre du jet. Les valeurs maximales de h_s se situent à l'axe du jet et diminuent continuellement vers les parois de la colonne. La chute la plus importante se produit à l'interface du jet et de l'anneau. L'influence du débit de gaz n'est pas important pour des particules dont le nombre d'Archimède est supérieur à environ 10^6. Finalement des corrélations permettant d'estimer les valeurs de h_s dans le jet et l'anneau ont été développées.

La construction et l'installation d'un échangeur de chaleur indirect dans le lit à jet au centre Biopro n'a pu être fait au cours de ce projet. Par contre, deux types d'échangeurs de chaleur peuvent être envisagés. Le premier serait un échangeur de type membrane (série de tubes verticaux reliés par des ailettes) qui s'étendrait dans l'anneau sans toucher au jet et le second serait un échangeur de type serpentin qui contournerait le jet.

De plus, en parallèle, j'ai contribué à une étude sur l'hydrodynamique dans un lit à jet conique. Un lit à jet conique ayant des particules inertes comme matériel de lit peut être utilisé pour sécher des boues très liquides. Afin de construire un lit à jet conique, il est nécessaire d'obtenir une valeur précise de la vitesse minimum de giclage (U_{ms}).

Les différentes corrélations disponibles dans la littérature prédisent des valeurs de U_{ms} ayant jusqu'à 500 % de différence entre elles pour une unité d'échelle pilote. En utilisant 111 données expérimentales de U_{ms} provenant de la littérature, il a été démontré que la plupart des équations ont un écart type de plus 45 % et sont généralement biaisées. Ces grandes imprécisions peuvent provenir du fait que la forme des différentes corrélations n'est pas tout à fait appropriée. Certaines corrélations utilisent des paramètres géométriques tel que le diamètre de la colonne qui n'a pas un effet sur la structure du lit pour une enceinte purement conique, d'autres prédisent des cas limites impossibles, e.g. U_{ms} tend vers zéro lorsque l'angle du cône est nul ou la hauteur de lit est très faible. Une nouvelle corrélation semi-empirique dérivée à partir d'une analyse hydrodynamique

approximative de l'équation d'Ergun a été développée. Cette équation demande l'ajustement d'un seul paramètre et prédit les données de la littérature avec un écart type de 30 % sans biais.

ABSTRACT

The disposal of sludge produced by municipal waste water plants, by industrial sources (e.g. pulp and paper sector) or by agricultural sources (e.g. pig farming) has become a serious problem in Quebec. Over the last few years, a sludge drying process using the spouted bed technology has been investigated at the Biopro research center in École Polytechnique de Montréal. The spouted bed dryer was successful in treating municipal waste water and paper deinking process sludge. However, the sludge drying system was not optimized for the production of hot gases nor for the destruction of pollutants and odors.

A new high thermal efficiency drying concept where the dirty drying gases are directed towards a combustion chamber has been developed. The combustion chamber uses a natural gas burner in order to provide the proper conditions for the incineration of the pollutants and odors in the dirty drying gases. The hot combustion gases are then used to supply heat for direct and indirect contact drying of the sludge.

The main objective of this project is to improve the thermal efficiency of the drying system at the Biopro research center by installing indirect heat transfer surfaces in the spouted bed dryer.

In order to accomplish this objective, it is initially necessary to conduct an experimental investigation on indirect heat transfer in spouted beds. An electrical probe able to measure heat transfer coefficients at different radial and axial positions in the bed was built. Values of heat transfer coefficients (h_s) vary between 95 and 230 $W/m^2°C$ and are 0 to 30 % lower in the annulus than in the spout. Maximum values of h_s are always at the spout axis and decrease monotonically towards the column wall. The drop is most

important at the spout-annulus boundary. The influence of gas velocity is not important for particles with an Archimedes number higher than around 10^6. Equations correlating values of h_s in the spout and the annulus were developed.

During this project, it was not possible to build and install an indirect heat exchanger in the spouted bed. However, two types of heat exchangers can be considered. The first would be a membrane type (vertical tubes joined together by fins) heat exchanger which would extend into the annulus without encroaching the spout. The second would be a coil type heat exchanger which would spiral around the spout.

Also, in parallel, I contributed to a study on the hydrodynamic behavior of a conical spouted bed. Conical spouted beds can be used for the drying of high moisture content sludge. In order to design a conical spouted bed it is necessary to obtain a precise value of the minimum spouting velocity (U_{ms}).

The different correlations available in the literature predict a 5-folds range of U_{ms} values for a typical pilot-scale conical bed. Using 111 data points of U_{ms} found in the literature, it was shown that the root mean standard deviation (RMSD) of the different equations is more than 45 % and that the correlations are generally biased. The lack of precision can come from the fact that the forms of the equations are questionable. Certain correlations include the column diameter which has no relevance for purely conical beds, or they predict impossible results for limiting cases, e.g. U_{ms} goes to zero when the cone angle is zero or the static bed height is very low.

A new correlation based on an approximate hydrodynamic analysis of the Ergun equation was derived. This equation requires only one adjustable parameter and is able to predict the literature data with a RMSD of 30 % without any bias.

TABLE DES MATIÈRES

DÉDICACE iv

REMERCIEMENTS v

RÉSUMÉ vi

ABSTRACT ix

TABLE DES MATIÈRES xi

LISTE DES TABLEAUX xiv

LISTE DES FIGURES xv

LISTE DES SIGLES ET ABRÉVIATIONS xvii

LISTE DES ANNEXES xxiv

CHAPITRE 1 INTRODUCTION 1

1.1 PROBLÉMATIQUE 1

1.2 SOLUTION ENVISAGÉE 3

1.3 OBJECTIF 7

CHAPITRE 2 ARTICLE SUR LE TRANSFERT DE CHALEUR INDIRECT EN LIT À JET 8

2.1 SOMMAIRE 8

2.2 TEXTE DE L'ARTICLE 10

2.2.1 Abstract 10

2.2.2 Résumé 11
2.2.3 Introduction 12
2.2.4 Experimental equipment and procedure 15
2.2.5 Experimental results 18
2.2.5.1 Effect of superficial gas velocity 18
2.2.5.2 Effect of particle diameter 20
2.2.5.3 Effect of the axial position of the probe 22
2.2.5.4 Effect of the static bed height 23
2.2.5.5 Effect of the inlet diameter 23
2.2.5.6 Effect of particle heat capacity and thermal conductivity 24
2.2.5.7 Effect of particle humidity 24
2.2.6 Discussion and correlation of the data 25
2.2.7 Conclusion 30
2.2.8 Acknowledgments 31
2.2.9 Nomenclature 32
2.2.10 References 35

CHAPITRE 3 ARTICLE SUR LA VITESSE MINIMUM DE GICLAGE D'UN LIT À JET CONIQUE 49

3.1 SOMMAIRE 49
3.2 TEXTE DE L'ARTICLE 51
3.2.1 Abstract 51
3.2.2 Introduction 52
3.2.3 Evaluation of existing correlations 53
3.2.4 A new semi-empirical correlation for U_{ms} in conical beds 55
3.2.5 Conclusion 60
3.2.6 Nomenclature 61
3.2.7 References 63

CONCLUSION ET RECOMMANDATIONS **73**

RÉFÉRENCES **76**

ANNEXE **82**

LISTE DES TABLEAUX

Table 2.1 Properties of the Particulate Material at 20°C 39

Table 2.2 Comparison of literature data with the predictions of equations 5 and 6. 40

Table 3.1 List of empirical equations for predicting U_{ms} in conical beds..... 66

Table 3.2 List of experimental data from the literature..... 67

Table 3.3 Root mean standard deviation of correlations in Table 2.1 68

Tableau A.1 Effet de la position radiale de la sonde sur h_s pour des particules de polyéthylène. H = 0.27 m, z = 0.21 m, U/U_{ms} = 1.3. 104

LISTE DES FIGURES

Figure 1.1 Schéma d'un lit à jet 4

Figure 1.2 Système intégré de séchage de boues en lit à jet 6

Figure 2.1 Schematic of heat transfer probe 41

Figure 2.2a Effect of superficial gas velocity on h_s in the annulus at r/R = 0.59 for nylon and polyethylene particles. H= 0.27 m, z = 0.21 m, and D_i = 0.019m. 42

Figure 2.2b Effect of superficial gas velocity on h_s in the annulus at r/R = 0.59 for glass and activated alumina particles. H = 0.27 m, z = 0.21 m and D_i = 0.019 m. .. 42

Figure 2.3a Effect of superficial gas velocity on h_s in the spout at r/R = 0 for nylon and polyethylene particles. H= 0.27 m, z = 0.21 m, and D_i = 0.019m. 43

Figure 2.3b Effect of superficial gas velocity on h_s in the spout at r/R = 0 for glass and activated alumina particles. H= 0.27 m, z = 0.21 m, and D_i = 0.019m. 43

Figure 2.4a Effect of superficial gas velocity on radial profiles of h_s for glass particles (dp = 1.6 mm). H = 0.27 m, z = 0.21 m and D_i = 0.019 m. 44

Figure 2.4b Effect of superficial gas velocity on radial profiles of h_s for nylon particles. H = 0.27 m, z = 0.21 m and D_i = 0.019 m. 44

Figure 2.5 Effect of particle diameter on radial profiles of h_s for glass particles at U/U_{ms} = 1.1. H = 0.27 m, z = 0.21m, D_i = 0.019 m 45

Figure 2.6a Effect of probe axial position on radial profiles of h_s for glass particles (d_p = 1.6 mm). H= 0.39 m, U/U_{ms} = 1.3, D_i = 0.019 m 45

Figure 2.6b Effect of probe axial position on radial profiles of h_s for polyethylene particles. H= 0.39 m, U/U_{ms} = 1.3, D_i = 0.019 m. 46

Figure 2.7 Effect of bed height on radial profiles of h_s for glass (d_p = 1.6 mm) and polyethylene particles. U/U_{ms} = 1.3, z = 0.21 m, D_i = 0.019 m. 46

Figure 2.8 Effect of inlet diameter on radial profiles of h_s for polyethylene particles. H = 0.27 m, z = 0.21 m, U/U_{ms} = 1.3 47

Figure 2.9 Effect of thermal properties on radial profiles of h_s. H = 0.27 m, z = 0.21 m, U/U_{ms} = 1.3, D_i = 0.019 m 47

Figure 2.10 Effect of particle humidity on h_s for activated alumina particles (d_p = 2.0mm). H = 0.27 m, z = 0.21 m, U/U_{ms} = 1. 3, D_i = 0.019 m. 48

Figure 2.11 Agreement between experimental and calculated values of h_s. 48

Figure 3.1 Schematic illustration of a conical-spouted bed. 69

Figure 3.2 Effect of cone angle and static bed height on $(Re_i)_{ms}$ based on data in Table3.2 70

Figure 3.3 $(Re_i)_{ms}/Ar^{0.5}$ and $(Re_b)_{ms}/Ar^{0.5}$ as functions of D_b/D_i based on data listed in Table 3.2 71

Figure 3.4 Comparison of literature data listed in Table 2.2 with equations (22), (24) and (25) 72

Figure A.1 Schéma du montage expérimental 83

Figure A.2 Effet de la position radiale sur h_s pour des particules de polyéthylène. U/U_{ms} = 1.3, z = 0.21 m, H = 0.27 m, D_i = 0.019 m 103

LISTE DES SIGLES ET ABRÉVIATIONS

Chapitre 2

a = variable in equation (4)

A = heat transfer surface area, m^2

Ar = Archimedes number $[=g \cdot d_p^3 \cdot (\rho_p - \rho_g)/\mu_g^2]$

b = variable in equation (4)

c = variable in equation (4)

C_p = particle heat capacity, J/kg°C

C_g = gas heat capacity, J/kg°C

d_p = particle diameter, mm

d_v = equivolume spherical diameter, m [diameter of a sphere having the same volume of the particle]

D_i = spouted bed inlet diameter, m

g = gravitational acceleration, m/s^2

G_s = dry air mass flowrate, kg/s

H = static bed height, m

h_{gc} = gas convective heat transfer coefficient, $W/m^{2o}C$

h_{pc} = particle convective heat transfer coefficient, $W/m^{2o}C$

h_s = surface-to-bed heat transfer coefficient, $W/m^{2o}C$

$h_{s\,calc}$ = surface-to-bed heat transfer coefficient predicted from equation 5, $W/m^{2o}C$

$h_{s\,exp}$ = experimental surface-to-bed heat transfer coefficient, $W/m^{2o}C$

$h_{s\,max}$ = maximum surface-to-bed heat transfer coefficient, $W/m^{2o}C$

h_w = wall-to-bed heat transfer coefficient, $W/m^{2o}C$

k_g = gas thermal conductivity, W/m°C

k_p = particle thermal conductivity, W/m°C

Nu = Nusselt number [$=h_s \cdot d_p/k_g$]

Nu_{gc} = gas convective Nusselt number [$=h_{gc} \cdot d_p/k_g$]

Nu_{max} = maximum Nusselt number [$=h_{s\,max} \cdot d_p/k_g$]

P = Power, W

Pe = Polyethylene

Pp = Polypropylene

Ps = Polystyrene

Pr = Prandl number, [$=\mu_g \cdot C_g/k_g$]

r = radial position of the heat transfer probe, m

R = spouted bed column radius, m

T = temperature, °C

T_b = bed temperature, °C

T_s = probe surface temperature, °C

U = superficial gas velocity, m/s

U_{ms} = minimum spouting superficial gas velocity, m/s

X = dry basis solid moisture, kg water/kg dry solid

X_1 = dry basis solid moisture at time t_1, kg water/kg dry solid

X_2 = dry basis solid moisture at time t_2, kg water/kg dry solid

Y_{in} = dry basis gas humidity at the spouted bed inlet, kg water/kg dry air

Y_{out} = dry basis gas humidity at the spouted bed outlet, kg water/kg dry air

z = axial position of the heat transfer probe, m

Greek letters

β = variable in equation (3)

δ = variable in equation (3)

ε_b = static bed voidage,

ε_{mf} = bed voidage at minimum fluidization,

ϕ = sphericity [surface of a sphere having the same volume as the particle divided by the surface of the particle]

γ = variable in equation (3)

μ_g = gas viscosity, kg/m·s

ρ_g = gas density, kg/m^3

ρ_p = particle density, kg/m^3

Δ_t = drying experiment sampling period, s

Chapitre 3

Ar = Archimedes number $[=gd_p^3(\rho_p-\rho_g)\rho_g/\mu_g^2]$

D = diameter of the column at a height of h, m

D_c, D_c' = diameter of the cylindrical section, m

D_i = inlet diameter, m

D_b = diameter at the bed surface, m

d_p = particle diameter, m

F = drag force between gas and particles, N

F_g = gravitational force, N

F_m = the bias of an equation as defined in Table 3.3

g = gravitational acceleration, m/s^2

H = static bed height, m

h = distance above the distributor, m

H_c = height of the cone section, m

Q_{mf} = volume flow rate at U_{ms}, m^3/s

Re_{mf} = Reynolds number at U_{mf} $(=\rho_g U_{mf} d_p/\mu_g)$

$(Re_i)_{mf}$ = Reynolds number at $(U_i)_{mf}$ $[=\rho_g (U_i)_{mf} d_p/\mu_g]$

Re_{ms} = Reynolds number at U_{ms} $[=\rho_g U_{ms} d_p/\mu_g]$

$(Re_i)_{ms}$ = Reynolds number at $(U_i)_{ms}$ $[=\rho_g (U_i)_{ms} d_p/\mu_g]$

$(Re_b)_{ms}$ = Reynolds number at $(U_b)_{ms}$ $[=\rho_g (U_b)_{ms} d_p/\mu_g]$

Re_t = Reynolds number at U_t $[=\rho_g U_t d_p/\mu_g]$

RMSD = root mean standard deviation

U_{mf} = minimum fluidization velocity, m/s

U_{ms} = minimum spouting velocity based on D_c, m/s

$(U_i)_{ms}$ = minimum spouting velocity based on D_i, m/s

$(U_b)_{ms}$ = minimum spouting velocity based on D_b, m/s

Greek letters

γ = included cone angle, degree

ε = voidage

ε_{mf} = bed voidage at U_{mf}

ε_{ms} = bed voidage at U_{ms}

μ_g = gas viscosity, Pa.s

ρ_p = particle density, kg/m^3

ρ_g = gas density, kg/m^3

ϕ = sphericity of particles

Annexe

A = surface de transfert de chaleur, m^2

Al = surface de transfert de chaleur par conduction axiale, m^2

C_p = capacité calorifique de la particule, J/kg°C

d_p = diamètre de la particule, mm

D_i = diamètre de l'orifice du lit à jet, m

D_t = diamètre de la surface de transfert de chaleur, m

H = hauteur du lit au repos, m

h_s = coefficient de transfert de chaleur indirect, $W/m^2°C$

k = conductivité thermique, W/m°C

L = longueur de la surface de transfert de chaleur, m

P = Puissance de la cartouche chauffante, W

P_{part} = pression partielle de la vapeur d'eau, kPa

P_{sat} = tension de vapeur de l'eau, kPa

$q_{axiale\ max}$ = transfert de chaleur maximum par conduction axiale, W

r = position radiale de la surface de transfert de chaleur, m

R = rayon de la colonne du lit à jet, m

T_0 = température ambiante, °C

T_1 = température à l'entrée du lit à jet, °C

T_2 = température à la surface de la sonde, °C

T_3 = température à la surface de la sonde, °C

T_4 = température dans le lit, °C

T_5 = température dans le lit, °C

T_b = température du lit, °C

T_s = température de la surface de transfert de chaleur, °C

U = vitesse superficielle du gaz basée sur le diamètre de la colonne, m/s

U_{ms} = vitesse minimum de giclage du gaz basée sur le diamètre de la colonne, m/s

V = tension, volt

Y = humidité absolue de l'air sur base sèche, kg eau/kg air sec

z = position axiale de la surface de transfert de chaleur, m

Symboles grecs

ε_b = porosité du lit au repos,

ρ_p = densité de la particule, kg/m^3

ΔT_{max} = différence maximum de température entre la surface de transfert de chaleur et le lit, °C

ΔX = longueur axiale du bouchon de Téflon, m

LISTE DES ANNEXES

ANNEXE Détails expérimentaux des essais de transfert de chaleur indirect en lit à jet 82

CHAPITRE 1

INTRODUCTION

1.1 PROBLÉMATIQUE

La gestion des boues de procédés d'assainissement, qu'elles proviennent de l'épuration des eaux usées domestiques, de sources industrielles (e.g. du secteur des pâtes et papier) ou de sources agricoles (e.g. l'élevage de porcs), devient un problème incontournable au Québec.

L'assainissement des eaux usées urbaines au Québec est en plein développement. En 1980, les eaux usées domestiques déversées dans les réseaux d'égouts et traitées représentaient l'équivalent de la consommation en eau de moins de 2 % de la population alors qu'en 1997, ce pourcentage devrait dépasser 85 %. Le volume de boues produites est donc en pleine croissance et devrait dépasser annuellement 180 000 tonnes (base sèche) d'ici l'an 2000 (MENVIQ, 1991).

De son côté, l'industrie canadienne des pâtes et papiers est aussi en pleine évolution. Le recyclage de vieux papiers est devenu une pratique courante. Au Québec, on compte déjà huit usines qui ont recours à l'incorporation d'une certaine quantité de fibres recyclées (entre 10 et 60 %) dans leurs produits (ACDI, 1996). De ce fait, il y a une augmentation considérable de boues de désencrage produites. De plus, afin de se conformer aux normes environnementales, les usines de pâtes et papier ont dû réduire leurs rejets dans les cours d'eau. Les usines ont donc fait l'achat d'équipements de

traitement secondaire, augmentant ainsi considérablement la quantité de boues produites (ACDI, 1996).

Aujourd'hui environ 40 % des boues sont enfouies, 58,5 % sont incinérées et seulement 1,5 % des boues générées par ces secteurs trouvent une application pratique sous forme d'engrais horticole, agricole ou sylvicole (Cayer, 1996). L'enfouissement des boues humides deviendra une option moins intéressante à cause des coûts d'enfouissement qui augmenteront à mesure que les normes gouvernementales deviendront plus sévères et que la quantité de sites propices diminuera. Une déshydratation mécanique poussée (par filtre à pressoir ou à sabots) ne permet d'obtenir des siccités que de l'ordre de 35 à 45 % de solides. Afin d'obtenir des siccités supérieures qui sont nécessaires pour une stabilisation des boues, il est nécessaire d'utiliser des méthodes thermiques de séchage. Dans ce domaine, plusieurs manufacturiers offrent des équipements de séchage plus ou moins sophistiqués qui comportent certains avantages et inconvénients (Rioux, 1993). De façon générale par contre, tous ces systèmes offrent des rendements énergétiques relativement faibles à cause des modes de contact non-optimaux entre la source de chaleur et les boues. De plus, ces systèmes génèrent des courants gazeux et/ou liquides qui nécessitent des traitements subséquents.

Quant à l'industrie de l'élevage du porc au Québec, elle a joui d'une importante croissance au cours des dix dernières années. La confiance du consommateur envers la viande de porc est à son meilleur. Aujourd'hui, le Québec produit plus de 5 millions de porcs par année. Cette industrie qui représente 2 milliards de dollars par an dont le quart des activités est relié à l'exportation. Plus de 30 000 emplois dépendent de cette industrie (Orr, 1996).

Chaque porc produit environ deux fois plus de rejets qu'un être humain, soit l'équivalent des rejets annuels de 10 millions de personnes. Le lisier de porc est une boue très liquide

et peut contenir plus de 92 % massique d'eau. Jusqu'à présent, les producteurs porcins épandent le lisier brut sur les champs. Cette option est peu coûteuse (environ $3.50/espace porc/année), mais elle résulte en une pollution de l'air et des eaux. En effet, l'épandage du lisier nuit à cause de son odeur nauséabonde. De plus, dans certaines régions, le lisier sature le sol et les cours d'eau souterrains en phosphore et azote car la surface disponible pour son épandage est trop petite. Dans les régions de l'Assomption, Chaudière et Yamaska, l'excès de lisier de porc est estimé à 1,5 millions de tonnes par année.

À cause de ce surplus, l'élevage du porc doit être réduit ou maintenu à son niveau actuel. Ceci empêche une croissance d'activité et affaiblit la position du Québec comme un des principaux éleveur de porc au monde. Le ministère de l'environnement et de la faune (MEF) doit délibérer sur plus de 323 demandes de permis d'augmentation de production dans les fermes actuelles ou pour la construction de nouvelles (Orr, 1996). Il est donc essentiel de trouver un moyen simple et efficace pour régler cet important problème écologique et économique.

1.2 SOLUTION ENVISAGÉE

Depuis quelques années, une technologie de séchage des boues basée sur le lit à jet est à l'étude au centre Biopro de l'École Polytechnique de Montréal. Le système s'est avéré très performant pour le séchage des boues d'épuration des eaux usées ainsi que pour des boues de désencrage, Rioux (1993).

Les principales composantes d'un lit à jet sont illustrées à la figure 1.1.

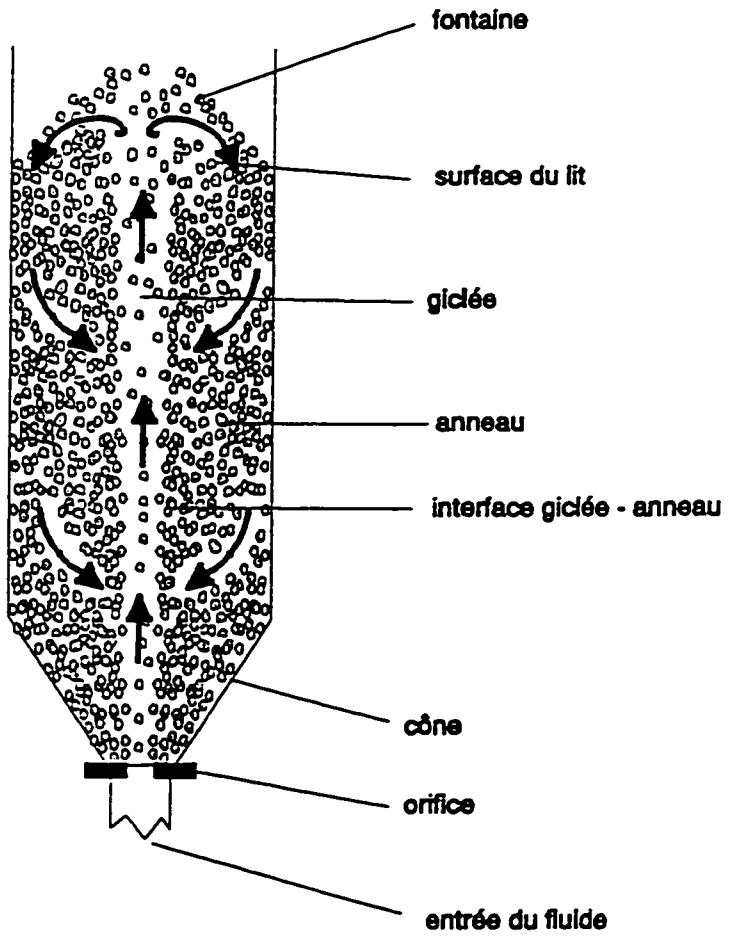

Figure 1.1 Schéma d'un lit à jet.

Cet appareil fonctionne de la façon suivante: L'air chaud est introduit verticalement par un orifice central situé à la base du cône au travers du lit de particules de boues. Lorsque la vitesse du fluide est suffisante, il se forme une cavité qui pénètre le lit jusqu'à la surface. Les particules de boues sont entraînées dans le jet central jusqu'à la surface du lit où elles sont désengagées dans la région nommée "la fontaine". Les solides retombent alors sur la périphérie du lit et sont entraînés dans le mouvement descendant de l'anneau où ils seront réentraînés dans le jet. La forme conique de la base est nécessaire pour éviter la présence de zones mortes (Mathur et Epstein, 1974).

Le lit à jet est particulièrement approprié pour traiter du matériel collant ou qui peut le devenir. Il est simple de construction et ne requiert pas de pièces mécaniques internes pour éviter le colmatage, accroître les surfaces d'échange et faire avancer les solides dans le séchoir. Pour des particules grossières et non-conventionnelles, la technique du lit à jet offre un excellent contact gaz-solide. Le mouvement intense des particules prévient la formation de zones de surchauffe et assure une humidité uniforme du produit. Finalement, en cours de séchage en lit à jet, les granules de boues peuvent être enrobées d'éléments fertilisants (azote, phosphore et potassium) injectés dans le courant d'air chaud et qui ont la capacité de se fixer aux granules lors du séchage.

Cependant, le système de séchage de boues développé à Biopro n'a pas été optimisé en fonction de la production des gaz chauds ni des émissions de polluants et d'odeurs. Un nouveau concept de séchage à haut rendement énergétique qui consiste à acheminer les gaz de séchage qui sortent du séchoir en lit à jet vers une chambre de combustion a été mis au point. Cette chambre de combustion utilisera un brûleur au gaz naturel afin de procurer un environnement de destruction efficace des composés organiques volatiles et des odeurs présents dans les gaz de séchage. Les gaz de combustion seront ensuite utilisés comme source d'énergie pour le séchage. D'abord, un premier échangeur de chaleur produira l'air chaud pour sécher par contact direct les boues dans le lit à jet. Ensuite, les gaz de combustion partiellement refroidis seront dirigés vers les surfaces d'échange de chaleur indirectes placées dans la chambre de séchage. Les gaz de combustion, qui auront donc été traités dans la chambre de combustion, seront ensuite déchargés à l'atmosphère. Le procédé n'aura donc pas d'effluent liquide qui pourrait nécessiter un traitement coûteux (voir figure 1.2).

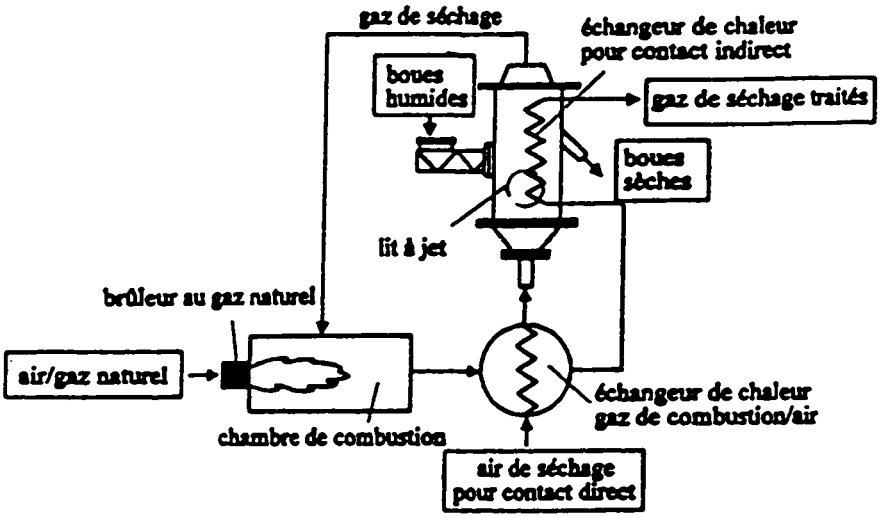

Figure 1.2 Système intégré de séchage de boues en lit à jet.

Pour un même débit de boues à traiter, l'ajout de surfaces d'échange de chaleur indirectes dans le séchoir devrait diminuer le volume de gaz nécessaire au procédé de séchage et par conséquent la puissance du ventilateur, la taille du séchoir et de tout l'équipement nécessaire pour l'épuration des gaz de séchage (cyclone, filtre à manche, colonne d'absorption, chambre de combustion avec brûleur au gaz naturel, etc.).

Pour les unités de grosse taille, l'utilisation d'échangeur de chaleur interne, de forme tubulaire par exemple, est un moyen plus efficace pour favoriser le transfert de chaleur que l'utilisation d'une veste chauffante autour des parois de la colonne. Lors de la conception d'un séchoir en lit à jet avec des échangeurs de chaleur internes, il est nécessaire d'estimer le coefficient de transfert de chaleur indirect afin de déterminer la taille de la surface et la quantité de chaleur qu'elle dissipera au lit. Jusqu'à présent, il n'existe pas de corrélation ou de modèle permettant de calculer ce coefficient.

De plus, pour ces unités de séchage de taille industrielle, on utilise souvent des lits coniques. Un lit à jet conique ayant des particules inertes comme matériel de lit est souvent utilisé pour le séchage de solutions et de suspensions (boues à haute teneur en eau tel que le lisier de porc). Dans ce type de séchoir, le lit de particules inertes est maintenu dans la région conique et la vitesse superficielle du gaz est choisie à plus de 1,5 fois la vitesse minimum de giclage. Dans ce régime très turbulent, la porosité du lit et la circulation des particules sont élevées réduisant ainsi le danger de blocage. Lors de la conception d'un séchoir lit à jet conique, il est nécessaire d'estimer la vitesse minimum de giclage. Les différentes corrélations disponibles dans la littérature prédisent des valeurs ayant jusqu'à 500 % de différence entre elles pour une unité d'échelle pilote.

1.3 OBJECTIF

Ce projet vise donc à développer un nouveau procédé permettant de sécher différents types de boues dans un lit à jet et de traiter les odeurs et les composés organiques volatiles contenus dans les gaz de séchage dans une chambre de combustion utilisant du gaz naturel. L'objectif principal de ce projet est d'améliorer le rendement énergétique du système de séchage au centre Biopro par l'ajout de surfaces d'échange de chaleur indirect dans le lit à jet. En parallèle, j'ai aussi contribué à une étude sur l'hydrodynamique d'un lit à jet conique en vue de d'établir une nouvelle équation permettant de mieux estimer la valeur de la vitesse minimum de giclage.

Le chapitre 2 traite de l'étude expérimentale de l'effet des conditions d'opération d'un lit à jet sur le taux de transfert de chaleur indirect. Le chapitre 3 présente l'article sur la vitesse minimum de giclage en lit à jet conique. Je présente ce deuxième article comme coauteur dans un groupe de recherche sur le séchage de boues en lit à jet composé de Robert Legros, Jamal Chaouki, Xiaotao Bi et moi-même.

CHAPITRE 2

ARTICLE SUR LE TRANSFERT DE CHALEUR INDIRECT EN LIT À JET

2.1 SOMMAIRE

L'objectif de ce travail est d'évaluer les effets des propriétés des particules (diamètre, densité, capacité calorifique, conductivité thermique et teneur en eau), de la vitesse superficielle du gaz, de l'emplacement de la sonde (axiale et radiale) dans le lit et du diamètre de l'orifice de la colonne sur le taux de transfert de chaleur d'un tube vertical submergé dans un lit à jet. Ces résultats permettront d'acquérir des connaissances sur les mécanismes de transfert de chaleur impliqués. Ces résultats seront aussi importants pour bien situer et estimer la quantité de chaleur transmise par un échangeur de chaleur dans un séchoir lit à jet.

Une sonde permettant d'évaluer les coefficients de transfert de chaleur a été construite. La sonde est faite d'un tube de cuivre dans lequel on insère une cartouche chauffante. La température de surface du tube de cuivre est mesurée à l'aide de deux thermocouples miniatures. Deux bouchons de Téflon sont installés aux extrémités du tube de cuivre afin de limiter les pertes de chaleur par conduction axiale. La sonde est vissée à une série de tubes en acier inoxydable. Afin de déplacer la sonde de façon axiale, il faut enlever un ou plusieurs tubes d'acier. Les mouvements radiaux de la sonde se font en poussant ou en tirant sur le manche à l'extérieur du lit à jet. Le coefficient de transfert de chaleur indirect (h_s) en régime permanent s'obtient en divisant la puissance électrique fournie à la sonde par la surface de la sonde et le gradient de température entre la sonde et le lit. La

température du lit de particules est calculée à partir de la moyenne des mesures de deux thermocouples situés dans l'annulus.

Les coefficients de transfert de chaleur obtenus varient entre 95 et 230 $W/m^2°C$. Les valeurs de h_s sont de 0 à 30 % plus faibles dans l'anneau qu'au centre du jet. Les valeurs maximales de h_s se situent à l'axe du jet et diminuent continuellement vers les parois de la colonne. La chute la plus importante se produit à l'interface du jet et de l'anneau. Pour une hauteur de lit fixe, lorsque la sonde est déplacée vers le haut, les valeurs de h_s diminuent dans le jet et augmentent dans l'anneau. L'influence du débit de gaz jusqu'à U/U_{ms} = 1,5 n'est pas important pour des particules dont le nombre d'Archimède est supérieur à environ 10^6. Pour de plus petites particules ($Ar \approx 3{,}5X10^5$), les valeurs de h_s augmentent avec le débit de gaz, surtout dans l'anneau.

Dans un lit à jet deux principaux mécanismes de transfert de chaleur agissent en parallèle. Interviennent, la convection forcée du gaz passant sur l'échangeur de chaleur puis la convection des particules (c'est-à-dire la conduction transitoire de la chaleur aux particules au cours de leur période de contact avec l'échangeur, suivi de la décharge de ces particules et de leur chaleur au reste du lit). La contribution relative des mécanismes varie selon les profils de porosité et de vitesse des particules et du gaz. Les profils radiaux de h_s semblent être intimement liés aux profils de vitesse du gaz sans que la contribution des particules au transfert de chaleur soit négligeable.

Des corrélations permettant d'estimer les valeurs de h_s dans la partie supérieure du jet et de l'anneau à U/U_{ms} = 1,3 ont été développées. L'erreur maximale entre les valeurs prédites et les valeurs expérimentales est de 10 %. Les corrélations proposées n'incluent pas les différents mécanismes de transfert de chaleur impliqués et doivent tout simplement être utilisées comme outils pour estimer le coefficient de transfert de chaleur indirect en lit à jet. Finalement, afin de bien comprendre et cerner les mécanismes de transfert de

chaleur indirect en lit à jet, des données sur les écoulements du gaz et du solide doivent être obtenues simultanément avec les mesures de h_s.

2.2 TEXTE DE L'ARTICLE

An Investigation of Heat Transfer from a Vertical Tube in a Spouted Bed

Macchi, A., H.T. Bi, R. Legros* and J. Chaouki

Département de génie chimique, École Polytechnique de Montréal, Case Postale 6079, succursale Centre-Ville, Montréal, Québec, Canada H3C 3A7

Can. J. of Chem. Eng. (submitted)

2.2.1 Abstract

An experimental investigation on heat transfer from a vertical tube in a gas-solid spouted bed has been conducted. Values of heat transfer coefficients (h_s) have been found to vary between 95 and 230 W/m^2°C. Maximum values of h_s are always at the spout axis and decrease monotonically towards the column wall, the drop is most important at the spout-annulus boundary. Most of the effects from different parameters can be explained by the flow patterns of the gas, although particle convection still contributes to some extent to

the heat transfer rate. Finally, equations correlating values of h_s in the spout and the annulus have been developed.

2.2.2 Résumé

Cette étude porte sur l'effet des conditions d'opération d'un lit à jet gaz-solide sur le taux de transfert de chaleur indirect. Les coefficients de transfert de chaleur (h_s) obtenus varient entre 95 et 230 $W/m^2{}^oC$. Les valeurs maximales de h_s se situent sur l'axe du jet et diminuent continuellement vers les parois de la colonne. Les profils de h_s semblent être intimement liés aux profils de vitesse du gaz sans que la contribution au transfert de chaleur par les particules soit négligeable. Finalement, des corrélations permettant d'estimer les valeurs de h_s dans le jet et l'anneau ont été développées.

Keywords: gas-solid spouted bed, tube-to-bed heat transfer coefficient, indirect heat transfer mechanism.

*Author to whom correspondence may be addressed.
E-mail: rlegros@mailsrv.polymtl.ca

2.2.3 Introduction

A spouted bed is an ideal low cost dryer for the treatment and upgrading of sludge (Rioux, 1993). It is able to treat materials that are sticky, or prone to become sticky (Bridgewater, 1985). It is also simple in construction and does not require any internal equipment. For coarse particles, the good gas-solid contacting in spouted beds prevents the formation of hot zones and assures a uniform humidity of the product (Mathur and Epstein, 1974).

Spouted bed dryers offer the possibility of combining direct and indirect heat transfer by including heat exchangers. The use of heat exchangers can save substantially in both capital and operating costs (Reay, 1986). For the same drying duty, less hot air is required, leading to the reduction of the size of the blower, dryer and any subsequent equipment for the treatment of the drying gases, (e.g. cyclone, bag filter, gas fired combustion chamber, wet scrubber, etc.). At bed temperatures higher than 100°C, it becomes possible to uncouple the hydrodynamic requirement for gas flow and the drying capacity of the spouted bed as a result of indirect heat input.

For large industrial units, the use of immersed heating elements is a more efficient way to transfer heat than the use of a jacket around the column wall. The use of internal elements increases the heat transfer area per unit volume of bed and creates more turbulence in the gas stream, which leads to the reduction of the thickness of the thermal boundary layer and thus the increase of the heat transfer rate (Mathur and Epstein, 1974).

In the design of spouted bed dryers with internal heat exchangers, it is necessary to estimate the surface-to-bed heat transfer coefficient (h_w) in order to determine the size of the heat exchanger and the amount of heat transferred.

There have been very few studies on heat transfer from a submerged object in a spouted bed. In the early work of Zabrodsky and Mikhailik (1967), values of h_s were measured with small electrically heated cylinders placed both vertically and horizontally at different locations in the bed. They also investigated the effects of particle diameter and superficial gas velocity on the heat transfer coefficient. It is noted that the column and inlet diameter of the spouted bed were 9.4 cm and 1.5 cm respectively. The conical base had an included angle of 45°. The static bed height was 10 cm. For this column geometry, assuming that the orifice diameter is equal to the inlet diameter, the cone height is 9.5 cm. With the vertical probe being 3.5 cm long, the measurements might have been made in the cone region. Values of h_s are then for conical spouted beds not for the classical cylindrical-conical spouted bed where the heat exchanger would be normally placed in the cylindrical section. This remark seems plausible since most Russian work back then were on conical spouted beds (Mathur and Epstein, 1974).

Also, Zabrodsky and Mikhailik's (1967) experiments showed that starting from the spout axis, values of h_s increased radially and reached a maximum at the spout-annulus interface before dropping suddenly in the annulus to a relatively constant value. They presented their results as if the spout-annulus boundary was at the same position for particles of different size (2 mm < d_p < 7 mm), indicating that they used a constant superficial gas velocity. It appears to be more appropriate to present the effect of particle diameter at a constant excess gas velocity (U/U_{ms}). The gas velocity required for minimum spouting of the larger particles will be equal to a very high value of U/U_{ms} for the smaller particles. The hydrodynamics and bed structure will then be quite different for both cases (spouting vs. jet-spouting).

Klimenko et al. (1970) measured heat transfer coefficients from the surface of a brass ball of 25 mm in diameter. The probe was moved along the radial direction in both the top of the bed and the fountain region above the bed surface. They did not measure a maximum

at the spout-annulus interface. Instead, values of h_w decreased monotonically from the spout axis towards the column wall. It seems that the few heat transfer investigations that have been performed lack experimental details and the results obtained are subject to controversy when compared to each other.

At the present time, there exist no correlations or theoretical models to estimate the tube-to-bed heat transfer coefficient in spouted beds. As for the wall-to-bed heat transfer, empirical correlations based on dimensional analysis have been proposed by Malek and Lu (1964) and Uemaki and Kugo (1967). Epstein and Mathur (1971) demonstrated that there were serious contradictions between the two correlations and pointed out the inadequacy of empirical equations formulated without reference to the physical mechanism involved. Epstein and Mathur (1971) also proposed a theoretical model based on the two-dimensional penetration theory but has not been rigorously tested because this model requires the particle velocity at the wall and the bed effective thermal conductivity which are not readily available (Freitas and Freire, 1993).

The main objectives of this work are to study the effects of particle properties (diameter, density, heat capacity, thermal conductivity and humidity), superficial gas velocity, probe location (axial and radial) in the bed and the column inlet diameter on heat transfer from a vertical tube submerged in a spouted bed and to gain an insight on the heat transfer mechanism involved. The results will be important for properly locating and estimating the amount of heat transferred by a heat exchanger in a spouted bed dryer.

2.2.4 Experimental equipment and procedure

All experiments were performed in a spouted bed with a 0.21 m internal diameter column resting on a 60° included angle conical base with an inlet nozzle diameter varying between 0.019 m and 0.038 m. The height of the cone section is 0.165 m and the height of the cylindrical section is 1.02 m.

A schematic of the probe used to determine heat transfer coefficients is presented in figure 2.1. The heat transfer probe is a 0.5" diameter and 2" long copper tube inserted with a heating cartridge which can dissipate a power of 125 Watts at 240 Volts. The temperature at the surface of the copper tube is measured by two miniature K-type thermocouples mounted flush with the surface. Teflon caps are installed at both ends of the copper tube in order to limit heat loss by axial conduction and to keep the temperature of the tube constant on its entire length. The conical cap at the lower end of the tube minimizes flow perturbations around the tube so that the gas layer thickness is even all along the heat transfer surface. The top cap is pierced so that the thermocouple wires as well as the heating cartridge connecting wires can pass through. The probe is then connected to a series of stainless steel tubes by O-rings. Radial positioning is achieved by moving the handle from the exterior of the spouted bed. Axial positioning is achieved by removing or adding one or more stainless steel tubes above the copper tube.

The steady-state surface-to-bed heat transfer coefficient was calculated from the following equation:

$$h_s = \frac{P}{A*(T_s - T_b)} \qquad (1)$$

The bed temperature, T_b, was determined as the average value from two thermocouples situated in the annulus. Since ambient air was used for the experiments, the bed, gas and particle temperatures were uniform.

In a typical experiment, the electrical power input of the probe was controlled between 25 and 45 % of its maximum value. This power range resulted in a temperature difference between the tube surface and the bed between 20°C and 40°C. When the surface temperature of the probe reached a constant value, the value of h_s was calculated. After a change in operating conditions, the surface temperature of the probe was allowed to reach a new steady-state value before a new value of h_s was calculated.

With this method the surface temperature of the probe varied from one condition to another. A preliminary experiment was thus performed in order to determine if a change in probe surface temperature affects the value of h_s significantly. At constant operating conditions, the power input was varied between 25 and 45 % of its maximum value. The probe surface temperature responded to the change in power, but the heat transfer coefficient remained the same. This confirms that the power input will affect the value of h_s only if the change in surface temperature is so that the thermal conductivity of the gas film surrounding the probe is changed significantly. The mean heat transfer coefficients were calculated without taking into account heat losses through the probe ends. Repeated experiments showed that values of h_s are reproducible within 2 %.

Table 2.1 presents the properties at 20°C of the various solids used in this investigation. For nonspherical particles, the particle diameter (d_p) is estimated as the equivolume spherical diameter (d_v) multiplied its sphericity (ϕ).

All experiments in the present study were performed with the excess gas velocity, U/U_{ms}, ranging from 1.1 to 1.5. Values of U_{ms} were determined by the conventional method of plotting bed pressure drops against decreasing spouting velocities. All values were obtained without the heat transfer probe in the bed. For the effect of probe axial position on h_s, the static bed height was maintained at H = 0.39 m. All other experiments were performed with the heat transfer surface placed above the cone region (z = 0.21 m) and below the static bed height (H = 0.27 m).

The effect of particle humidity on the heat transfer coefficient was evaluated by performing drying experiments. Activated alumina particles were soaked in water for 24 hours. During a run with the wet particles, the air inlet temperature was chosen so that its wet bulb temperature was similar to that of the bed temperature during the experiments with the dry particles. The initial and final moisture contents of the particles were measured by drying 25 g of the wet particles in an oven at 105°C for 24 hours. The outlet gas humidity was measured by a hygrometer (Vaisala, model HMD 20 VB) at every 10 seconds. The average particle humidity was therefore obtained by mass balance starting with the final moisture content.

$$X_1 = X_2 + G_s * \left(Y_{out} - Y_{in}\right)_{ave} * \Delta_t \qquad (2)$$

Here X_1 and X_2 are the dry basis solid moisture contents at times t_1 and t_2 respectively, G_s is the dry air mass flow rate and $(Y_{out} - Y_{in})_{ave}$ is the time average dry basis gas humidity difference between the outlet and inlet of the dryer during sampling period, Δ_t. Calculated values of the initial humidity were within 5 % of the measured values, validating the method for estimating the average particle humidity.

2.2.5 Experimental results

2.2.5.1 Effect of superficial gas velocity

Figures 2.2a and 2.2b present the effect of superficial gas velocity on local heat transfer coefficients for different particles with the probe placed in the annulus (r/R = 0.59). As expected, values of h_s drop sharply with the transition from a spouted to a fixed bed. The drop is more pronounced for particles of small Ar number. Indeed, for the small glass and activated alumina particles the drop is around 45 % while for the large glass and activated alumina particles its around 22 %. This result indicates that, just as in fluidized beds, the relative contribution to heat transfer by particle convection is more important for the smaller particles.

During spouting h_s is seen to be practically independent of the superficial gas velocity for the large particles, while for the small glass and activated alumina particles, h_s decreased with decreasing the gas velocity. Similarly, Klassen and Gishler (1958), Malek and Lu (1964), and Freitas and Freire (1993) found that the wall-to-bed heat transfer coefficient was independent of the superficial gas velocity, but no explanation was given.

In spouted beds, particle circulation and mixing increase with an increase of the gas flowrate, while the average particle voidage in the annulus remains more or less constant and equal to ε_{mf} (Mathur and Epstein, 1974). Lim and Grace (1987) indicated that the average superficial gas velocity in the annulus is not strongly influenced by the overall superficial gas velocity for large polystyrene particles of 3.45 mm in diameter. However, He et al (1994a) noticed that the average annulus voidage increased with increasing superficial gas velocity for small glass particles of 1.41 mm in diameter. Therefore, it seems that the common assumption that all the excess gas ($U - U_{ms}$) passes through the

spout while the gas flow through the annulus remains constant (Epstein and Grace, 1984) is more accurate for the larger particles.

For the large particles, values of h_s remain constant with increasing the superficial gas velocity because most of the excess gas passes through the spout and the contribution from particle convection is not significant. With the small glass and activated alumina particles, with a 50 % increase in U/U_{ms}, heat transfer coefficients increase by 17 %. This small rise in h_s can result from the enhanced particle motion since the influence of particle convection on overall heat transfer is more important for small than for large particles and/or from the gas flaring out from the spout into the annulus.

Figures 2.3a and 2.3b present the effect of superficial gas velocity for different particles with the probe situated at the spout axis. Compared to figures 2.2a and 2.2b, the drop in heat transfer when the flow pattern transforms from a spouted to a fixed bed is seen to be more important in the spout than in the annulus du to a more significant reduction of the local gas velocity. Again the drop is more pronounced for the particles of smaller Ar number. During spouting heat transfer coefficients increased only slightly (< 8 %) with an increase of superficial gas velocity. Also, the effect of superficial gas velocity for the small particles was less noticeable in the spout than in the annulus.

For the large particles, if the excess gas passes through the spout only, heat transfer coefficients should increase considerably with increasing the superficial gas velocity. A possible explanation for our results is that the increase of local particle and gas velocity is counterbalanced by the reduction in particle concentration, especially in the upper portion of the spout were the probe is situated (He et al., 1994a; Day et al., 1987). Also the increase of local gas velocity in the spout is not proportional to the increase of gasflow rate because of the widening of the spout diameter and the leakage of gas into the

annulus for small particles. More information is, however, needed to fully understand the mechanism in play.

The effect of superficial gas velocity on the radial profiles of local heat transfer coefficients is shown in figures 2.4a and 2.4b. Radial profiles of h_s for the small glass particles, see figure 2.4a, tend to be more flat with an increase of superficial gas velocity du to the increase of h_s in the annulus. Also the change of h_s at the spout-annulus interface becomes less significant at high gas flowrate. For large nylon particles shown in figure 2.4b, the variation of superficial gas velocity has little effect on the radial profiles of h_s because the heat transfer coefficient in both the spout and the annulus is not sensitive to the superficial gas velocity.

Zabrodsky and Mikhailik (1967) measured values of h_s in the spout with a horizontal cylindrical probe. They used 2 mm in diameter silica gel particles as spouting material. In the upper part of the bed, the increase in h_s was proportional to the increase of the flowrate ($h_s \alpha U^1$) although in the lower part of the spout the increase was more significant.

2.2.5.2 Effect of particle diameter

Radial profiles of h_s for small, large and a 50-50 % (vol.) mixture of glass particles are given in Figure 2.5 for $U/U_{ms} = 1.1$. Values of h_s are seen to increase with increasing particle diameter at $U/U_{ms} = 1.1$. However, at higher gas velocities, as shown in figures 2.2b and 2.3b, values of h_s for the small particles approach the values of the larger particles, especially in the annulus.

Similar effect has also been reported by Zabrodsky and Mikhailik (1967) who showed that h_s obtained at the top of the bed with a vertical cylindrical probe increased with the particle diameter (2 to 7 mm) and by Malek and Lu (1964), Glassen and Gishler (1958) and Freitas and Freire (1993) who measured higher values of wall-to-bed heat transfer coefficients, h_w, for larger particles. Zabrodsky and Mikhailik (1967) attributed the increase of h_s with increasing d_p to the greater disturbance created by large particles in the gas stream surrounding the probe. Malek and Lu (1964), on the other hand, suggested that the increase in solids circulation rates associated with the larger particles was responsible for the increase of h_w because particle convection is important for wall-to-bed heat transfer. Such a mechanism, however, fails to explain why h_w remains the same as the particle circulation rate is increased with increasing the gas velocity.

The minimum spouting velocity is higher for the particle mixture than for the small particles alone and smaller than for the large particles alone. Therefore, values of h_s in the spout for the particle mixture are expected to be between those obtained for small and large particles. Epstein and Grace (1984) indicated that when particles of different sizes are used, the larger particles concentrate in the upper inside part of the annulus, especially at low values of U/U_{ms}. Further out in the annulus the particle mixture is rich in small particles. In the annulus, values of h_s of the mixture are higher than those for the small particles because of the higher particle circulation rate and gas velocity. Values of h_s of the particle mixture are also higher than those obtained for the large particles because the increase of heat transfer by particle convection (richer in small particles) seems more important than the decrease of heat transfer by gas convection du to the lower gas flowrate.

Also, Zabrodsky and Mikhailik's (1967) experiments showed that starting from the spout axis, values of h_s increased radially and reached a maximum at the spout-annulus interface before dropping suddenly in the annulus to a relatively constant value. They attributed

this maximum to the radial increase of particle concentration in the spout and to the ejection of short-circuiting particles from the annulus into the spout. In the present investigation, maximum values of h_s are always at the axis and monotonically decrease towards the column wall, although there exist a sharp drop at the spout-annulus boundary. Klimenko et al. (1970) who measured radial profiles of h_s just over the conical section at the top of the bed obtained, the same type of profiles as us.

2.2.5.3 Effect of the axial position of the probe

Radial profiles of h_s at different axial positions for $U/U_{ms} = 1.3$ are shown in figures 2.6a and 2.6b. With increasing the elevation of the axial position, it is seen that radial profiles of h_s tend to flatten out just like the radial profiles of gas velocity (He et al., 1992). Indeed, as gas travels up in the bed more and more gas has flowed out of the spout into the annulus (Mathur and Epstein 1974; Bridgewater, 1985). This effect is more pronounced for the smaller glass particles than for the larger polyethylene particles, indicating again that gas flares out more easily for smaller particles. In the annulus, values of h_s are higher at higher axial positions since gas and particle velocities are higher. In the spout, values of h_s at lower axial positions are higher because of the higher gas and particle velocities, although particle concentration is lower. With the horizontal cylindrical probe, Zabrodsky and Mikhailik (1967) also measured a decrease of h_s along the spout height and which leveled off in the upper part.

2.2.5.4 Effect of the static bed height

Figure 2.7 presents the effect of the static bed height for polyethylene and small glass particles at $U/U_{ms} = 1.3$. Grbavcic et al. (1976) found that for a given vessel geometry and fluid-solid combination, the annulus fluid velocity at any bed level was independent of the total bed height. For this reason, values of h_s for the polyethylene particles are seen to be relatively constant in the annulus, although the particle circulation rate is increased in deeper beds (Mathur and Epstein, 1974). However a slight increase of h_s is noticed for the small glass particles presumably because again some of the excess gas flares out into the annulus and the effect of particle circulation is more important for particles of small Ar number. In the spout, values of h_s are seen to be higher in the deeper bed because of the higher gas flow rate required for minimum spouting.

2.2.5.5 Effect of the inlet diameter

Radial profiles of h_s for different inlet diameters at $U/U_{ms} = 1.3$ are shown in figure 2.8 for polyethylene particles. The effect of the inlet diameter on the values of h_s is only marginal. Values of h_s are constant in the annulus because an increase of the inlet diameter does not significantly affect the average gas velocity (Lim and Grace, 1987) and particle circulation rate (Mathur and Epstein, 1974) in the annulus. In the spout, values of h_s increase slightly with an increase of inlet diameter because a higher gas flow rate is required for the minimum spouting velocity with larger inlet diameters.

As for wall-to-bed heat transfer coefficients, Malek and Lu (1964) did not find any significant effect of D_i while Uemaki and Kugo (1967) found that $h_w \propto D_i^{0.2}$.

2.2.5.6 Effect of particle heat capacity and thermal conductivity

Figure 2.9 presents radial profiles of h_s for polyethylene, polypropylene and polystyrene particles at U/U_{ms} = 1.3. All three particles have similar diameters and densities and therefore similar values of U_{ms}. If gas convection was the sole mechanism of heat transfer, values of h_s would be the same for all three profiles. The variation of h_s with particle heat capacity and thermal conductivity in figure 2.9 indicates that particle convection still plays a role in heat transfer although not necessarily predominant.

2.2.5.7 Effect of particle humidity

Figure 2.10 presents the effect of particle humidity for the small activated alumina particles (d_p = 2.0 mm). It is seen that particle moisture content has a positive effect on the values of h_s in the annulus and in the spout. In the annulus, the value of h_S for particles with 37 % humidity (dry basis) is 15 % higher than for the dry particles. In the spout, the value of h_s for the wet particles is only 5 % higher. This result indicates that heat transfer by particle convection is still significant, and is more important in the annulus.

Particle convection heat transfer is influenced by particle heat capacity and gas thermal conductivity. An increase of particle moisture content increases the heat capacity of the particles while an increase of gas humidity increases the thermal conductivity of the gas.

2.2.6 Discussion and correlation of the data

Values of heat transfer coefficients obtained in the present study vary between 95 and 230 W/m^2°C. Values of h_a in the annulus are similar to those reported by Grace (1986) for moving beds (50 - 150 W/m^2°C) while values of h_s in the upper part of the spout are similar to those reported by Botterill (1986) for large particle fluidized beds (150 - 250 W/m^2°C).

Like moving beds and fluidized beds, or any other gas-solid systems where there is a particle and gas flow pattern, two parallel heat transfer mechanisms are involved in spouted beds operated at low or moderate temperatures (T< 400°C), i.e. particle convection and gas convection.

Particle convection (h_{pc}) is the unsteady-state heat conduction through the gas layers between the particles and the heat transfer surface during the period of contact. The particles are then continuously released back into the bulk of the bed where they exchange heat by convection with the spouting gas and by conduction through the gas with the other particles. Heat transfer is then a function of particle concentration and residence time, gas film conductivity and thickness and particle volumetric heat capacity at the surface of the heat exchanger (Saxena, 1989). Gas convection (h_{gc}) is the heat exchanged with the gas percolating along the surface in the interstitial voids between the particles (Botterill, 1986). As a first approximation, the heat transfer coefficient can be taken as the addition of the two components (Botterill, 1986): $h_s = h_{pc} + h_{gc}$.

Although the mechanisms of heat transfer by gas and particle convection are well understood, there still seems to be some confusion about their relative importance at different areas of the bed and under different spouting conditions. Mathur and Epstein (1974) emphasized the role of particle convection in the annulus based on the

experimental data of Klimenko et al. (1970) which showed that values of h_s dropped by a factor of 2.5 just over the annulus. Furthermore, Mathur and Epstein (1971) modeled wall-to-bed heat transfer based on particle convection only. Similar to the packet model developed by Mickley and Fairbanks (1955) for particle convective heat transfer in fluidized beds, Mathur and Epstein (1971) replaced the packet renewal frequency by the residence time of the particles at the heat transfer surface. The particle residence time was approximated by the length of the surface divided by the axial velocity of the particle by assuming that particles flow along the surface over the entire length of heat transfer probe.

It is interesting to note that particle velocities in the annulus are in the order of 10 to 75 mm/s, depending on gas and solid properties, column geometry and operating conditions (He and al, 1994b; Benkrid and Caram, 1989; Roy et al., 1994). Also, particle velocities at the column wall are quite smaller than those further out in the annulus (He et al., 1994b). In the study of Malek and Lu (1964), the length of the heat transfer surface varied between 254 and 457 mm. If particles flow along the walls in a smooth laminar-like motion, it is then possible that the residence time of the particles at the wall is long enough for them to change in temperature and reduce the thermal driving force. By increasing the particle diameter and therefore the particle circulation rate, the residence time of the particles would be reduced and the heat transfer coefficient would increase. Also, the thermal time constant of particles increases with their diameter, requiring a greater amount of heat transferred to have a change of the temperature.

In a fluidized bed of large particles, such as those used in spouted beds, the predominant heat transfer mechanism is gas convection and values of h_s increase with particle diameter (Saxena, 1989). Zabrodsky and Mikhailik (1967) measured an increase in h_s with increasing particle diameter all across the spouted bed. They suggested that larger particles would cause a greater disturbance of the gas stream in the vicinity of the heater,

thereby increasing the contribution to heat transfer by gas convection. Grace (1982) thus suggested that even for wall-to-bed heat transfer coefficients, the primary mode of heat transfer is by gas convection since h_w increases with particle diameter. He then proposed the use of correlations for the gas convective component (h_{gc}) in a fluidized bed to estimate the overall wall-to-bed heat transfer coefficient in spouted beds.

In the present investigation, most of the effects from varying the different parameters could be explained by the gas flow pattern, although figures 2.9 and 2.10 showed that particle convection cannot be neglected. At a fix bed level in the cylindrical section of a spouted bed, radial profiles of particle velocity and voidage in the annulus are quite flat except near the wall (Benkrid and Caram, 1989; Roy et al., 1994; He et al., 1994a; 1994b). While the gas velocity monotonically decreases from the axis towards the column wall. This radial gas velocity profile flattens out progressively with the elevation of the bed level since more and more gas has moved from the spout into the annulus (Mathur and Epstein, 1974; Kmiec, 1980; Lim and Grace 1987; He et al., 1992). Such a radial gas velocity profile is in correspondence with that of local heat transfer coefficients obtained by Klimenko et al. (1970) and in this investigation in which h_s decreased from the axis towards the column wall. This suggests that local heat transfer coefficients are strongly interrelated to local gas velocities. Also for the larger particles, the contribution of particle heat transfer seems to be small since an increase of gas flow does not substantially increase the annulus gas velocity (Lim and Grace, 1987) and particle voidage (Epstein and Grace, 1984) while particle circulation is enhanced (Mathur and Epstein, 1974; He et al., 1994b) which would lead to an increase of h_s if particle convection was important.

In gas-solid fluidized beds of large particles, the gas convective term can be correlated in the following form (Grace, 1982):

$$Nu_{gc} = \beta * Ar^{\delta} * Pr^{\gamma} \tag{3}$$

Since gas convection appears to be the predominant mode of tube-to-bed heat transfer in spouted beds while particle convection is also not negligible, the following equation is proposed.

$$Nu = a * Ar^{b} * \left(\frac{\rho_p \cdot (1-\varepsilon_b) \cdot C_p}{\rho_g \cdot C_g} \right)^{c} \tag{4}$$

Here the Prandl number is omitted since only ambient air was used in the experiments. The ratio of particle to gas volumetric heat capacity takes into account the contribution to heat transfer by particle convection.

Values of (a, b and c) in the proposed correlation were evaluated based on the data obtained at $U/U_{ms} = 1.3$, $z = 0.21$ m and $H = 0.27$ m when a stable spouting condition was maintained with the probe placed in the annulus ($r/R = 0.59$) as well in the spout ($r/R = 0$).

By least square fitting the following correlations were obtained:

$$Nu = 0.0196 * Ar^{0.359} * \left(\frac{\rho_p \cdot (1-\varepsilon_b) \cdot C_p}{\rho_g \cdot C_g} \right)^{0.284} \quad \text{in the spout at } r/R = 0 \tag{5}$$

$$Nu = 0.009 * Ar^{0.348} * \left(\frac{\rho_p \cdot (1-\varepsilon_b) \cdot C_p}{\rho_g \cdot C_g} \right)^{0.379} \quad \text{in the annulus at } r/R = 0.59 \tag{6}$$

As expected, the effect of particle heat capacity is less important in the spout than in the annulus. Although the particle diameter does not have a direct influence on the heat transfer coefficient at U/U_{ms} =1.3 ($h_s \alpha d_p^{0.08}$), it is very important for the structure of the spouting bed and the form of the h_s radial profiles. It has been shown that operating conditions affect values of h_s differently for small and large particles.

The agreement between experimental and calculated values of h_S from equations 5 and 6 is shown in figure 2.11. The average deviation is 4 % while the maximum deviation is 10 % with h_S ranging from 100 to 230 $W/m^2°C$.

Table 2.2 compares the predicted values from equations 5 and 6 with the experimental data from Zabrodsky and Mikhailik (1967) and Klimenko et al. (1970). The density and heat capacity of the particles used in their experiments were not mentioned. The physical and thermal properties were therefore taken from Kunni and Levenspiel (1991) and Kirk-Othmer (1979). The static bed voidage (ε_b) was taken as 0.4.

Experimental values of h_s from Klimenko et al. (1970) are predicted with than 22 % error in the spout and 6 % error in the annulus while the average relative error with Zabrodsky and Mikhailik (1967) data is around 39 %. It is interesting to note that for particles of similar size, density and heat capacity, values of h_s from Zabrodsky and Mikhailik (1967) are considerably higher than those obtained by Klimenko et al. (1970), especially in the annulus. If particle properties of silica (ρ_p = 2300 kg/m^3; C_p = 740 J/kg°C) are used instead of those for silica gel, values of h_s from Zabrodsky and Mikhailik (1967) are predicted with an average error of 15 %.

2.2.7 Conclusion

An experimental investigation on heat transfer from a vertical tube in a cylindrical-conical spouted bed using ambient air and a variety of solid particles has been conducted. Values of the heat transfer coefficients obtained in the present study vary between 95 and 230 $W/m^2{}^oC$ and are about 0 to 30 % lower in the annulus (r/R = 0.59) than at the spout axis, depending on particle properties, spouting conditions and probe axial positions.

As in fluidized beds, particle diameter has significant influence on the heat transfer coefficient in spouted beds. Indeed, the influence of the different operating conditions on the gas-solid flow structure of the bed is dependent on particle size and density. Also, within the cylindrical section of the bed, the heat transfer behavior is different in the spout from in the annulus.

Maximum values of h_s are always at the spout axis and decrease monotonically towards the column wall, the drop is most important at the spout-annulus boundary. At a given bed height, when the probe is moved upward, values of h_S decrease in the spout and increase in the annulus. The influence of gas velocity (up to U/U_{ms} = 1.5) is not important for particles with an Ar number higher than about 10^6. As for the small glass and activated alumina particles ($Ar \approx 3.5 \times 10^5$)with an increase of gas velocity, values of h_S increase and approach the values of the larger particles, especially in the annulus.

It seems that the common assumption that the excess gas above U_{ms} passes through the spout while the gas flow through the annulus remains constant is more accurate for the larger particles. For the smaller particles, a larger portion of the excess gas flares out of the spout into the annulus. In the present investigation, most of the effects from varying the different parameters could be explained by the flow patterns of the gas, although particle convection still has some importance in determining the heat transfer rate.

Two equations correlating values of h_s obtained with the probe placed in the spout and in the annulus at $U/U_{ms} = 1.3$ have been developed. The maximum deviation from the predicted and experimental values of h_s from the present investigation is 10 %. The proposed correlations could serve as a tool for the estimation of the tube-to-bed heat transfer coefficient in a spouted bed. Finally, in order to fully understand the complex mechanism of indirect heat transfer in spouted beds and then to predict the heat transfer rate, hydrodynamic and heat transfer data must be obtained under the same operating conditions.

2.2.8 Acknowledgments

The authors gratefully acknowledge financial support from the Natural Sciences and Engineering Research Council of Canada and the FCAR of Quebec. A. Macchi also would like to thank Gaz Métropolitain inc. for contributing to a graduate fellowship.

2.2.9 Nomenclature

a = variable in equation (4)

A = heat transfer surface area, m^2

Ar = Archimedes number $[=g \cdot d_p^3 \cdot (\rho_p - \rho_g)/\mu_g^2]$

b = variable in equation (4)

c = variable in equation (4)

C_p = particle heat capacity, J/kg°C

C_g = gas heat capacity, J/kg°C

d_p = particle diameter, mm

d_v = equivolume spherical diameter, m [diameter of a sphere having the same volume of the particle]

D_i = spouted bed inlet diameter, m

g = gravitational acceleration, m/s^2

G_s = dry air mass flowrate, kg/s

H = static bed height, m

h_{gc} = gas convective heat transfer coefficient, $W/m^{2\circ}C$

h_{pc} = particle convective heat transfer coefficient, $W/m^{2\circ}C$

h_s = surface-to-bed heat transfer coefficient, $W/m^{2\circ}C$

$h_{s\,calc}$ = surface-to-bed heat transfer coefficient predicted from equation 5, $W/m^{2\circ}C$

$h_{s\,exp}$ = experimental surface-to-bed heat transfer coefficient, $W/m^{2\circ}C$

$h_{s\,max}$ = maximum surface-to-bed heat transfer coefficient, $W/m^{2\circ}C$

h_w = wall-to-bed heat transfer coefficient, $W/m^{2\circ}C$

k_g = gas thermal conductivity, W/m°C

k_p = particle thermal conductivity, W/m°C

Nu = Nusselt number $[=h_s \cdot d_p/k_g]$

Nu_{gc} = gas convective Nusselt number $[=h_{gc} \cdot d_p/k_g]$

Nu_{max} = maximum Nusselt number $[=h_{s\,max} \cdot d_p/k_g]$

P = Power, W

Pe = Polyethylene

Pp = Polypropylene

Ps = Polystyrene

Pr = Prandl number, [$=\mu_g \cdot C_g/k_g$]

r = radial position of the heat transfer probe, m

R = spouted bed column radius, m

T = temperature, °C

T_b = bed temperature, °C

T_s = probe surface temperature, °C

U = superficial gas velocity, m/s

U_{ms} = minimum spouting superficial gas velocity, m/s

X = dry basis solid moisture, kg water/kg dry solid

X_1 = dry basis solid moisture at time t_1, kg water/kg dry solid

X_2 = dry basis solid moisture at time t_2, kg water/kg dry solid

Y_{in} = dry basis gas humidity at the spouted bed inlet, kg water/kg dry air

Y_{out} = dry basis gas humidity at the spouted bed outlet, kg water/kg dry air

z = axial position of the heat transfer probe, m

Greek letters

β = variable in equation (3)

δ = variable in equation (3)

ε_b = static bed voidage,

ε_{mf} = bed voidage at minimum fluidization,

ϕ = sphericity [surface of a sphere having the same volume as the particle divided by the surface of the particle]

γ = variable in equation (3)

μ_g = gas viscosity, kg/m·s

ρ_g = gas density, kg/m^3

ρ_p = particle density, kg/m^3

Δ_t = drying experiment sampling period, s

2.2.10 References

Benkrid, A. and H. S. Caram, "Solid Flow in the Annular Region of a Spouted Bed", AIChE J. **35**, 1328-1336 (1989).

Botterill, J. S. M., "Fluid Bed Heat Transfer", Chapt. 9 in "Gas Fluidization Technology", D. Geldart, Ed., John Wiley & Sons Ltd., New York (1986), pp. 219-258.

Bridgewater, J., "Spouted beds", Chapt. 6 in "Fluidization", 2nd edition, J. F. Davidson, R. Clift and D. Harrison, Eds., Academic Press, London (1985), pp. 201-224.

Day, J. Y., M. H. Morgan, III and H. Littman, "Measurements of Spout Voidage Distributions, Particle Velocities and Particle Circulation rates in Spouted Beds of Coarse Particles - II. Experimental Verification", Chem. Eng. Sci. **42**, 1461-1470 (1987).

Epstein, N. and K. B. Mathur, "Heat and Mass Transfer in Spouted Beds - A Review", Can. J. Chem. Eng. **49**, 467-476 (1971).

Epstein, N. and J. R. Grace, "Spouting of Particulate Solids", Chapt. 11 in "Handbook of Powder Science and Technology", M.E. Fayed and L. Otten, Eds., Van Nostrand Reinhold Co., New York (1984), pp. 507-536.

Freitas, L. A. P. and J. T. Freire, "Heat Transfer in Spouted Beds", Drying Technology **11**, 303-317 (1993).

Grace, J. R., "Fluidized-Bed Heat Transfer", Chapt. 8.2 in "Handbook of Multiphase Systems", G. Hestroni, Ed., Hemisphere/McGraw Hill (1982), pp. 8-65 - 8-83.

Grace, J.R., "Contacting Modes and Behaviour Classification of Gas-Solid and Other Two Phase Suspensions," Can. J. Chem. Eng. **64**, 353-363 (1986).

Grbavcic, Z. B., D. V. Vukovic, F. K. Zdanski and H. Littman, "Fluid Flow Pattern, Minimum Spouting Velocity and Pressure Drop in Spouted Beds", Can. J. Chem. Eng. **54**, 33-42, (1976).

He, Y. L., C. J. Lim and J. R. Grace, "Spouted Bed and Spout-Fluid Bed Behaviour in a Column of Diameter 0.91 m", Can. J. Chem. Eng. **70**, 848-857 (1992).

He, Y. L., C. J. Lim, J. R. Grace, J. X. Zhu and S.Z. Qin, "Measurements of Voidage Profiles in Spouted Beds", Can. J. Chem. Eng. **72**, 229-234 (1994a).

He, Y.L., S. Z. Qin, C. J. Lim and J.R. Grace, "Particle Velocity Profiles and Solid Flow Patterns in Spouted Beds", Can. J. Chem. Eng. **72**, 561-568 (1994b).

Kirk-Othmer, "Encyclopedia of Chemical Technology", 3rd ed., vol. 8, John Wiley & Sons Ltd., New York (1979), p.124.

Klassen, J. and P. E. Gishler, "Heat Transfer from Column Wall to Bed in Spouted, Fluidized and Packed Systems", Can. J. Chem. Eng. **36**, 12-18 (1958).

Klimenko et al., "Heat Transfer Between a Spouting Bed and the Surface of a Spherical Probe", Heat Transfer - Soviet Research **Vol.2 No. 1**, 90-94 Jan. (1970).

Kmiec, A., "Hydrodynamics of Flows and Heat Transfer in Spouted Beds", Chem. Eng. J. **19**, 189-200 (1980).

Kunni, D. and O. Levenspiel, "Fluidization Engineering", 2nd ed., Butterworth-Heinemann, Boston (1991), Chapt. 13, pp. 313-336.

Lim, C. J. and J. R. Grace, "Spouted Bed Hydrodynamics in a 0.91 m Diameter Vessel", Can. J. Chem. Eng. **65**, 366-372 (1987).

Malek, M. A. and B. C. Y. Lu, "Heat Transfer in Spouted Beds", Can. J. Chem. Eng. **42**, 14-20 (1964).

Mathur, K. B. and N. Epstein, "Spouted Beds", Academic Press Inc., New York (1974).

Mikley, H. S. and D. F. Fairbanks, "Mechanism of Heat Transfer to Fluidized Beds", AICheE J. **1**, 374-384 (1955).

Molerus, O., A. Burschka and S. Dietz, "Particle Migration at Solid Surfaces and Heat Transfer in Bubbling Fluidized Beds - II. Prediction of Heat Transfer in Bubbling Fluidized Beds", Chem. Eng. Sci. **50**, 879-885 (1995).

Reay, D., "Fluidized Bed Drying", Chapt. 10 in "Gas Fluidization Technology", D. Geldart, Ed., John Wiley & Sons Ltd., New York (1986), pp. 259-283.

Rioux, M., "Séchage des Boues de Procédés d'Usines d'Épuration par Lit à Jet", M.Sc.A mémoire, École Polytechnique de Montréal, Montréal, Canada (1993).

Roy D., F. Larachi, R. Legros and J. Chaouki, "A Study of Solid Behavior in Spouted Beds Using 3-D Particle Tracking", Can. J. Chem. Eng. **72**, 945-952 (1994).

Saxena, S. C., "Heat Transfer between Immersed Surfaces and Gas-Fluidized Beds", in "Advances in Heat Transfer", vol. 19, J.P. Harnett and T.F. Irvine Jr., Eds., Academic Press Inc., New York (1989), pp. 97-190.

Uemaki, O. and M. Kugo, "Heat Transfer in Spouted Beds", Kagaku Kogaku **31**, 348-353 (1967)

Zabrodsky S. S. and V. D. Mikhailik, "The Heat Exchange of the Spouting Bed with a submerged Heating Surface", Collected papers on "Intensification of Transfer of Heat and Mass in Drying and Thermal Processes", Nauka i Tekhnica BSSR, 130-137 (1967). (Quoted in Mathur and Epstein (1974))

Table 2.1 Properties of the Particulate Material at 20°C

Material	d_v (mm)	ϕ	d_p (mm)	ε_b (at rest)	ρ_p (kg/m^3)	k_p (W/m°C)	C_p (J/kg°C)	Ar
Glass	3.00	1	3.00	0.38	2400	0.90	765	2.35×10^6
Glass	1.60	1	1.60	0.36	2400	0.90	765	3.57×10^5
Activated Alumina	3.75	1	3.75	0.39	1290	33	1005	2.47×10^6
Activated Alumina	1.98	1	1.98	0.36	1320	33	1005	3.72×10^5
Nylon	2.90	1	2.90	0.40	1120	0.24	1599	9.90×10^5
Polystyrene (Ps)	3.40	0.85	2.89	0.45	1087	0.11	1194	9.51×10^5
Polyethylene (Pe)	3.70	0.83	3.07	0.37	943	0.48	1855	9.90×10^5
Polypropylene (Pp)	3.70	0.87	3.22	0.35	880	0.12	1789	1.06×10^6

Table 2.2 Comparison of literature data with the predictions of equations 5 and 6.

	Klimenko et al. (1970) Silica-alumina catalyst d_p = 2.4 mm ρ_p = 1250 kg/m^3 C_p = 1060 J/kg°C			Zab. and Mik. (1967) Silica gel particles d_p = 2.0 mm ρ_p = 1200 kg/m^3 C_p = 921 J/kg°C			Zab. and Mik. (1967) Silica gel particles d_p = 4.0 mm ρ_p = 1200 kg/m^3 C_p = 921 J/kg°C		
r/R	$h_{s\,exp}$ (W/m^2°C)	$h_{s\,cal}$ (W/m^2°C)	error (%)	$h_{s\,exp}$ (W/m^2°C)	$h_{s\,cal}$ (W/m^2°C)	error (%)	$h_{s\,exp}$ (W/m^2°C)	$h_{s\,cal}$ (W/m^2°C)	error (%)
0	208	162	22	235	150	36	260	158	39
4/7	127	119	6	190	109	43	195	113	42

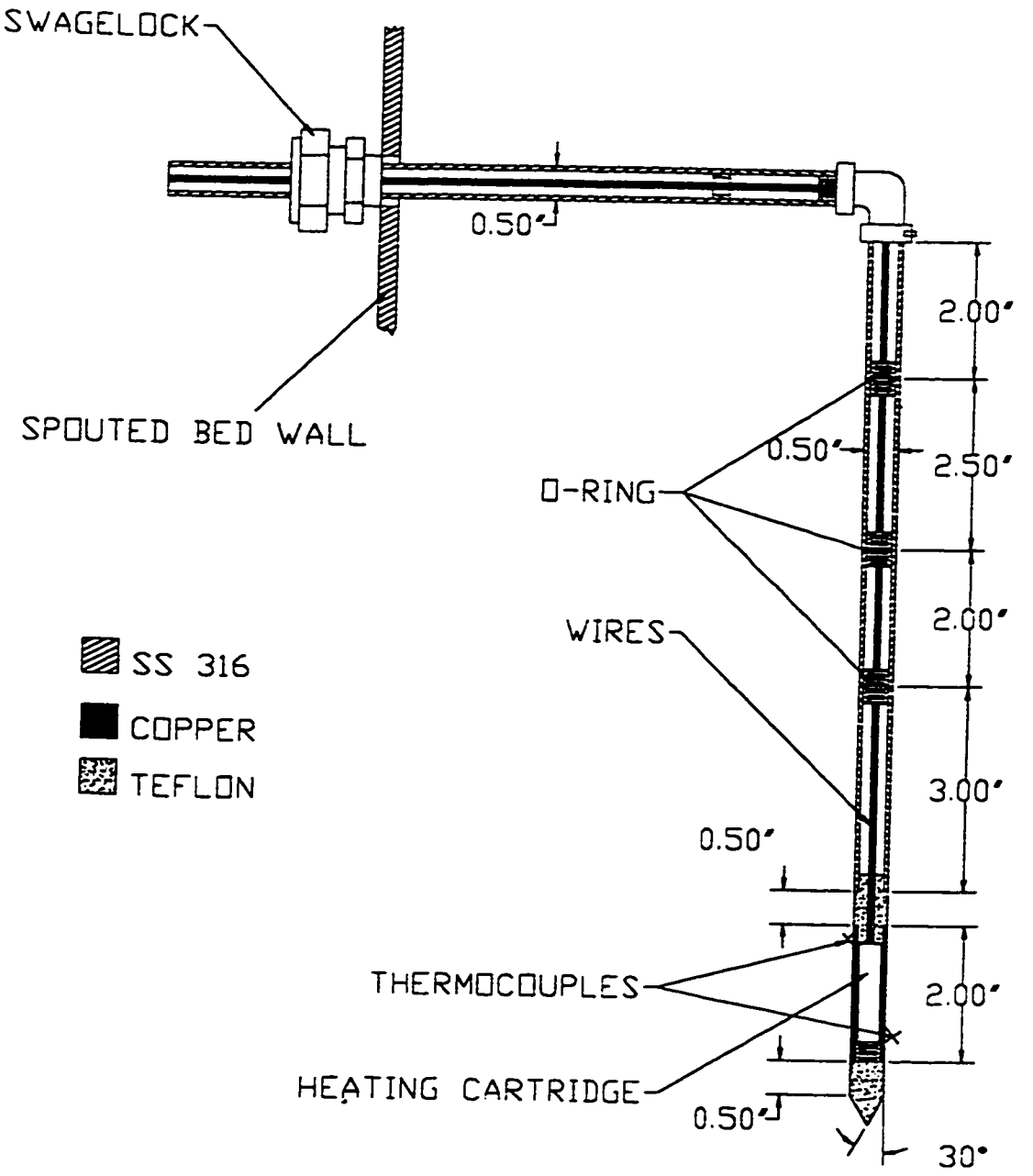

Figure 2.1 Schematic of heat transfer probe.

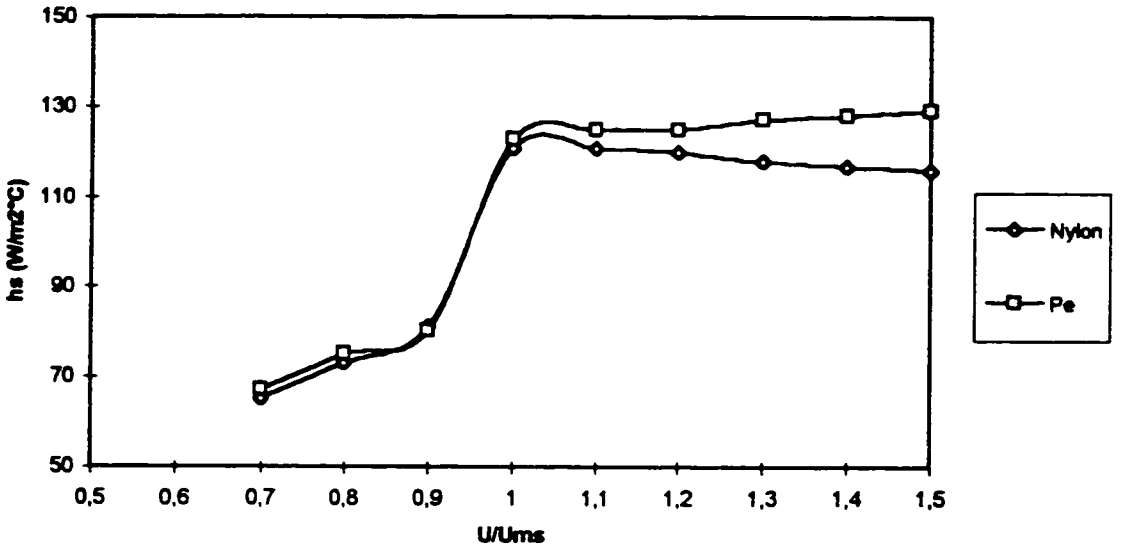

Figure 2.2a Effect of superficial gas velocity on h_s in the annulus at r/R = 0.59 for nylon and polyethylene particles. H= 0.27 m, z = 0.21 m, and D_i = 0.019m.

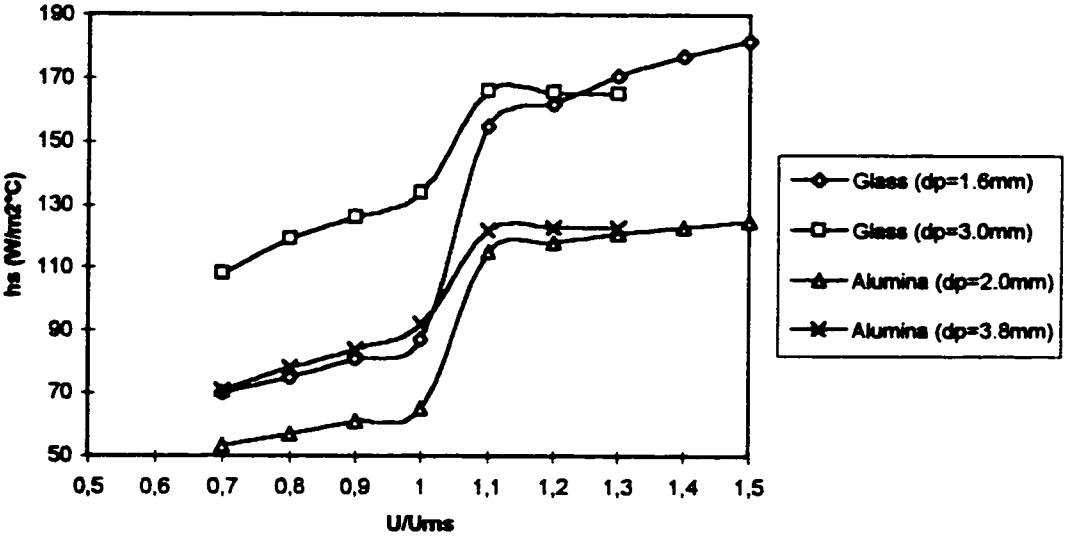

Figure 2.2b Effect of superficial gas velocity on h_s in the annulus at r/R = 0.59 for glass and activated alumina particles. H = 0.27 m, z = 0.21 m and D_i = 0.019 m.

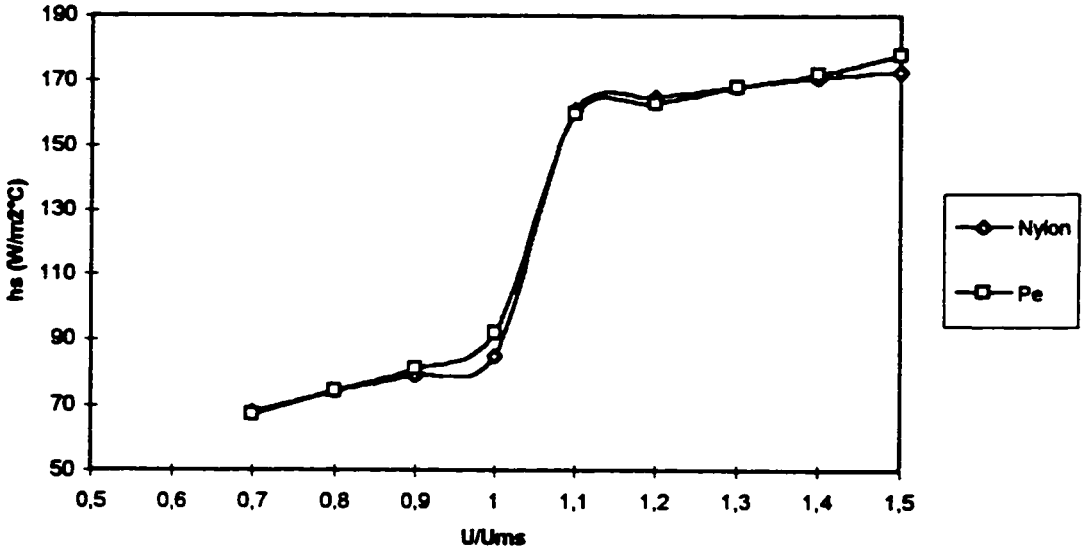

Figure 2.3a Effect of superficial gas velocity on h_s in the spout at r/R = 0 for nylon and polyethylene particles. H= 0.27 m, z = 0.21 m, and D_i = 0.019m.

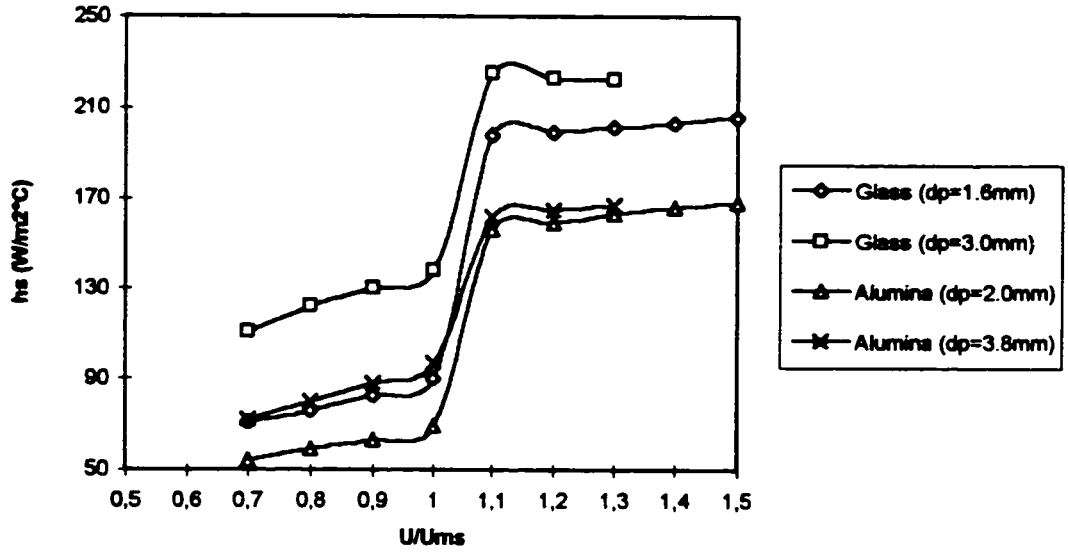

Figure 2.3b Effect of superficial gas velocity on h_s in the spout at r/R = 0 for glass and activated alumina particles. H= 0.27 m, z = 0.21 m, and D_i = 0.019m.

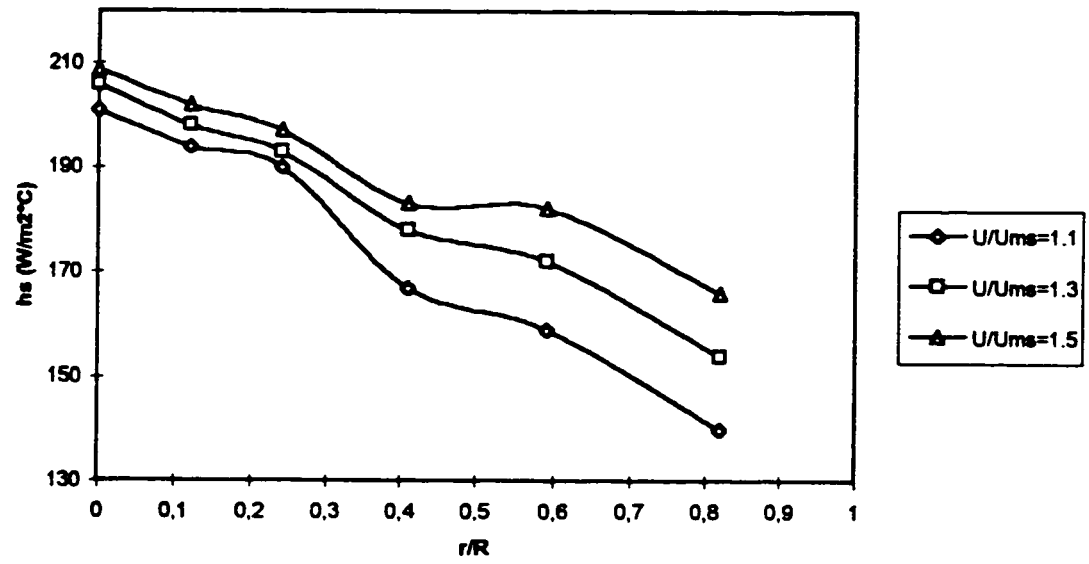

Figure 2.4a Effect of superficial gas velocity on radial profiles of h_s for glass particles (dp = 1.6 mm). H = 0.27 m, z = 0.21 m and D_i = 0.019 m.

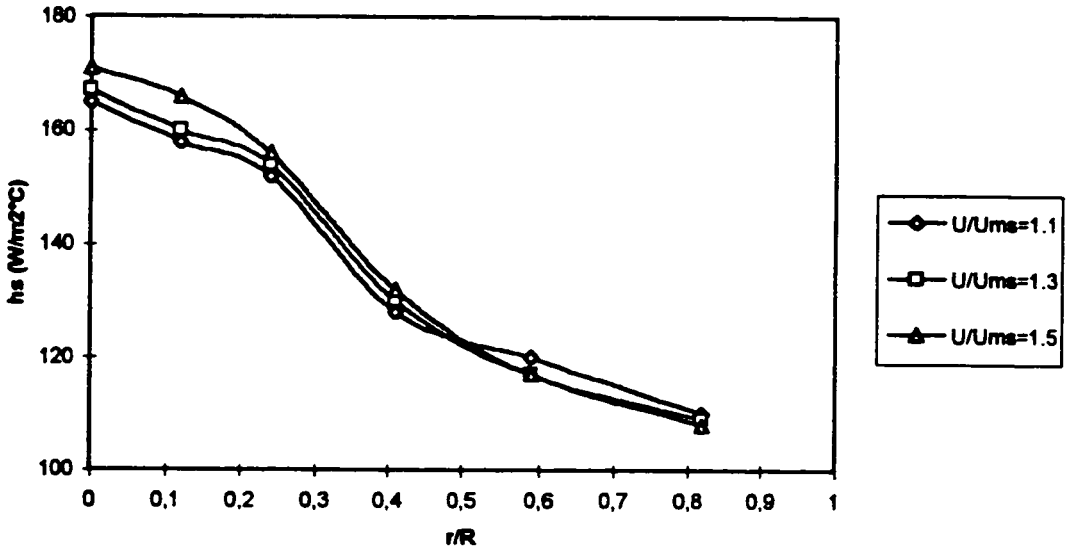

Figure 2.4b Effect of superficial gas velocity on radial profiles of h_s for nylon particles. H = 0.27 m, z = 0.21 m and D_i = 0.019 m.

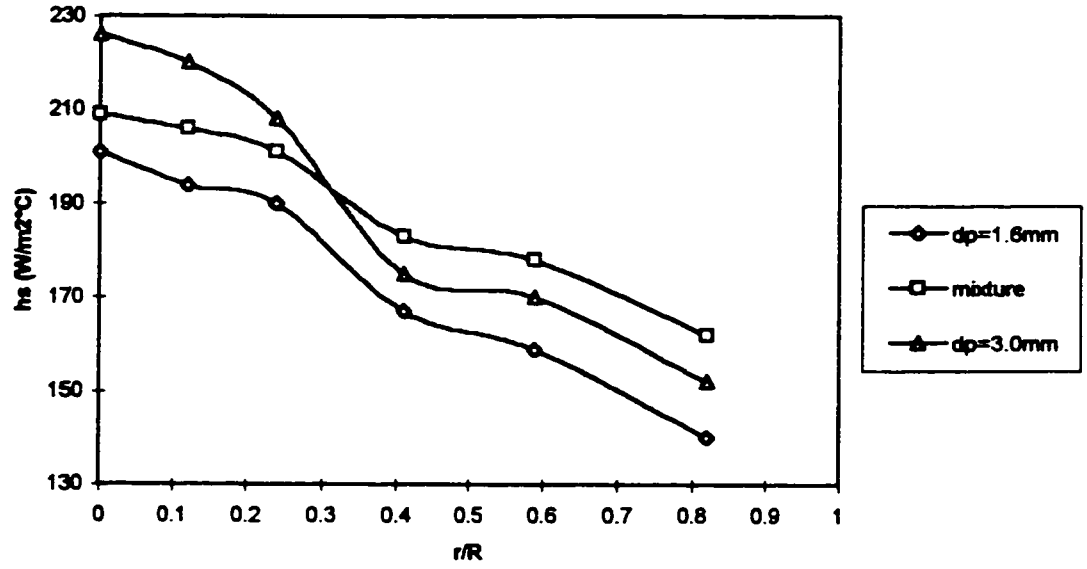

Figure 2.5 Effect of particle diameter on radial profiles of h_s for glass particles at $U/U_{ms} = 1.1$. $H = 0.27$ m, $z = 0.21$m, $D_i = 0.019$ m.

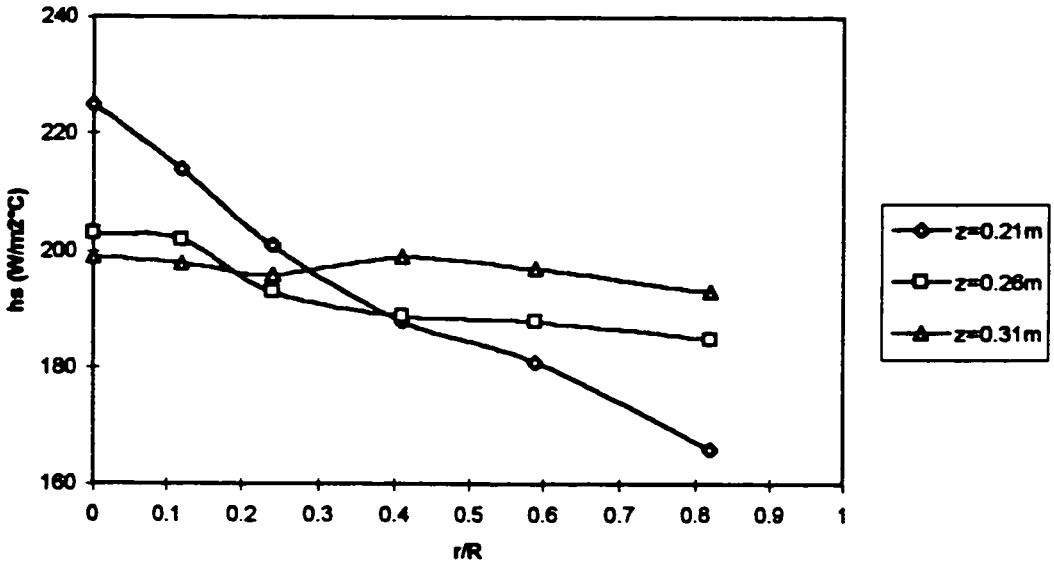

Figure 2.6a Effect of probe axial position on radial profiles of h_s for glass particles ($d_p = 1.6$ mm). $H = 0.39$ m, $U/U_{ms} = 1.3$, $D_i = 0.019$ m.

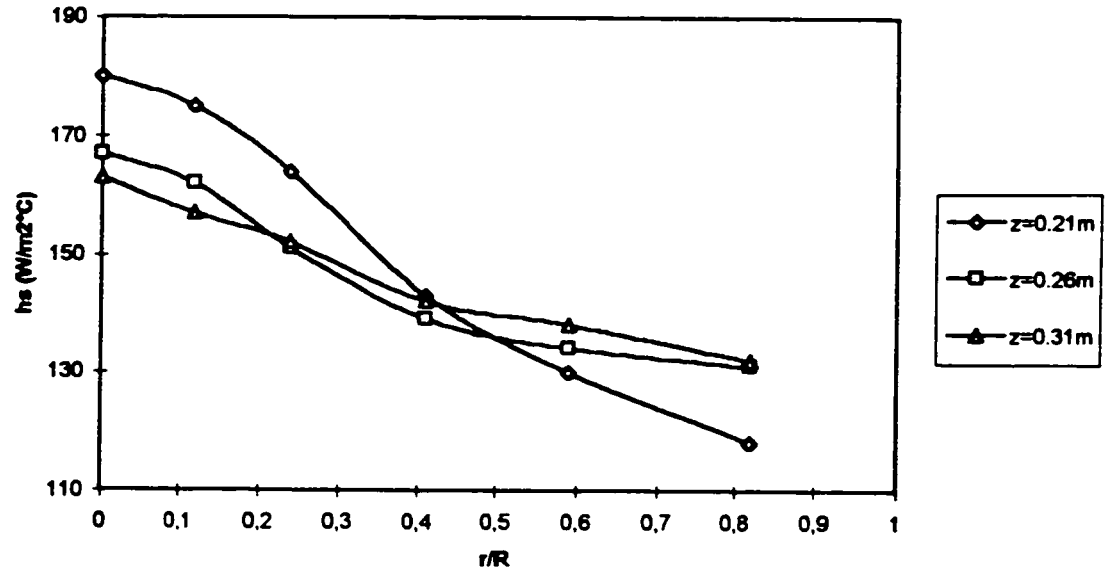

Figure 2.6b Effect of probe axial position on radial profiles of h_s for polyethylene particles. H= 0.39 m, U/U_{ms} = 1.3, D_i = 0.019 m.

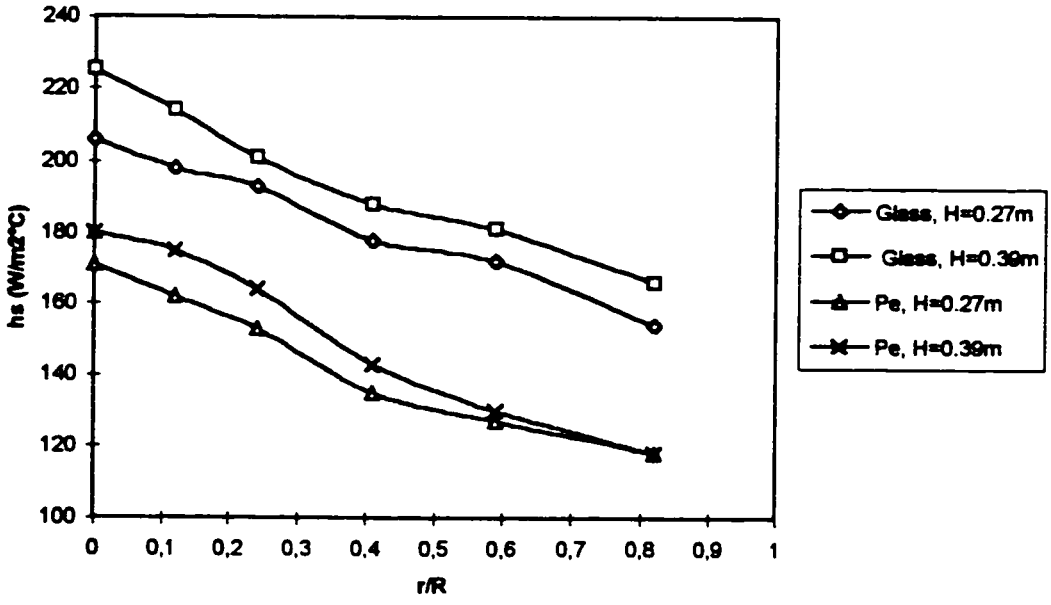

Figure 2.7 Effect of bed height on radial profiles of h_s for glass (d_p = 1.6 mm) and polyethylene particles. U/U_{ms} = 1.3, z = 0.21 m, D_i = 0.019 m.

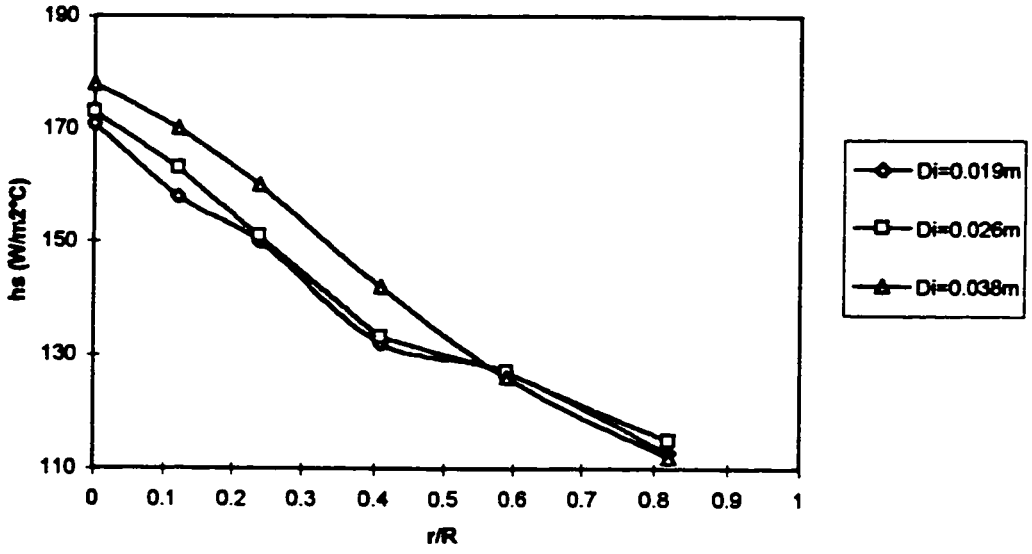

Figure 2.8 Effect of inlet diameter on radial profiles of h_s for polyethylene particles. H = 0.27 m, z = 0.21 m, U/U_{ms} = 1.3.

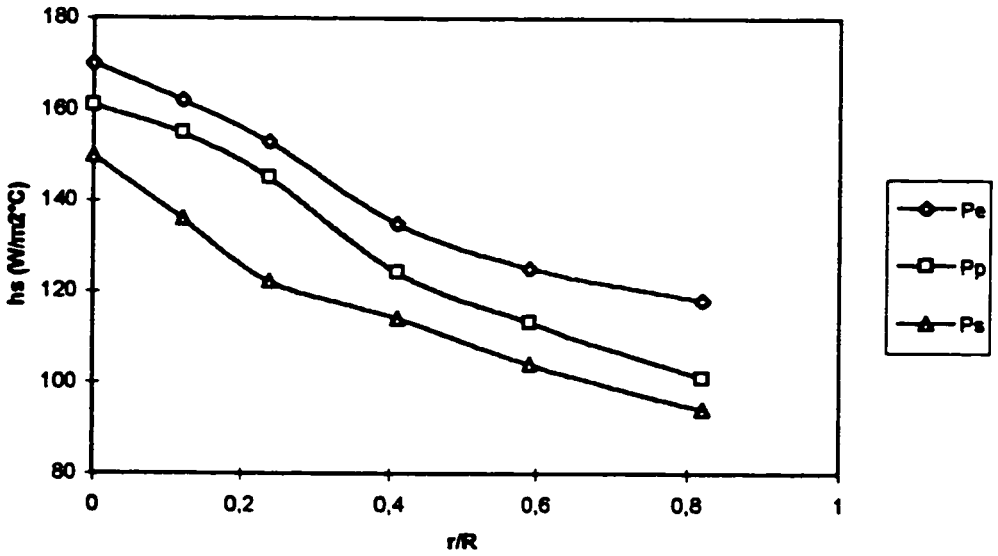

Figure 2.9 Effect of thermal properties on radial profiles of h_s. H = 0.27 m, z = 0.21 m, U/U_{ms} = 1.3, D_i = 0.019 m.

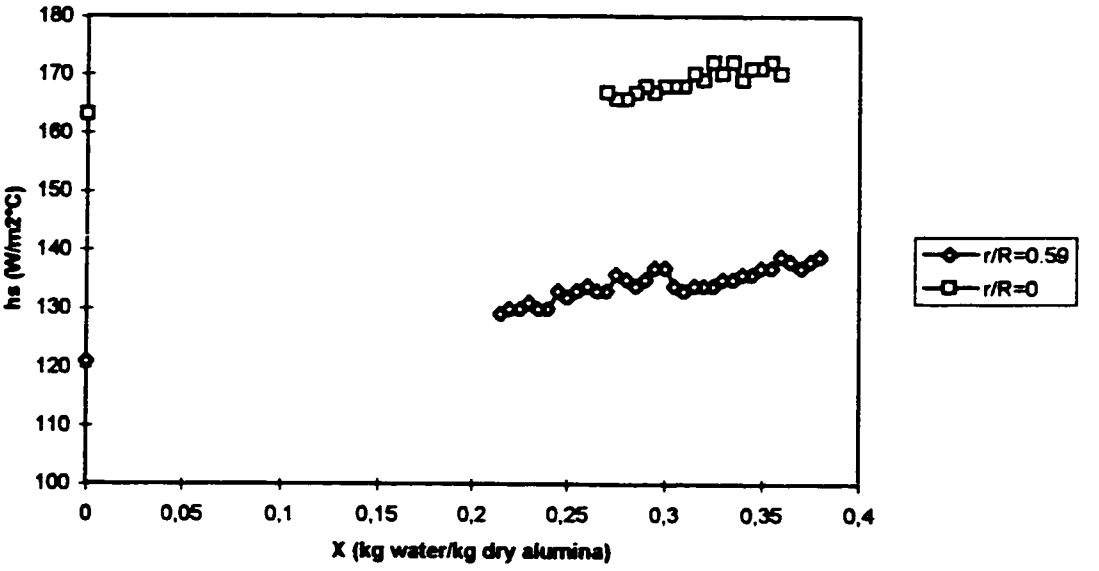

Figure 2.10 Effect of particle humidity on h_s for activated alumina particles (d_p = 2.0 mm). H = 0.27 m, z = 0.21 m, U/U_{ms} = 1. 3, D_i = 0.019 m.

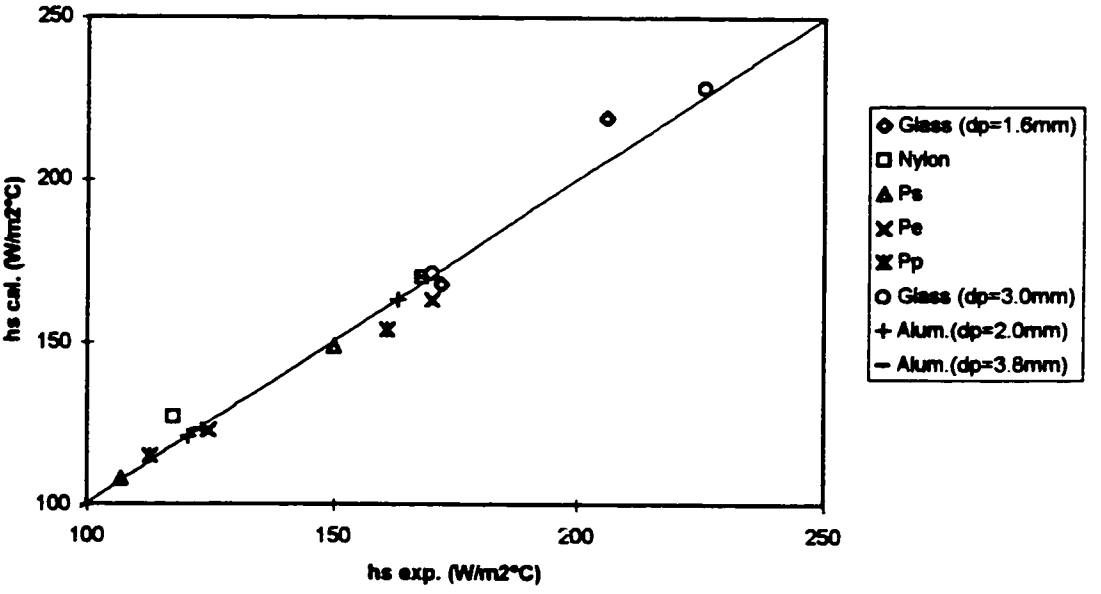

Figure 2.11 Agreement between experimental and calculated values of h_s.

CHAPITRE 3

ARTICLE SUR LA VITESSE MINIMUM DE GICLAGE D'UN LIT À JET CONIQUE

3.1 SOMMAIRE

Afin de dimensionner et d'effectuer une mise à l'échelle d'un lit à jet conique, il est important de prédire la vitesse minimale de giclage (U_{ms}) pour des unités de différentes tailles et conditions d'opération.

L'équation de Mathur et Gishler (1955) prédit bien U_{ms} pour un lit à jet classique dans lequel le lit est maintenu relativement haut dans la section cylindrique. Par contre, Kmiec (1983), Markowski et Kaminski (1983) et Choi et Meisen (1992) ont tous démontré que cette corrélation surestime les valeurs de U_{ms} pour un lit à jet conique dans lequel le lit est entièrement confiné dans la section conique.

Les différentes corrélations disponibles dans la littérature prédisent des valeurs ayant jusqu'à 500 % de différence entre elles pour une unité pilote. En utilisant 111 données expérimentales de U_{ms} provenant de la littérature, il a été démontré que la plupart des équations ont un écart type de plus 45 % et sont généralement biaisées. Ces grandes imprécisions peuvent provenir du fait que la forme des différentes corrélations n'est pas tout à fait appropriée. Les paramètres géométriques utilisés dans ces équations sont la hauteur du lit, le diamètre de la section cylindrique, l'angle et le diamètre de l'entrée du cône. Les corrélations utilisant le diamètre de la section cylindrique comme paramètre ne peuvent pas être appliquées à toutes les opérations car ce dernier n'a pas d'effets sur la

structure et l'hydrodynamique du système lorsque le lit est bien confiné dans la section conique. De plus, la plupart des corrélations prédisent que $U_{ms} = 0$ lorsque l'angle du cône est nul. Ceci est contraire au fait que la vitesse minimum de giclage est égale à la vitesse minimum de fluidization (U_{mf}) lorsque l'angle du cône approche zéro ou la hauteur de lit est faible, e.g. $D_b/D_i \rightarrow 1$.

Une nouvelle corrélation semi-empirique dérivée à partir d'une analyse hydrodynamique approximative de l'équation d'Ergun a été développée. Cette équation ne requiert l'ajustement que d'un seul paramètre et prédit les données de la littérature avec un écart type de 30 % sans biais.

De plus, dans un lit à jet classique, le ratio U_{ms}/U_{mf} augmente avec la hauteur du lit et éventuellement le haut du lit devient fluidisé lorsque la hauteur du lit est égale ou supérieure à la hauteur maximum de giclage. Ce travail a permis de démontrer qu'il n'existe pas de hauteur maximum pour une opération stable dans un lit à jet conique, puisque le ratio de U_{ms}/U_{mf} basé sur la surface supérieure du lit diminu lorsque la hauteur du lit augmente. Finalement, cette étude a aussi démontré qu'il existe une hauteur minimum de giclage à partir de laquelle le lit fluidise au lieu de gicler.

3.2 TEXTE DE L'ARTICLE

Minimum Spouting Velocity of Conical Spouted Beds

H.T. Bi, A. Macchi, J. Chaouki and R. Legros*
Department of Chemical Engineering, Ecole Polytechnique de Montreal
P. O. Box 6079, Station A, Montreal, Quebec H3C 3A7

Can. J. Chem. Eng. (accepted)

3.2.1 Abstract

Existing correlations for predicting minimum spouting velocity in conical spouted beds have been found to give poor agreement with available literature data. A new correlation has been developed based on literature data to give much better prediction of the minimum spouting velocity for both small and pilot-scale conical-spouted beds.

Keywords: Minimum spouting, conical spouted beds, scale-up

Author to whom correspondence may be addressed.
E-mail: legros@mailsrv.polymtl.ca

3.2.2 Introduction

Conical spouted beds have been commonly used for drying suspensions, solutions and pasty materials because vigorous solids motion and intimate gas-solids contact are attained (Olazar et al., 1992). When the conical bed is operated at much higher gas velocities than used in conventional spouted beds with static bed height lower than $2D_i$ and $U > 1.5U_{ms}$, bed expansion is so high that a jet spouting regime is reached where internal solids circulation rate is much higher than in conventional spouted beds. It has been demonstrated by Markowski and Kaminski (1983) that the heat and mass transfer rates in a jet spouted bed can be 10 to 15 times higher than those in commercial spray dryers. To properly design and scale up conical spouted beds, one needs to predict the minimum spouting velocity in specific systems having different dimensions and gas and particle properties.

The minimum spouting velocity in conventional spouted beds has been extensively studied and the well-known Mathur and Gishler (1955) correlation has been found to give the most accurate prediction of experimental data in relatively deep beds with $H/D_c \geq 1$ (Mathur and Epstein, 1974). In conical beds where the solids inventory is restrained within the conical region below the cylindrical section, the ratio of H/D_c in most cases is smaller than unity. The hydrodynamics of the conical spouted bed is thus expected to be quite different from the conventional spouted bed (Mathur and Epstein, 1974). Choi and Meisen (1992) and Olazar et al. (1992) found that $U_{ms} \propto H^{1\sim1.3}$ in conical beds, different from $U_{ms} \propto H^{0.5}$ in conventional spouted beds as revealed by the Mathur and Gishler (1955) correlation. Kmiec (1983), Markowski and Kaminski (1983) and Choi and Meisen (1992) showed that the Mathur and Gishler (1955) correlation overestimated their U_{ms} data in conical beds. In relatively shallow spouted beds with $H/D_c = 1$ to 2, Fane and Mitchell (1984) found that the Mathur and Gishler (1955) correlation increasingly underestimated U_{ms} as D_c increases beyond 0.4 m. All of these studies

suggest that the minimum spouting velocity in conical beds is significantly different from that in conventional spouted beds.

The few correlations that have been developed to predict U_{ms} in conical beds are listed in Table 3.1. The geometrical parameters used in these equations include the bed height, H, diameter of the cylindrical section, D_c, inlet diameter, D_i, and the included cone angle, γ. These equations predict a 5-folds range of U_{ms} values for a typical pilot-scale conical bed. Therefore, in this study a thorough comparison of the predictions of these correlations and available literature data is carried out and a new correlation based on the Ergun equation is developed.

3.2.3 Evaluation of existing correlations

A typical conical bed is illustrated in Figure 3.1. The minimum spouting velocity in such a unit with a static bed height, H, smaller than the height of the cone region, H_c, depends on the geometry of the unit defined by H, D_b, D_i and γ, as well as gas and particle properties. Since $D_b = D_i + 2H\cdot\tan(\gamma/2)$, the geometry of the unit can be completely described by three parameters, for example, H, D_i and D_b. The diameter of the cylindrical section of the bed, D_c, should not be used in the correlation for predicting U_{ms} in conical spouted beds, because U_{ms} will remain unchanged with variations in D_c as long as the bed stays entirely in the conical section (see Figure 3.1). In conventional spouted beds where particles occupy both the cone and the cylindrical sections, D_c becomes an important parameter as reflected in the Mathur and Gishler (1955) correlation.

Twelve correlations found in the open literature for the prediction of U_{ms} in conical beds are listed in Table 3.1. It is seen that most equations predict that $(U_i)_{ms} = 0$ in columns whose cone angle γ is zero. This is in contradiction to the fact that $(U_i)_{ms} = U_{mf}$ when $\gamma = 0$, as in a fluidized bed. In Equations (1) to (6), D_c is included as a parameter. These equations may work well for specific units or dimensionally scaled units of similar geometry, but they cannot be used for all systems because D_c may not necessarily be related to the other three parameters. Equations (7) to (12) in Table 3.1 do not include D_c and may be used for all systems, although the accuracy of these six equations needs to be examined.

The minimum spouting velocity in conical beds has also been calculated based on model equations developed from force and momentum balances in the spout region of the bed (Kmiec, 1983; Hadzismajlovic et al., 1986; Legros et al., 1995). Several model parameters, e.g. spouting angle, void fraction in the spout region and friction coefficient between the core and the annulus or the breaking force coefficient, still need to be provided experimentally in order to calculate U_{ms}.

To help evaluate the accuracy of Equations (1) to (12), literature data on U_{ms} in conical beds with a static bed height within the conical section were collected and are listed in Table 3.2. Sixty eight data points are from Kmiec (1983) and 43 data points are from other authors. The ranges of conditions for the data reported here are: $0.088 \le D_c \le 1.10$ m, $0.015 \le D_i \le 0.30$ m, $0.05 \le H \le 0.71$ m, $24 \le \gamma \le 60°$, $0.88 \le d_p \le 6.17$ mm, $845 \le \rho_p \le 2986$ kg/m^3, which cover both bench and pilot scale conical bed units.

Table 3.3 shows the root-mean standard deviation (RMSD) and the bias F_m as proposed by Bolles and Fair (1979) between experimental data in Table 3.2 and values calculated from Equations (1) to (12). It is seen that RMSD from Equations (1) to (12) is generally higher than 0.45 for all data listed in Table 3.2, while the bias F_m, which is close to 1 in a

non-biased system, is generally much away from unity. A better correlation is thus needed in order to give reliable prediction of U_{ms} in conical beds.

3.2.4 A new semi-empirical correlation for U_{ms} in conical beds

The minimum spouting velocity corresponds to the onset of spouting of particles in the conical bed when particles start to be suspended and move upward in the spout region. $(U_i)_{ms}$ is expected to be the same as U_{mf} when the cone angle approaches zero, i.e. $(U_i)_{ms}/U_{mf} = 1$ for $D_b/D_i = 1$. In fluidized beds, the minimum fluidization velocity has been generally derived by assuming that the pressure drop at the onset of minimum fluidization still follows the Ergun equation which can be written as:

$$-dP = (AU + BU^2)dh \tag{13}$$

where,

$$A = 150\frac{(1-\varepsilon)^2}{\varepsilon^3}\frac{\mu_g}{d_p^2} \tag{14}$$

and

$$B = 1.75\frac{(1-\varepsilon)}{\varepsilon^3}\frac{\rho_g}{d_p} \tag{15}$$

At the minimum fluidization point, the drag force between particles and interstitial gas is in equilibrium with the gravity force of the particles. As a result, the Reynolds number at U_{mf} can be expressed as a function of Archimedes number (Grace, 1986),

$$Re_{mf} = \sqrt{C_1^2 + C_2 Ar} - C_1 \tag{16}$$

where C_1 and C_2 are mainly functions of the void fraction at minimum fluidization. Experimentally, C_1 has been found to be around 30 and C_2 ranges from 0.036 to 0.06 (see Grace, 1986).

In a conical bed as shown in Figure 3.1, the force exerted by the fluid in an elemental volume with an elemental height dh of the bed at a distance h from the inlet is:

$$dF = \frac{\pi}{4} D^2 (AU + BU^2) dh \tag{17}$$

Integrating over the entire bed height H gives:

$$F = \frac{\pi}{4} D_i^2 H \left[AU_i + BU_i^2 \left(\frac{D_i}{D_b} \right) \right] \tag{18}$$

The effective weight of the particle bed in the same elemental volume is:

$$dF_p = (1-\varepsilon)(\rho_p - \rho_g) g \frac{\pi}{4} D^2 dh \tag{19}$$

The integration of Equation (19) over the entire bed height H gives:

$$F_p = \frac{\pi}{4} (1-\varepsilon)(\rho_p - \rho_g) g \left[\left(\frac{D_b}{D_i} \right)^2 + \frac{D_b}{D_i} + 1 \right] / 3 \tag{20}$$

By assuming that at minimum fluidization the flow is uniform at each cross section of the bed, the pressure drop follows the Ergun equation and the drag force between particles and interstitial gas is in equilibrium with the gravity force of the particles, i.e. $F = F_p$, one

is able to derive an equation similar to Equation (16) but which allows for the increase in cross-sectional area with height (Venkatesh et al., 1996):

$$(Re_i)_{mf} = [\sqrt{C_1^2 + C_2 Ark_1 k_2} - C_1]/k_1 \qquad (21)$$

with $k_1 = (D_i / D_b)$

$$k_2 = [(D_b / D_i)^2 + (D_b / D_i) + 1]/3$$

$$C_1 = 300(1 - \varepsilon_{mf})/7$$

$$C_2 = \varepsilon_{mf}^3 / 1.75$$

For particles of several millimeters in diameter as commonly used in conical spouted beds, Equation (21) can be further approximated by,

$$(Re_i)_{mf} \cong [C_2 Ark_2 / k_1]^{0.5} \qquad (22)$$

In conical beds the point at which pressure drop over the bed reaches a constant after a maxima is defined as the minimum spouting velocity, instead of minimum fluidization velocity. Therefore, Equation (22) is expected to be applicable to the minimum spouting condition. It has been reported that $(Re_i)_{ms} \propto Ar^{0.5\sim0.59}$ (Olazar et al., 1992) in conical spouted beds. This can also be seen from Figure 3.2 where experimental data are plotted with $(Re_i)_{ms}/Ar^{0.5}$ as a function of H/D_i for different particles in columns having the same cone angle. It is seen that all data obtained in columns with the same cone angle are well correlated by a single line, confirming that the effect of particle properties can be well represented by the ratio $(Re_i)_{ms}/Ar^{0.5}$, in agreement with Equation (22).

Figure 3.3 shows $(Re_i)_{ms}/Ar^{0.5}$ as a function of (D_b/D_i) based on all data listed in Table 3.2. It is seen that $(Re_i)_{ms}/Ar^{0.5}$ increases with increasing (D_b/D_i) and all the data can

be fairly correlated by this parameter. It is also interesting to see that the minimum spouting velocity based on the bed surface, $(U_b)_{ms}$, is lower than U_{mf}, as shown in Figure 3.3. $(Re_b)_{ms}/Ar^{0.5}$ also tends to decrease with increasing (D_b/D_i). This indicates that under the minimum spouting condition the superficial gas velocity in the inlet of the conical bed is higher than the minimum fluidization velocity, and that at the upper bed surface is lower than the minimum fluidization velocity. The latter finding is contradictory to the conventional spouted bed where, as shown by the Mathur and Gishler (1955) correlation, U_{ms}/U_{mf} increases with increasing bed height and eventually the top of the bed becomes fluidized when the bed height is equal to or higher than a maximum spoutable bed height. Also, this finding explains the non-existence of a maximum spoutable bed height in the conical spouted bed because the top of the bed will never be fluidized with increasing bed height.

Figure 3.4 shows comparison of experimental data with Equation (22). It is seen that the data with small (D_b/D_i) are in reasonable agreement with Equation (22) with C_2 = 0.0408, a value commonly used in fluidized beds. However, a value of C_2 = 0.084 is required to give the best fit of experimental data with large (D_b/D_i) values, although the slope of the curve at large (D_b/D_i) values is in good agreement with the slope predicted by Equation (22). The indication is that the voidage at minimum spouting, which affects the value of C_2, is a function of (D_b/D_i). A least-square-fit of all data in Figure 3.4 gives,

$$C_2 = [0.30 - 0.27/(D_b/D_i)^2]^2 \qquad (23)$$

when (D_b/D_i) is smaller than about 1.66, C_2 predicted by Equation (23) is smaller than 0.0408, lower than at minimum fluidization. Therefore, C_2 should be taken as 0.0408 for $(D_b/D_i) < 1.66$.

Combining Equations (22) and (23), one arrives a complete equation for the prediction of $(U_i)_{ms}$ in a conical spouted bed,

$$(Re_i)_{ms} = [0.30 - 0.27/(D_b/D_i)^2]\sqrt{Ar(D_b/D_i)[(D_b/D_i)^2 + (D_b/D_i) + 1]/3} \qquad (24)$$

for $(D_b/D_i) \geq 1.66$, and

$$(Re_i)_{ms} = 0.202\sqrt{Ar(D_b/D_i)[(D_b/D_i)^2 + (D_b/D_i) + 1]/3} \qquad (25)$$

for $(D_b/D_i) < 1.66$. Equations (24) and (25) suggest that there exists a minimum spoutable bed height below which the conical bed is fluidized, instead of spouted. This finding is consistent with the experimental observations of Olazar et al. (1992).

The root-mean standard deviation between experimental data and calculated values from Equations (24) and (25) is 0.23 for Kmiec's (1983) data and 0.31 for all the data in Table 3.2. Equations (24) and (25) are recommended for the estimation of U_{ms} in conical spouted beds.

It should be noted that the use of Equations (24) and (25) is limited to the conical region of spouted beds with conical bases, i.e. $H \leq H_c$, because D_b will be the same as D_c when $H > H_c$. For $H > H_c$ and $H/D_c > 2$, the Mathur and Gishler (1955) correlation could be used to predict U_{ms}. However, caution still needs to be exercised when U_{ms} is to be predicted in a spouted bed operated in the transition region with $H/H_c > 1$ and $H/D_c < 2$.

3.2.5 Conclusion

The minimum fluidization velocity in conical spouted beds is different from that in conventional spouted beds. Since the ratio of U_{ms}/U_{mf} based on the upper surface of the conical spouted bed always increases with increasing bed height, a maximum spoutable bed height does not exist in conical spouted beds. Existing correlations are unable to give an accurate prediction of the minimum spouting velocity in conical spouted beds. A new correlation is thus developed based on the Ergun equation and validated by comparing with experimental data obtained for a wide range of conditions.

3.2.6 Nomenclature

Ar = Archimedes number $[=gd_p^3(\rho_p-\rho_g)\rho_g/\mu_g^2]$

D = diameter of the column at a height of h, m

D_c, D_c' = diameter of the cylindrical section, m

D_i = inlet diameter, m

D_b = diameter at the bed surface, m

d_p = particle diameter, m

F = drag force between gas and particles, N

F_g = gravitational force, N

F_m = the bias of an equation as defined in Table 3

g = gravitational acceleration, m/s^2

H = static bed height, m

h = distance above the distributor, m

H_c = height of the cone section, m

Q_{mf} = volume flow rate at U_{ms}, m^3/s

Re_{mf} = Reynolds number at U_{mf} $(=\rho_g U_{mf} d_p/\mu_g)$

$(Re_i)_{mf}$ = Reynolds number at $(U_i)_{mf}$ $[=\rho_g (U_i)_{mf} d_p/\mu_g]$

Re_{ms} = Reynolds number at U_{ms} $[=\rho_g U_{ms} d_p/\mu_g]$

$(Re_i)_{ms}$ = Reynolds number at $(U_i)_{ms}$ $[=\rho_g (U_i)_{ms} d_p/\mu_g]$

$(Re_b)_{ms}$ = Reynolds number at $(U_b)_{ms}$ $[=\rho_g (U_b)_{ms} d_p/\mu_g]$

Re_t = Reynolds number at U_t $[=\rho_g U_t d_p/\mu_g]$

RMSD = root-mean standard deviation

U_{mf} = minimum fluidization velocity, m/s

U_{ms} = minimum spouting velocity based on D_c, m/s

$(U_i)_{ms}$ = minimum spouting velocity based on D_i, m/s

$(U_b)_{ms}$ = minimum spouting velocity based on D_b, m/s

Greek letters

γ = included cone angle, degree

ε = voidage

ε_{mf} = bed voidage at U_{mf}

ε_{ms} = bed voidage at U_{ms}

μ_g = gas viscosity, Pa.s

ρ_p = particle density, kg/m^3

ρ_g = gas density, kg/m^3

ϕ = sphericity of particles

3.2.7 References

Bolls, W.L. and J.R. Fair, "Performance and design of packed distillation columns," Inst. Chem. Eng. Symp. Ser. **56**, 35-89, 1979.

Choi, M. and A. Meisen, "Hydrodynamics of Shallow, Conical Spouted Beds," Can. J. Chem. Eng. **70**, 916-924 (1992).

Fane, A.G. and R.A. Mitchell, "Minimum Spouting Velocity of Scaled-Up Beds," Can. J. Chem. Eng. **62**, 437-439 (1984).

Goltsiker, A.D., PhD dissertation, Lensovet Technology Institute, Leningrad (1967) (Quoted in Mathur and Epstein, 1974).

Gorshtein, A.E. and I.P. Mukhlenov, "Hydraulic Resistance of a Fluidized Bed in a Cyclone Without a Grate. Critical Gas Rate Corresponding to the Beginning of Jet Formation," Zh. Prikl. Khim. (Leningrad) **37**, 1887-1893 (1964).

Grace, J.R., "Contacting Modes and Behaviour Classification of Gas-Solid and Other Two-Phase Suspensions," Can. J. Chem. Eng. **64**, 353-363 (1986).

He, Y.-L., C.J. Lim and J.R. Grace, "Spouted Bed and Spout-Fluid Bed Behaviour in a Column of Diameter 0.91 m," Can. J. Chem. Eng. **70**, 848-857 (1992).

Kmiec, A., "Expansion of Solid-Gas Spouted Bed," Chem. Eng. J. **13**, 143-147 (1977).

Kmiec, A. "The Minimum Spouting Velocity in Conical Beds," Can. J. Chem. Eng. **61**, 274-280 (1983).

Legros, R., S. Charbonneau and R.C. Mayer, "Prediction of Minimum Spouting Velocities in Liquid-Solids Conical Beds," in "Fluidization VIII", editors C. Laguerie and J.F. Large, Engineering Foundation, New York, 401-408 (1995).

Markowski, A. and W. Kaminski, "Hydrodynamic Characteristics of Jet-Spouted Beds," Can. J. Chem. Eng. **61**, 377-381 (1983).

Mathur, K.B. and P.E. Gishler "A Technique for Contacting Gases with Solid Particles," AIChE J. **1**, 157-164 (1955).

Mathur, K.B. and N. Epstein, "Spouted Beds," Academic Press, New York (1974).

Mukhlenov, I.P. and A.E. Gorshtein, "Investigation of a Spouted Bed," Khim. Prom. **41**(6), 443-446 (1965).

Nikolaev, A.M. and L.G. Golubev, "Basic Hydrodynamic Characteristics of the Spouting Bed," Izv. Vyssh. Ucheb. Zaved. Khim. Khim. Tekhnol. 7, 855-867 (1964).

Olazar, M., M.J. San Jose, A.T. Aguayo, J.M. Arandes and J. Bilbao, "Stable Operation Conditions for Gas-Solid Contact Regimes in Conical Spouted Beds," Ind. Eng. Chem. Res. **31**, 1784-1792 (1992).

Pham, Q.T. "Behaviour of a Conical Spouted-Bed Dryer for Animal Blood," Can. J. Chem. Eng. **61**, 426-434 (1983).

Rocha, S.C.S., O.P. Taranto and G.E. Ayub, "Aerodynamics and Heat Transfer During Coating of Tablets in Two-Dimensional Spouted Bed," Can. J. Chem. Eng. **73**, 308-312 (1995).

Tsvik, M.Z., M.N. Nabiev, N.U. Rizaev, K.V. Merenkov and V.S. Vyzgo, "The Velocity for External Spouting in the Combined Process for Production of Granulated Fertilizer," Uzb. Khim. Zh. **11**(2), 50-59 (1967).

Venkatesh, R.D., J. Chaouki and D. Klvana, "Fluidization of Cryogels in a Conical Column," Powder Technol., in press (1996).

Wan-Fyong, F., P.G. Romankov and N.B. Rashkovskaya, "Research on the Hydrodynamics of the Spouting Bed," Zh. Prikl. Khim. (Leningrad) **42**, 609-617 (1969).

Table 3.1 List of empirical equations for predicting U_{ms} in conical beds.

Author	Correlation	
Nikolaev and Golubev (1964)	$(Re_i)_{ms} = 0.051Ar^{0.59}(H/D_c)^{0.25}(D_i/D_c)^{0.1}$	(1)*
Kmiec (1977)	$Re_{ms} = 0.0176Ar^{0.714}(H/D_c)^{1.535}\gamma^{0.714}\varepsilon_{ms}^{2.21}$	(2)*
Markowski and Kaminski (1983)	$Re_{ms} = 0.028Ar^{0.57}(H/D_i)^{0.48}(D_c/D_i)^{1.27}$	(3)*
Kmiec (1983)	$(Re_i)_{ms}^2[1.75+150(1-\varepsilon_{ms})/(Re_i)_{ms}] = 31.31Ar(H/D_i)^{1.757}(D_i/D_c)^{0.029}(\tan\frac{\gamma}{2})^{2.07}\varepsilon_{ms}^3$	(4)*
Choi and Meisen (1992)	$U_{ms}/\sqrt{2gH} = 0.147(\frac{\rho_p-\rho_g}{\rho_g})^{0.477}(d_p/D_c)^{0.61}(H/D_c)^{0.508}(D_i/D_c)^{0.243}$	(5)*
Rocha et al. (1995)	$Q_{ms} = 5.92x10^{-5}[d_p/(D_c\phi)]^{0.05}(D_i/D_c)^{-2.6}[2gH(\rho_p-\rho_g)/\rho_g](\tan\frac{\gamma}{2})^{0.06}$	(6)*
Gorshtein and Mukhlenov (1964)	$(Re_i)_{ms} = 0.174Ar^{0.5}[1+2\tan(\gamma/2)H/D_i]^{0.25}(\tan\frac{\gamma}{2})^{-1.25}$	(7)
Mukhlenov and Gorshtein (1965)	$(Re_i)_{ms} = 3.32Ar^{0.33}(H/D_i)(\tan\frac{\gamma}{2})^{0.55}$	(8)
Goltsiker (1967)	$(Re_i)_{ms} = 73Ar^{0.14}(H/D_i)^{0.9}(\rho_p/\rho_g)^{0.47}$	(9)
Tsvik et al. (1967)	$(Re_i)_{ms} = 0.4Ar^{0.52}(H/D_i)^{1.24}(\tan\frac{\gamma}{2})^{0.42}$	(10)
Wan-Fyong et al. (1969)	$(Re_i)_{ms} = 1.24Re_t(H/D_i)^{0.82}(\tan\frac{\gamma}{2})^{0.92}$	(11)
Olazar et al. (1992)	$(Re_i)_{ms} = 0.126Ar^{0.5}[1+2\tan(\gamma/2)H/D_i]^{1.68}(\tan\frac{\gamma}{2})^{-0.57}$	(12)

* Equations including D_c as a parameter.

Table 3.2 List of experimental data from the literature.

Source	D_c m	D_i m	γ, degree	d_p mm	ρ_p kg/m^3	Range of H m	Number of data
Kmiec (1983)	0.088	0.015	30	3.32	1293	0.432	1
				0.875	2646	0.06-0.12	2
	0.088	0.015	60	2.16	2986	0.065-0.106	4
				5.48	1496	0.065	1
				3.32	1293	0.065-0.12	3
				2.24	1293	0.065-0.12	3
	0.18	0.035	24	5.48	1496	0.06-0.09	2
				2.24	1293	0.06-0.12	2
	0.18	0.035	53	6.17	2451	0.06	1
				5.48	1496	0.06	1
				3.32	1293	0.06-0.15	4
				2.24	1293	0.09	1
				0.875	2646	0.06-0.12	2
	0.308	0.05	33.8	3.16	2384	0.06-0.30	5
				2.24	2384	0.16-0.20	2
				3.72	2178	0.05-0.165	3
				2.24	845	0.22-0.30	2
	0.308	0.071	34.8	3.16	2384	0.06-0.30	4
				3.72	2178	0.05-0.13	3
	0.308	0.082	33.8	3.16	2384	0.06-0.30	5
	0.90	0.15	33.8	3.16	2384	0.06-0.30	5
				2.14	1074	0.05-0.51	7
				2.24	2384	0.05-0.22	4
Pham (1983)	1.044	0.24	60	4	900	0.34-0.73	4
Markowski and Kaminski (1983)	0.30	0.056	37	4.38	2178	0.072-0.13	3
	0.48	0.20	37	4.09	2178	0.20-0.30	2
	1.10	0.30	37	4.09	2178	0.30-0.40	2
He et al. (1992)	0.91	0.18	60	3.25	1018	0.55	1
Olazar et al. (1992)	0.36	0.04	36	3.0	2420	0.015-0.08	6
	0.36	0.03	28	1.0	2420	0.025-0.195	9
	0.36	0.03	28	8.0	2420	0.025-0.17	6
Choi and Meisen (1992)	0.24	0.025	60	2.3	1045	0.12-0.19	3
	0.45	0.025	60	2.3	1045	0.11-0.35	7

Table 3.3 Root mean standard deviation of correlations in Table 2.1

Equation	RMSD for Kmiec's data	RMSD for all data	Bias, F_m
1	0.91	0.91	0.18
2	ε_{ms} not available	ε_{ms} not available	Not available
3	0.97	0.98	0.41
4	0.51	ε_{ms} not available	Not available
5	0.47	0.45	1.13
6	98.5	98.5	8.33
7	21.4	21.6	1.76
8	0.54	0.56	0.45
9	2.07	2.00	33.1
10	0.53	0.53	1.11
11	1.31	1.36	1.60
12	0.49	0.49	0.50
24 & 25	0.23	0.31	0.99

RMSD: Root-mean-standard-deviation is defined as

$$\text{RMSD} = \sqrt{\frac{1}{n}\sum_{i=1}^{n}\left[(U_{i,ms,cal} - U_{i,ms,exp})/U_{i,ms,exp}\right]^2}$$

F_m: The bias of an equation is defined as

$$F_m = \exp\left(\sum_{i=1}^{n} \ln(U_{ims,exp}/U_{ims,cal})/n\right)$$

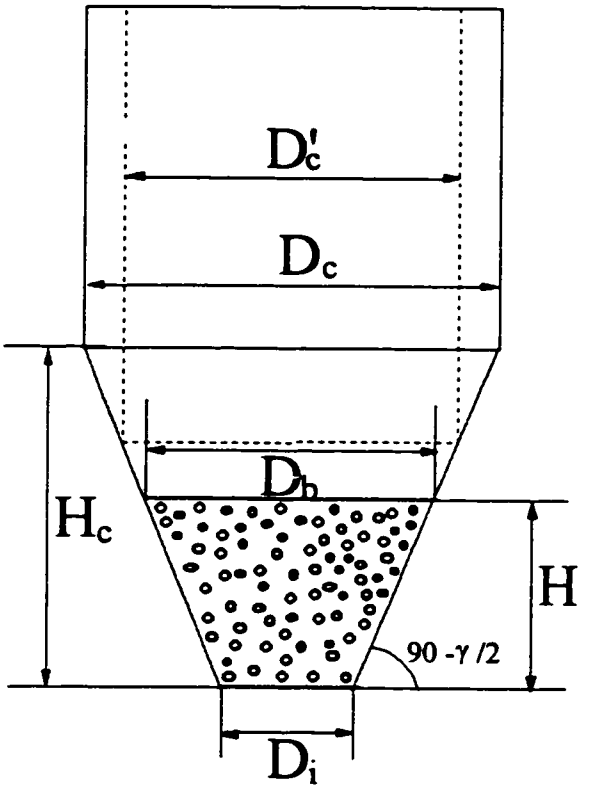

Figure 3.1 Schematic illustration of a conical-spouted bed.

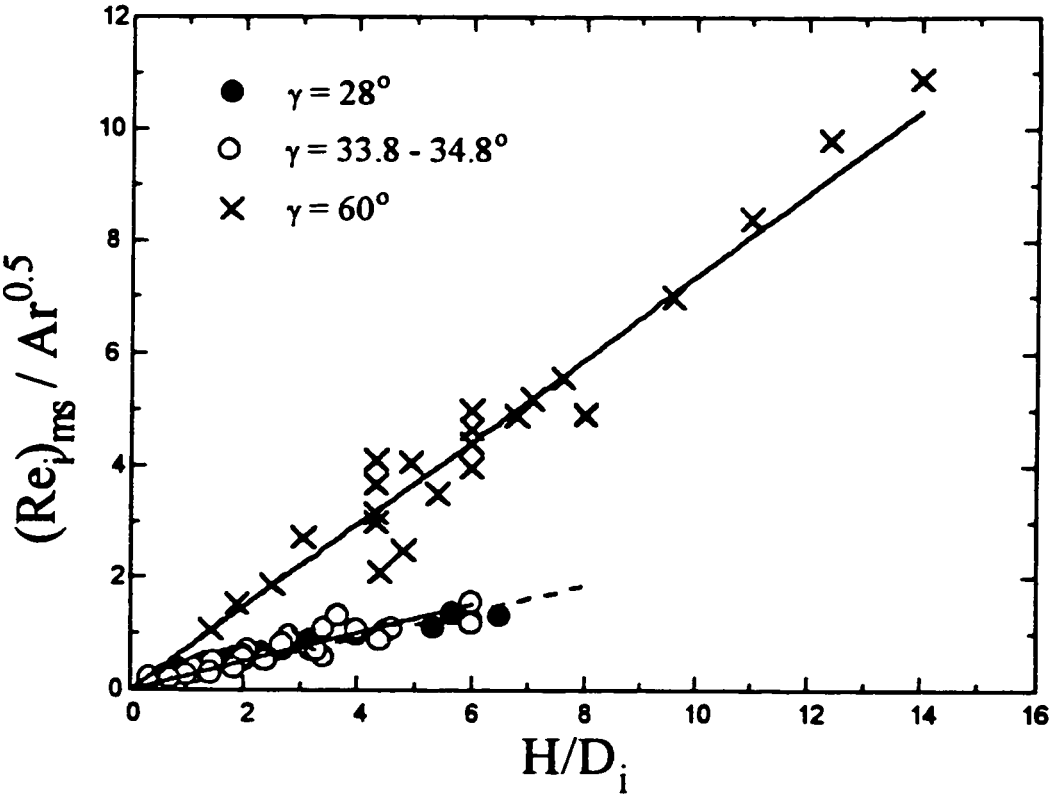

Figure 3.2 Effect of cone angle and static bed height on $(Re_i)_{ms}$ based on data in Table 3.2.

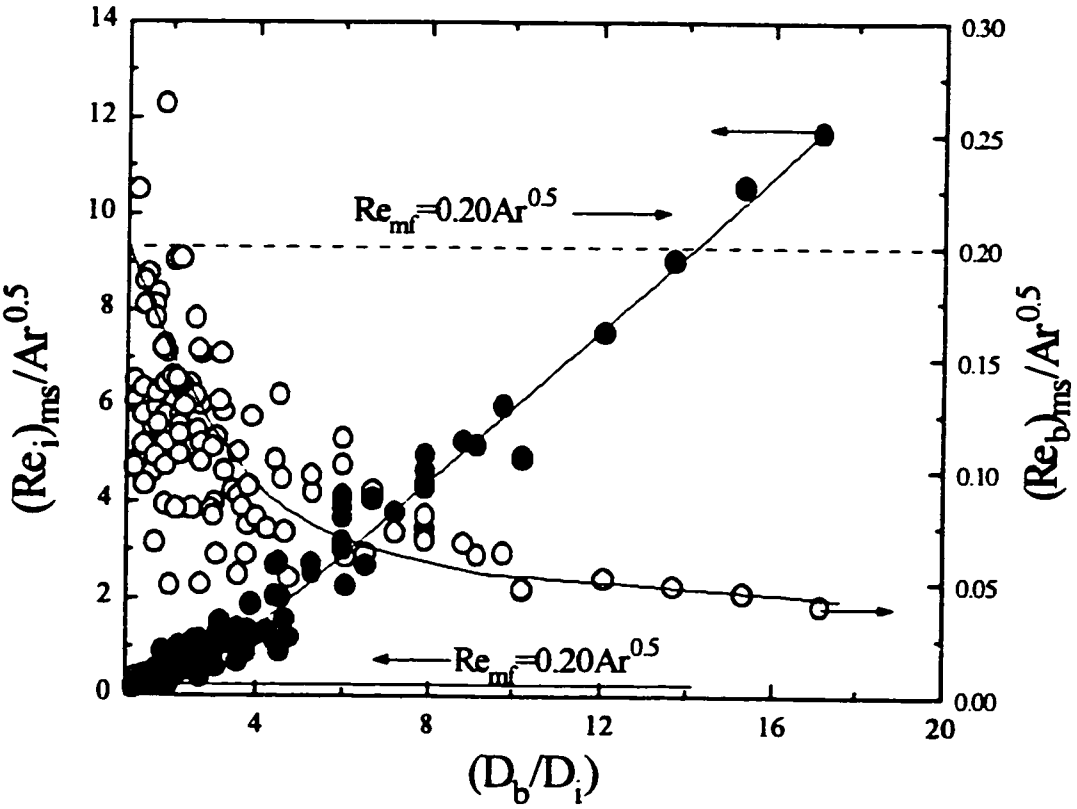

Figure 3.3 $(Re_i)_{ms}/Ar^{0.5}$ and $(Re_b)_{ms}/Ar^{0.5}$ as functions of D_b/D_i based on data listed in Table 3.2.

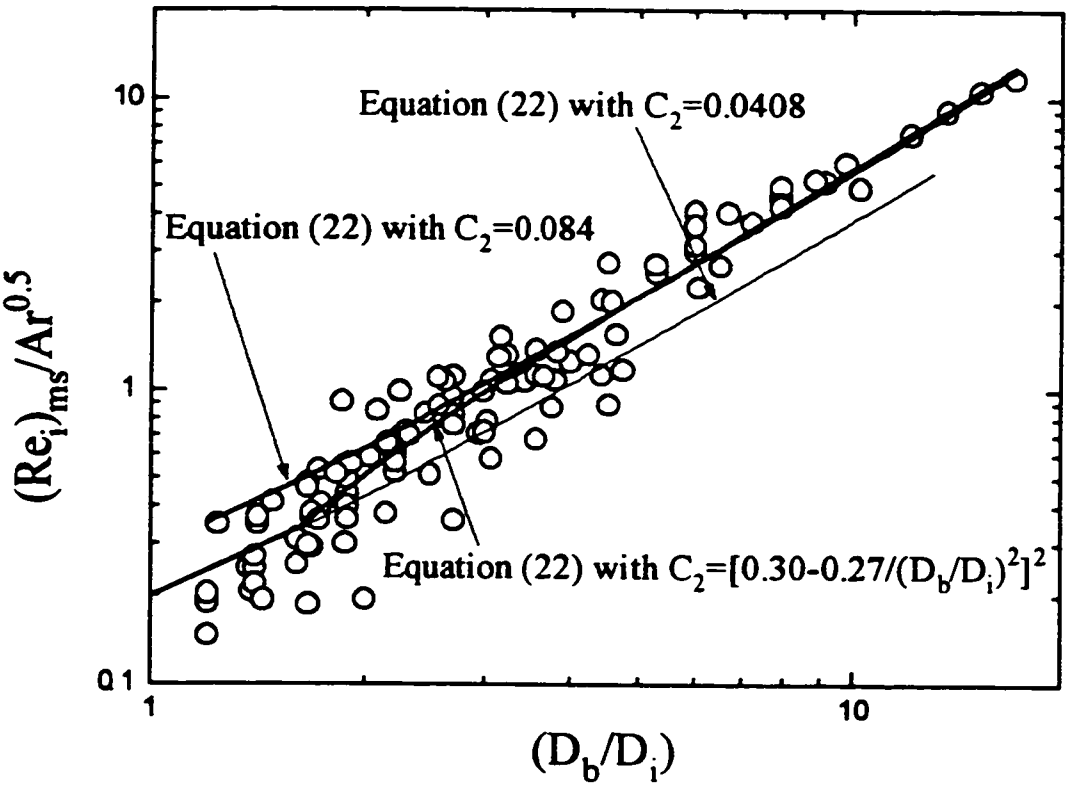

Figure 3.4 Comparison of literature data listed in Table 2.2 with equations (22), (24) and (25).

CONCLUSION ET RECOMMANDATIONS

Ce projet visait à développer un nouveau procédé permettant de sécher différents types de boues dans un lit à jet et de traiter les odeurs et les composés organiques volatiles contenus dans les gaz de séchage dans une chambre de combustion au gaz naturel. L'objectif principal de ce projet était d'améliorer le rendement énergétique du système de séchage au centre Biopro par l'ajout de surfaces d'échange de chaleur indirect dans le lit à jet.

Afin de réaliser cet objectif, il fallait tout d'abord estimer le coefficient de transfert de chaleur indirect (h_s). Puisqu'il n'existe pas de corrélation ou de modèle, une sonde permettant d'évaluer h_s à différentes positions radiales et axiales dans le lit à jet a été développée. Les coefficients de transfert de chaleur obtenus varient entre 95 et 230 $W/m^{2o}C$ et étaient de 0 à 30 % plus faibles dans l'anneau qu'au centre du jet. Les valeurs maximales de h_s se situent à l'axe du jet et diminuent continuellement vers les parois de la colonne. La chute la plus importante se produit à l'interface du jet et de l'anneau. Les profils radiaux de h_s semblent être intimement liés aux profils de vitesse du gaz sans que la contribution des particules au transfert de chaleur soit négligeable. Des corrélations permettant d'estimer les valeurs de h_s dans le jet et l'anneau ont été développées. L'erreur maximale entre les valeurs prédites et les valeurs expérimentales est de 10 %. Cette étude a donc permis de produire un outil pour prédire le coefficient de transfert de chaleur indirect en lit à jet et d'aquérir de l'information sur les mécanismes de transfert de chaleur impliqués.

La construction et l'installation d'un échangeur de chaleur indirect dans le lit à jet au centre Biopro n'a pu être fait au cours de ce projet. Par contre, sachant que l'insertion d'un objet dans le jet rend le giclage instable, surtout à de basses valeurs de U/U_{ms}, et en

tenant compte des résultats de l'étude expérimentale, deux types d'échangeurs de chaleur peuvent être envisagés. Le premier serait un échangeur de type membrane (série de tubes verticaux reliés par des ailettes) qui s'étendrait dans l'anneau sans toucher au jet. Le second serait un échangeur de type serpentin qui contournerait le jet. Cette dernière configuration ressemblerait beaucoup à un lit à jet dans lequel le jet est guidé par un tube de monté.

De plus, en parallèle, j'ai contribué à une étude sur l'hydrodynamique dans un lit à jet conique. Un lit à jet conique ayant des particules inertes comme matériel de lit peut être utilisé pour sécher des boues très liquides. Dans ce type de séchoir, le lit de particules inertes est maintenu dans la région conique et la vitesse superficielle du gaz est choisie à plus de 1,5 fois la vitesse minimale de giclage (U_{ms}). Afin de construire un lit à jet conique, il est nécessaire d'obtenir une valeur précise de U_{ms}.

Les différentes corrélations disponibles dans la littérature prédisent des valeurs de U_{ms} ayant jusqu'à 500 % de différence entre elles pour une unité d'échelle pilote. En utilisant 111 données expérimentales de U_{ms} provenant de la littérature, il a été démontré que la plupart des équations ont un écart type de plus 45 % et sont généralement biaisées. Ces grandes imprécisions peuvent provenir du fait que la forme des différentes corrélations n'est pas tout à fait appropriée. Certaines corrélations utilisent des paramètres géométriques tel que le diamètre de la colonne qui n'a pas d'effet sur la structure du lit pour une enceinte purement conique. De plus, la plupart des corrélations prédisent que $U_{ms} = 0$ lorsque l'angle du cône est nul. Ceci est contraire au fait que la vitesse minimum de giclage est égale à la vitesse minimum de fluidization (U_{mf}) lorsque l'angle du cône approche zéro ou la hauteur de lit est très faible.

Une nouvelle corrélation semi-empirique dérivée à partir d'une analyse hydrodynamique approximative de l'équation d'Ergun a été développée. Cette équation ne requiert

l'ajustement que d'un seul paramètre et prédit les données de la littérature avec un écart type de 30 % sans biais. Cette corrélation, ayant une base théorique, sera dorénavant un excellent outil pour la conception et la mise à l'échelle d'un lit à jet conique. De plus cette étude a démontré qu'il n'y a pas de hauteur maximum de giclage dans un lit à jet conique, mais qu'il existe une hauteur minimale à partir de laquelle le lit devient fluidisé.

RÉFÉRENCES

ACDI (Association des Industries Forestières du Québec), "La gestion des matières résiduelles de l'industrie forestière", pp. 1-31 (Août 1996).

BENKRID, A. and H. S. CARAM, "Solid Flow in the Annular Region of a Spouted Bed", AIChE J. **35**, 1328-1336 (1989).

BOLLS, W.L. and J.R. FAIR, "Performance and design of packed distillation columns," Inst. Chem. Eng. Symp. Ser. **56**, 35-89, 1979.

BOTTERILL, J. S. M., "Fluid Bed Heat Transfer", Chapt. 9 in "Gas Fluidization Technology", D. Geldart, Ed., John Wiley & Sons Ltd., New York (1986), pp. 219-258.

BRIDGEWATER, J., "Spouted beds", Chapt. 6 in "Fluidization", 2nd edition, J. F. Davidson, R. Clift and D. Harrison, Eds., Academic Press, London (1985), pp. 201-224.

CAYER, M., "Disposer des boues industrielles, des solutions économiques et profitables", L'ingénieur, vol. 9, no. 6, p. 11 (1996).

CHOI, M. and A. MEISEN, "Hydrodynamics of Shallow, Conical Spouted Beds," Can. J. Chem. Eng. **70**, 916-924 (1992).

DAY, J. Y., M. H. MORGAN, III and H. LITTMAN, "Measurements of Spout Voidage Distributions, Particle Velocities and Particle Circulation rates in Spouted Beds of Coarse Particles - II. Experimental Verification", Chem. Eng. Sci. **42**, 1461-1470 (1987).

EPSTEIN, N. and K. B. MATHUR, "Heat and Mass Transfer in Spouted Beds - A Review", Can. J. Chem. Eng. **49**, 467-476 (1971).

EPSTEIN, N. and J. R. GRACE, "Spouting of Particulate Solids", Chapt. 11 in "Handbook of Powder Science and Technology", M.E. Fayed and L. Otten, Eds., Van Nostrand Reinhold Co., New York (1984), pp. 507-536.

FANE, A.G. and R.A. MITCHELL, "Minimum Spouting Velocity of Scaled-Up Beds," Can. J. Chem. Eng. **62**, 437-439 (1984).

FREITAS, L. A. P. and J. T. FREIRE, "Heat Transfer in Spouted Beds", Drying Technology **11**, 303-317 (1993).

GOLTSIKER, A.D., PhD dissertation, Lensovet Technology Institute, Leningrad (1967) (Quoted in Mathur and Epstein, 1974).

GORSHTEIN, A.E. and I.P. MUKHLENOV, "Hydraulic Resistance of a Fluidized Bed in a Cyclone Without a Grate. Critical Gas Rate Corresponding to the Beginning of Jet Formation," Zh. Prikl. Khim. (Leningrad) **37**, 1887-1893 (1964).

GRACE, J. R., "Fluidized-Bed Heat Transfer", Chapt. 8.2 in "Handbook of Multiphase Systems", G. Hestroni, Ed., Hemisphere/McGraw Hill (1982), pp. 8-65 - 8-83.

GRACE, J.R., "Contacting Modes and Behaviour Classification of Gas-Solid and Other Two-Phase Suspensions," Can. J. Chem. Eng. **64**, 353-363 (1986).

GRBAVCIC, Z. B., D. V. VUKOVIC, F. K. ZDANSKI and H. LITTMAN, "Fluid Flow Pattern, Minimum Spouting Velocity and Pressure Drop in Spouted Beds", Can. J. Chem. Eng. **54**, 33-42, (1976).

HE, Y. L., C. J. LIM and J. R. GRACE, "Spouted Bed and Spout-Fluid Bed Behaviour in a Column of Diameter 0.91 m", Can. J. Chem. Eng. **70**, 848-857 (1992).

HE, Y. L., C. J. LIM, J. R. GRACE, J. X. ZHU and S.Z. QIN, "Measurements of Voidage Profiles in Spouted Beds", Can. J. Chem. Eng. **72**, 229-234 (1994a).

HE, Y.L., S. Z. QIN, C. J. LIM and J.R. GRACE, "Particle Velocity Profiles and Solid Flow Patterns in Spouted Beds", Can. J. Chem. Eng. **72**, 561-568 (1994b).

KIRK-OTHMER, "Encyclopedia of Chemical Technology", 3rd ed., vol. 8, John Wiley & Sons Ltd., New York (1979), p.124.

KLASSEN, J. and P. E. GISHLER, "Heat Transfer from Column Wall to Bed in Spouted, Fluidized and Packed Systems", Can. J. Chem. Eng. **36**, 12-18 (1958).

KLIMENKO et al., "Heat Transfer Between a Spouting Bed and the Surface of a Spherical Probe", Heat Transfer - Soviet Research **Vol.2 No. 1**, 90-94 Jan. (1970).

KMIEC, A., "Expansion of Solid-Gas Spouted Bed," Chem. Eng. J. **13**, 143-147 (1977).

KMIEC, A., "Hydrodynamics of Flows and Heat Transfer in Spouted Beds", Chem. Eng. J. **19**, 189-200 (1980).

KMIEC, A. "The Minimum Spouting Velocity in Conical Beds," Can. J. Chem. Eng. **61**, 274-280 (1983).

KUNNI, D. and O. LEVENSPIEL, "Fluidization Engineering", 2nd ed., Butterworth-Heinemann, Boston (1991), Chapt. 13, pp. 313-336.

LEGROS, R., S. CHARBONNEAU and R.C. MAYER, "Prediction of Minimum Spouting Velocities in Liquid-Solids Conical Beds," in "Fluidization VIII", editors C. Laguerie and J.F. Large, Engineering Foundation, New York, 401-408 (1995).

LIM, C. J. and J. R. GRACE, "Spouted Bed Hydrodynamics in a 0.91 m Diameter Vessel", Can. J. Chem. Eng. **65**, 366-372 (1987).

MALEK, M. A. and B. C. Y. LU, "Heat Transfer in Spouted Beds", Can. J. Chem. Eng. **42**, 14-20 (1964).

MARKOWSKI, A. and W. KAMINSKI, "Hydrodynamic Characteristics of Jet-Spouted Beds," Can. J. Chem. Eng. **61**, 377-381 (1983).

MATHUR, K.B. and P.E. GISHLER "A Technique for Contacting Gases with Solid Particles," AIChE J. **1**, 157-164 (1955).

MATHUR, K. B. and N. EPSTEIN, "Spouted Beds", Academic Press Inc., New York (1974).

MENVIQ (Ministère de l'Environement du Québec), "État de situation de la valorisation des boues de stations d'épuration des eaux usées municipales au Québec", pp. 1-15 (1991).

MIKLEY, H. S. and D. F. FAIRBANKS, "Mechanism of Heat Transfer to Fluidized Beds", AICheE J. **1**, 374-384 (1955).

MOLERUS, O., A. BURSCHKA and S. DIETZ, "Particle Migration at Solid Surfaces and Heat Transfer in Bubbling Fluidized Beds - II. Prediction of Heat Transfer in Bubbling Fluidized Beds", Chem. Eng. Sci. **50**, 879-885 (1995).

MUKHLENOV, I.P. and A.E. GORSHTEIN, "Investigation of a Spouted Bed," Khim. Prom. **41**(6), 443-446 (1965).

NIKOLAEV, A.M. and L.G. GOLUBEV, "Basic Hydrodynamic Characteristics of the Spouting Bed," Izv. Vyssh. Ucheb. Zaved. Khim. Khim. Tekhnol. **7**, 855-867 (1964).

OLAZAR, M., M.J. SAN JOSE, A.T. AGUAYO, J.M. ARANDES and J. BILBAO, "Stable Operation Conditions for Gas-Solid Contact Regimes in Conical Spouted Beds," Ind. Eng. Chem. Res. **31**, 1784-1792 (1992).

ORR, R., "Researchers strive to deodorize pig manure", The Gazette, Oct. 26 (1996).

PHAM, Q.T. "Behaviour of a Conical Spouted-Bed Dryer for Animal Blood," Can. J. Chem. Eng. **61**, 426-434 (1983).

REAY, D., "Fluidized Bed Drying", Chapt. 10 in "Gas Fluidization Technology", D. Geldart, Ed., John Wiley & Sons Ltd., New York (1986), pp. 259-283.

RIOUX, M., "Séchage des Boues de Procédés d'Usines d'Épuration par Lit à Jet", M.Sc.A mémoire, École Polytechnique de Montréal, Montréal, Canada (1993).

ROCHA, S.C.S., O.P. TARANTO and G.E. AYUB, "Aerodynamics and Heat Transfer During Coating of Tablets in Two-Dimensional Spouted Bed," Can. J. Chem. Eng. **73**, 308-312 (1995).

ROY D., F. LARACHI, R. LEGROS and J. CHAOUKI, "A Study of Solid Behavior in Spouted Beds Using 3-D Particle Tracking", Can. J. Chem. Eng. **72**, 945-952 (1994).

SAXENA, S. C., "Heat Transfer between Immersed Surfaces and Gas-Fluidized Beds", in "Advances in Heat Transfer", vol. 19, J.P. Harnett and T.F. Irvine Jr., Eds., Academic Press Inc., New York (1989), pp. 97-190.

TSVIK, M.Z., M.N. NABIEV, N.U. RIZAEV, K.V. MERENKOV and V.S. VYZGO, "The Velocity for External Spouting in the Combined Process for Production of Granulated Fertilizer," Uzb. Khim. Zh. **11**(2), 50-59 (1967).

UEMAKI, O. and M. KUGO, "Heat Transfer in Spouted Beds", Kagaku Kogaku **31**, 348-353 (1967)

VENKATESH, R.D., J. CHAOUKI and D. KLVANA, "Fluidization of Cryogels in a Conical Column," Powder Technol., in press (1996).

WAN-FYONG, F., P.G. ROMANKOV and N.B. RASHKOVSKAYA, "Research on the Hydrodynamics of the Spouting Bed," Zh. Prikl. Khim. (Leningrad) **42**, 609-617 (1969).

ZABRODSKY S. S. and V. D. MIKHAILIK, "The Heat Exchange of the Spouting Bed with a submerged Heating Surface", Collected papers on "Intensification of Transfer of Heat and Mass in Drying and Thermal Processes", Nauka i Tekhnica BSSR, 130-137 (1967). (Quoted in Mathur and Epstein (1974))

ANNEXE

DÉTAILS EXPÉRIMENTAUX DES ESSAIS DE TRANSFERT DE CHALEUR INDIRECT EN LIT À JET

A.1 MONTAGE EXPÉRIMENTAL

Voici le schéma du montage lit à jet dans lequel les expériences de transfert de chaleur indirect ont été effectuées.

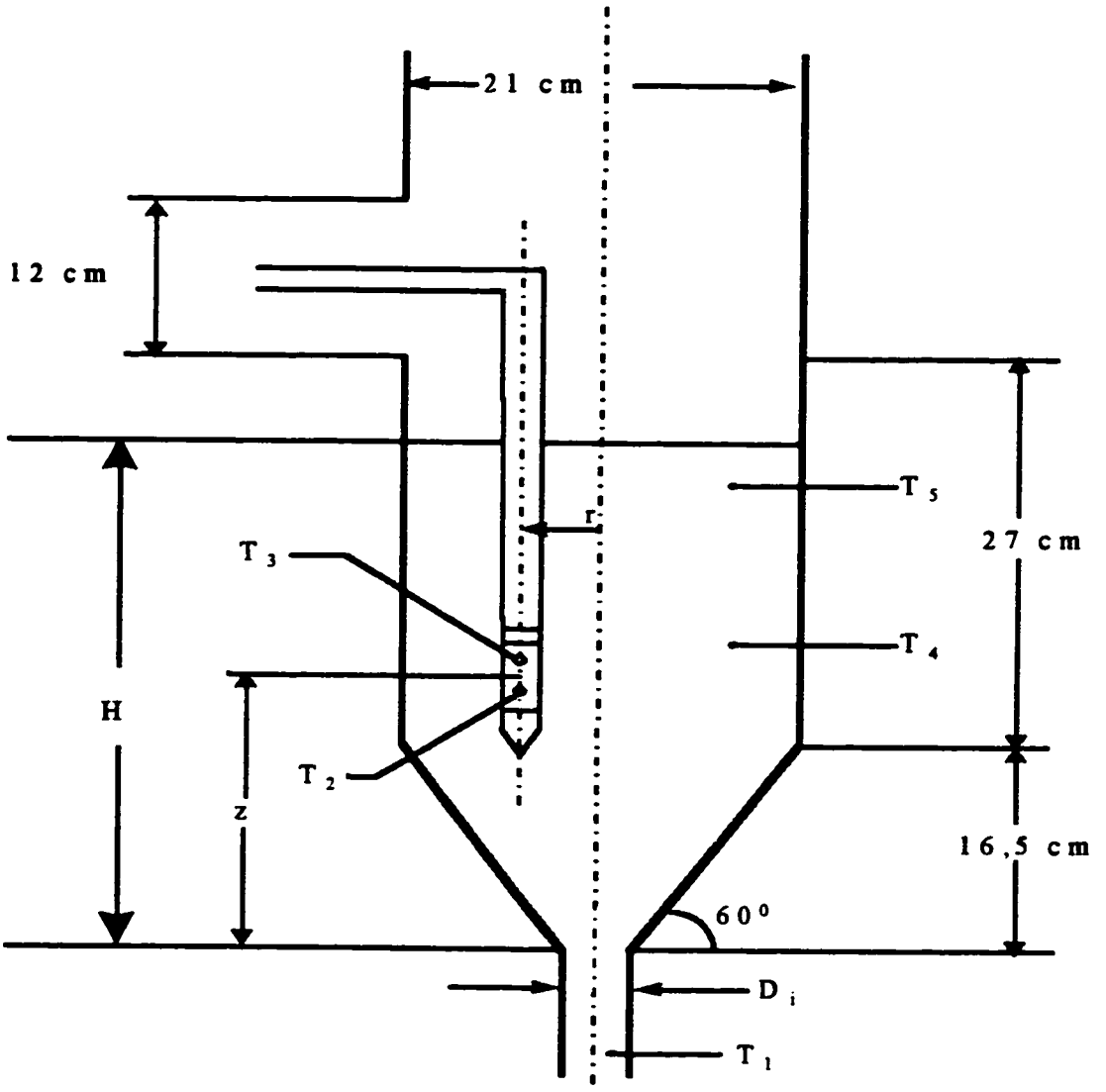

Figure A.1 Schéma du montage expérimental

D_i : Diamètre de l'orifice

H : Hauteur du lit au repos

r : Position radiale de la sonde

T_0 : Température ambiante

T_1 : Température à l'entrée du lit à jet

T_2 : Température à la surface de la sonde

T_3 : Température à la surface de la sonde

T_4 : Température dans le lit

T_5 : Température dans le lit

z : Position axiale de la sonde

A.2 CALCUL DU COEFFICIENT DE TRANSFERT DE CHALEUR INDIRECT

On calcul le coefficient de transfert de chaleur indirect (h_s) à l'aide de l'équation suivante :

$$h_s = \frac{P}{A*(T_s - T_b)}$$

où

- $P\ (watts) = \left(\text{fraction de puissance de chauffe de la cartouche}\right) * \left(\frac{\text{Voltage}}{240\ \text{volts}}\right)^2 * 125$

  Le voltage ne peut être directement lu par le système d'acquisition de données. On utilise donc un interface qui donne un signal calibré en fonction du voltage. Voici l'équation de la courbe de calibration :

$$V\,(volts) = 0.06454 * Lecture + 5.27 \qquad (R^2 = 0.99)$$

- $A = \pi * D_t * L = \pi * 0.0127 * 0.0508 = 0.002027\ m^2$
- $T_s = \frac{(T_2 + T_3)}{2}$
- $T_b = \frac{(T_4 + T_5)}{2}$

A.3 CALCUL DE L'HUMIDITÉ ABSOLUE DE L'AIR SORTANT DU LIT

L'humidité relative de l'air est mesurée à l'aide d'un hygromètre à capacitance. Voici l'équation de la courbe de calibration :

Humidité relative (%) = 0.059*Lecture - 20.96

L'humidité absolue est déduite de la mesure de la température à l'endroit de la sonde par les calculs successifs de la tension de vapeur (P_{sat}) et de la pression partielle (P_{part})de la vapeur d'eau,
sachant que :

$P_{part} = P_{sat} *$(humidité relative)

L'humidité absolue (Y) est alors définie par l'équation suivante :

$$Y\ (\text{kg eau / kg air sec}) = 0.622 * \left(\frac{P_{sat}}{P_{atm} - P_{part}} \right)$$

A.4 EXEMPLE D'UNE EXPÉRIENCE TYPIQUE.

Le programme d'acquisition de données utilisé est "Boues avec contrôle de puissance" et le fichier d'acquisition est "c :\arturo\heat.nch ".

A.4.1 Conditions d'opération

- Particules de Polyéthylène (d_p = 3.1 mm, ρ_p = 943 kg/m^3, c_p = 1855 J/kg°C, ε_b = 0.35)
- Vitesse minimum de giclage (U_{ms}) basée sur le diamètre de la colonne = 0.68 m/s
- Vitesse superficielle du gaz U/U_{ms} = 1.3
- Hauteur du lit au repos : H = 0.27 m
- Position axiale de la sonde : z = 0.21 m
- Diamètre de l'orifice : D_i = 0.019 m
- Positions radiales de la sonde: r/R = (0, 0.118, 0.235, 0.412, 0.588, 0.823)
- Pourcentage de puissance de chauffe de la cartouche : 30 %
  (la cartouche chauffe à sa capacité maximale 0.3 s à chaque seconde)

A.4.2 Données brutes et transformations.

Les pages suivantes présentent les données brutes et les transformations permettant d'obtenir l'humidité de l'air et le graphe du coefficient de transfert de chaleur indirect (h_s) en fonction du temps.

	ch[0]	ch[1]	ch[2]	ch[3]	ch[4]	ch[5]	ch[6]	ch[7]
canaux	0	2	1	3	4	5	6	7
hrs(sec.)	**T0**	**T1**	**T2**	**T3**	**T4**	**T5**	**Voltage**	**humidité de l'air**
	(°C)	**(°C)**	**(°C)**	**(°C)**	**(°C)**	**(°C)**	**Lecture**	**Lecture**
r/R = 0.823								
0	17.1	18.28	23.02	22.31	18.76	18.76	1703	426
10	16.63	18.28	26.35	25.16	18.52	18.76	1701	426
20	16.86	18.28	28.96	28.01	18.52	18.52	1698	426
30	16.63	18.28	31.81	31.09	18.52	18.76	1703	427
40	16.86	18.28	34.42	33.47	18.52	18.76	1700	426
50	16.63	18.05	36.8	35.61	18.52	18.76	1701	427
60	16.63	18.28	38.47	37.75	18.52	18.76	1704	427
70	16.86	18.28	40.61	39.42	18.52	18.76	1701	428
80	16.86	18.28	42.04	40.85	18.52	18.52	1701	428
90	16.63	18.28	43.23	42.27	18.52	18.52	1699	428
100	16.63	18.28	44.9	43.47	18.52	18.76	1702	428
110	16.86	18.28	45.61	44.66	18.52	18.52	1701	428
120	16.86	18.05	46.8	45.37	18.28	18.28	1701	428
130	16.86	18.05	47.52	46.33	18.28	18.52	1702	429
140	16.63	18.28	48.23	47.04	18.28	18.52	1700	429
150	16.86	18.28	48.71	47.99	18.52	18.52	1698	430
160	16.86	18.28	49.9	48.47	18.52	18.76	1668	430
170	16.86	18.28	50.38	48.95	18.52	18.52	1699	430
180	16.86	18.28	50.86	49.66	18.52	18.52	1701	430
190	16.86	18.28	51.1	49.9	18.28	18.52	1699	430
200	16.86	18.28	51.33	50.38	18.28	18.52	1699	431
210	16.63	18.28	51.81	50.86	18.28	18.52	1698	431
220	16.86	18.28	52.29	51.1	18.52	18.76	1697	432
230	17.1	18.52	52.53	51.57	18.76	18.76	1699	432
240	17.1	18.52	52.77	51.81	18.76	19	1698	433
250	16.63	18.28	53	51.57	18.52	18.52	1697	433
260	16.86	18.28	52.77	52.05	18.52	18.52	1700	433
270	16.86	18.28	53	52.05	18.28	18.52	1696	433
280	16.86	18.28	53.24	52.29	18.52	18.52	1694	433
290	16.86	18.28	53.72	52.53	18.52	18.76	1700	434
300	17.1	18.28	53.72	52.77	18.28	18.52	1695	434
310	16.63	18.28	53.96	52.77	18.52	18.76	1697	434
320	16.63	18.28	53.96	52.77	18.28	18.52	1703	434
330	16.86	18.52	54.2	53	18.52	18.52	1705	435
340	16.63	18.28	54.44	53	18.52	18.76	1698	435
350	17.1	18.52	54.44	53.24	18.76	18.76	1699	434
360	17.1	18.52	54.2	53.24	18.52	18.76	1695	432

hrs(sec.)	T0	T1	T2	T3	T4	T5	Voltage	humidité de l'air
	(°C)	(°C)	(°C)	(°C)	(°C)	(°C)	Lecture	Lecture
370	17.1	18.52	54.68	53.48	18.52	18.76	1701	430
380	17.1	18.52	54.68	53.48	18.76	18.76	1696	428
390	17.1	18.52	54.44	53.48	18.52	18.76	1698	426
400	17.1	18.52	54.68	53.48	18.52	18.76	1698	425
410	16.86	18.52	54.68	53.48	18.76	18.76	1703	424
420	16.86	18.52	54.44	53.48	18.76	18.76	1704	423
430	16.86	18.76	54.91	53.72	18.76	18.76	1703	423
440	16.86	18.52	54.68	53.72	18.52	18.76	1704	422
450	16.86	18.52	55.15	53.72	18.52	18.76	1702	421
460	16.86	18.52	54.68	53.48	18.52	18.76	1702	421
470	17.1	18.52	54.91	53.96	18.76	18.76	1705	421
480	17.1	18.52	54.91	53.96	18.52	18.76	1702	420
490	16.86	18.52	54.68	53.96	18.52	18.52	1702	420
500	17.1	18.52	55.39	53.96	18.76	18.76	1705	420
510	16.86	18.52	55.15	54.2	18.76	18.76	1706	420
520	17.1	18.52	54.91	53.96	18.76	18.76	1707	420
530	17.1	18.76	55.39	54.2	18.76	18.76	1704	420
540	16.86	18.52	54.91	54.2	18.76	18.76	1705	421
550	16.63	18.52	55.15	54.2	18.76	18.52	1706	421
560	17.1	18.52	55.15	53.96	18.76	19	1705	421
570	17.1	18.52	55.15	54.44	18.76	19	1704	421
580	16.86	18.52	55.39	54.2	18.76	18.76	1707	422
590	16.86	18.52	55.15	54.2	18.76	18.76	1706	422
600	16.86	18.52	54.44	53.72	18.52	18.52	1703	423
r/R = 0.588								
610	16.86	18.52	54.68	53.72	18.52	18.76	1701	423
620	16.63	18.52	54.44	53.24	18.52	18.76	1704	424
630	16.86	18.52	54.2	53.24	18.52	18.76	1707	424
640	16.86	18.52	53.96	53	18.52	18.76	1706	424
650	17.1	18.76	54.2	53	18.76	18.76	1705	424
660	17.34	18.76	53.72	52.77	18.76	19	1705	425
670	17.1	18.76	53.96	52.77	18.76	19	1703	425
680	17.1	18.76	53.48	52.53	18.76	19	1705	425
690	17.34	18.76	53.48	52.53	18.76	19	1711	426
700	17.1	18.76	53.72	52.05	18.76	19	1709	426
710	17.34	18.76	53.72	52.53	18.76	19.23	1711	426
720	17.1	18.76	53.48	52.53	19	19	1709	426
730	17.1	18.76	53.48	52.29	19	19	1707	427
740	17.34	19	53.48	52.29	19	19.23	1707	427
750	17.1	18.76	53.24	52.05	19	19	1709	427
760	17.1	18.76	53.24	52.05	18.76	19	1706	427

hrs(sec.)	T0	T1	T2	T3	T4	T5	Voltage	humidité de l'air
	(°C)	(°C)	(°C)	(°C)	(°C)	(°C)	Lecture	Lecture
770	17.1	18.76	53	52.05	18.76	19	1705	427
780	17.1	18.76	53	52.05	19	19.23	1708	428
790	17.1	19	53.48	51.81	19	19	1706	428
800	17.1	18.76	53	52.05	19	19	1705	428
810	17.1	18.76	53	52.05	18.76	19	1704	428
820	16.86	18.52	52.53	51.81	18.76	18.76	1708	428
830	17.1	18.76	53	52.05	18.76	19	1708	429
840	17.1	18.76	53	51.81	18.76	19	1708	429
850	17.1	18.76	53	51.81	19	19	1706	429
860	17.1	18.76	53.24	52.05	19	19	1709	429
870	17.1	18.76	53	51.81	19	19	1711	430
880	17.1	19	52.77	52.05	19	19	1704	429
890	17.1	19	53.24	52.05	19	19	1708	430
900	17.1	18.76	53	51.81	18.76	19	1711	430
910	17.1	18.76	53	51.81	19	19	1708	430
920	17.1	18.76	53	52.05	19	19	1708	430
930	17.1	19	53.48	52.05	19.23	19.23	1707	430
940	17.1	18.76	53.24	51.81	19	19	1710	430
950	16.86	18.76	53	52.05	19	19	1708	431
960	17.1	18.76	53	52.05	19	19	1705	431
970	17.1	18.76	53.48	52.05	19	19	1703	431
980	17.1	18.76	53.48	52.05	19	19.23	1705	431
990	17.1	18.76	53	51.81	19	19.23	1701	431
1000	17.1	19	53.24	52.05	19	19	1704	431
1010	16.86	19	53.24	52.05	19	19.23	1705	431
1020	17.1	18.76	53	52.05	19	19.23	1706	432
1030	17.1	18.76	53	51.81	19	19	1706	432
1040	17.1	18.76	53	51.81	18.76	19	1705	432
1050	17.1	18.76	53	52.05	19	19	1701	432
1060	17.1	18.76	52.77	52.05	19	19	1704	432
1070	17.34	19	53.48	52.05	19	19.23	1704	433
1080	17.34	19	53.24	51.81	19	19.23	1703	433
1090	17.1	18.76	53	51.81	19	19	1705	433
1100	16.86	18.76	53	51.81	19	19	1705	433
r/R = 0.412								
1110	16.63	18.76	52.53	51.33	18.76	19	1708	433
1120	16.63	18.76	52.05	51.1	18.76	19	1704	433
1130	17.1	19	52.53	51.1	19	19.23	1705	433
1140	17.1	18.76	52.05	50.86	18.76	19	1705	434
1150	16.86	18.76	51.81	50.62	18.76	19	1699	434
1160	17.1	18.76	51.81	50.62	19	19	1703	434

hrs(sec.)	T0	T1	T2	T3	T4	T5	Voltage	humidité de l'air
	(°C)	(°C)	(°C)	(°C)	(°C)	(°C)	Lecture	Lecture
1170	17.34	19	52.29	50.86	19.23	19	1707	434
1180	16.86	18.76	52.05	50.38	18.76	19	1703	434
1190	16.86	18.76	51.1	50.38	18.76	19	1707	434
1200	16.86	18.52	51.33	50.14	18.76	18.76	1707	433
1210	16.63	18.52	51.57	50.14	18.76	18.76	1704	432
1220	16.86	18.76	51.33	50.14	19	19	1702	430
1230	16.86	18.76	51.1	50.14	19	19	1703	427
1240	16.86	18.52	51.33	49.9	18.76	18.76	1704	426
1250	16.86	18.76	51.33	50.14	18.76	19	1705	425
1260	17.1	19	51.57	50.14	19	19	1704	424
1270	17.1	18.76	51.57	49.9	19	19.23	1708	423
1280	16.86	18.76	51.33	50.14	19	19	1703	422
1290	16.86	18.76	51.1	50.14	19	19	1706	422
1300	17.1	18.76	51.1	49.9	19	19	1704	421
1310	17.1	18.76	51.1	49.9	19	19	1706	421
1320	16.86	18.76	51.33	50.14	18.76	19	1701	420
1330	17.1	19	51.1	49.9	19	19.23	1702	420
1340	17.1	19	51.33	49.9	19	19	1705	420
1350	16.86	18.76	51.1	49.9	18.76	19.23	1705	420
1360	17.1	18.76	51.33	49.9	19	19.23	1705	420
1370	17.1	19	50.86	49.9	19	19	1706	420
1380	16.86	19	51.33	49.9	19	19.23	1704	420
1390	16.86	18.76	50.86	49.9	19	19.23	1706	420
1400	17.1	19	51.1	49.66	19	19.23	1703	421
1410	17.1	18.76	50.86	49.9	19	19.23	1705	421
1420	16.86	18.76	50.86	49.9	19	19.23	1702	421
1430	17.1	19	51.1	49.9	19	19.23	1701	422
1440	16.86	18.76	50.62	49.66	19	19	1702	423
1450	16.63	18.76	50.86	49.66	19	19	1703	423
1460	16.86	18.76	50.86	49.66	19	19	1706	423
1470	17.1	18.76	50.62	49.66	19	19.23	1706	424
1480	17.34	19	51.1	49.9	19	19.23	1703	425
1490	17.1	19	51.1	49.9	19	19.23	1702	425
1500	17.1	19	51.1	49.9	19	19.23	1703	425
1510	16.86	19	51.1	49.9	19	19.23	1700	426
1520	17.1	19	51.1	50.14	19	19.23	1695	426
1530	16.86	19	51.57	50.14	19.23	19.23	1702	426
1540	17.1	19	51.33	50.38	19.23	19.47	1704	426
1550	17.1	19	51.1	49.9	19	19.23	1704	426
1560	17.1	18.76	51.33	50.14	19.23	19.23	1704	427
1570	17.1	19	50.86	50.14	19.23	19.23	1705	427
1580	17.34	19	51.33	50.14	19.23	19.47	1705	428

hrs(sec.)	T0	T1	T2	T3	T4	T5	Voltage	humidité de l'air
	(°C)	(°C)	(°C)	(°C)	(°C)	(°C)	Lecture	Lecture
1590	17.34	19	51.33	50.14	19.23	19.23	1706	428
1600	17.34	19	51.33	50.14	19.23	19.23	1705	428
r/R = 0.235								
1610	17.1	19	50.86	49.9	19	19.23	1701	428
1620	16.63	19	50.14	49.43	19	19.23	1701	428
1630	16.86	18.76	49.9	48.71	19	19	1706	428
1640	17.1	18.76	49.66	48.71	19	19.23	1706	428
1650	16.86	18.76	49.19	48.47	18.76	19	1704	429
1660	16.63	18.76	48.71	47.99	18.76	19	1700	429
1670	17.1	18.76	48.71	47.76	19	19.23	1705	429
1680	17.1	18.76	48.71	47.52	19	19.23	1702	429
1690	17.1	18.76	48.23	47.76	19	19.23	1708	430
1700	17.1	19	48.47	47.52	19.23	19.47	1704	430
1710	17.1	19	48.47	47.28	19.23	19.47	1708	430
1720	17.1	19	48.23	47.04	19	19.23	1703	430
1730	17.1	19	48.23	47.04	19.23	19.23	1704	430
1740	16.86	18.76	47.99	47.04	19	19	1706	430
1750	17.1	19	47.52	47.04	19	19.23	1705	430
1760	16.86	19	47.76	47.04	19	19	1704	430
1770	17.1	19	47.76	46.8	19	19	1708	431
1780	17.1	18.76	47.52	46.8	19	19.23	1707	431
1790	16.86	18.76	47.52	46.8	18.76	19.23	1708	431
1800	17.1	19	47.99	46.8	19	19.23	1707	431
1810	17.1	19	47.99	46.8	19	19.23	1706	431
1820	17.1	19	47.76	46.8	19.23	19.47	1709	432
1830	16.86	19	47.76	46.56	19.23	19.23	1702	432
1840	17.1	18.76	47.76	46.56	19	19.23	1706	432
1850	17.1	19	47.76	47.04	19	19.23	1706	432
1860	17.1	19	47.52	46.8	19	19.23	1705	432
1870	17.1	19	47.76	46.8	19.23	19.23	1704	433
1880	17.1	19	47.76	47.04	19.23	19.23	1708	433
1890	17.1	19	47.76	46.56	19	19	1706	433
1900	17.1	19	47.52	46.8	19	19.23	1707	433
1910	17.34	19	47.99	46.8	19.23	19.23	1702	433
1920	17.34	19	47.52	46.8	19.23	19.23	1700	434
1930	17.1	19.23	47.99	46.8	19.23	19.47	1706	434
1940	17.1	19.23	47.52	47.04	19.23	19.23	1708	434
1950	17.1	19	47.99	47.04	19.23	19.23	1705	434
1960	16.63	19	47.52	46.8	19	19.23	1704	434
1970	16.86	19	47.52	46.8	19	19.23	1706	434
1980	17.1	18.76	47.52	46.56	19	19.23	1706	432

hrs(sec.)	T0	T1	T2	T3	T4	T5	Voltage	humidité de l'air
	(°C)	(°C)	(°C)	(°C)	(°C)	(°C)	Lecture	Lecture
1990	17.1	19	47.76	46.8	19	19.23	1706	430
2000	17.1	19	47.76	46.8	19	19.23	1706	428
2010	17.1	19	47.52	46.8	19	19.23	1706	426
2020	16.86	19	47.76	46.8	19	19.23	1700	425
2030	16.86	19	47.99	46.8	19	19.23	1700	423
2040	16.86	19	47.76	46.8	19.23	19	1704	422
2050	16.86	19	47.76	46.56	19.23	19.47	1707	422
2060	16.86	18.76	47.52	46.56	19	19.23	1705	420
2070	16.86	18.76	47.52	46.56	19	19.23	1706	420
2080	17.1	18.76	47.52	46.56	18.76	19.23	1707	420
2090	17.1	18.76	47.76	46.33	19	19.23	1706	419
2100	16.63	18.76	47.76	46.56	19	19	1705	419
2110	16.63	19	47.99	46.8	19.23	19.23	1705	419
2120	16.63	19	47.52	46.56	19	19.23	1709	419
2130	16.86	19	47.52	46.8	19.23	19.23	1709	419
2140	17.1	19	47.52	46.8	19.23	19.47	1704	419
2150	17.1	19	47.52	46.8	19.23	19.47	1707	419
2160	17.1	19	47.52	46.56	19	19.23	1709	419
2170	17.1	19	47.52	47.04	19.23	19.47	1709	419
2180	17.1	19	47.28	46.56	19	19.23	1705	420
2190	16.86	19	47.52	46.56	19	19.23	1706	420
2200	16.86	19	47.52	46.33	18.76	19.23	1702	420
r/R = 0.118								
2210	16.86	19	47.04	46.56	19	19.23	1706	421
2220	16.86	19	47.28	46.09	19	19.23	1707	421
2230	17.1	19	46.8	46.09	19	19.47	1708	422
2240	17.1	19	46.56	45.85	19.23	19.47	1707	422
2250	17.1	19.23	46.8	46.09	19.23	19.47	1710	423
2260	17.34	19.23	46.56	45.85	19.23	19.47	1705	423
2270	17.1	19	46.56	45.61	19	19.23	1705	423
2280	17.34	19.23	46.33	45.85	19.23	19.47	1708	424
2290	17.1	19	46.33	45.37	19.23	19.23	1710	424
2300	17.1	19	46.33	45.61	19	19.47	1709	424
2310	17.1	19.23	46.33	45.37	19.23	19.47	1708	424
2320	17.1	19	46.33	45.37	19.23	19.47	1708	425
2330	17.1	19	46.09	45.37	19.23	19.47	1709	425
2340	17.34	19.23	46.33	45.37	19.23	19.47	1711	425
2350	17.34	19.23	46.33	45.61	19.23	19.47	1709	425
2360	17.34	19.23	46.09	45.37	19.23	19.47	1704	425
2370	17.1	19	46.33	45.13	19.23	19.23	1710	426
2380	17.1	19	45.85	45.37	19.23	19.47	1709	426

hrs(sec.)	T0	T1	T2	T3	T4	T5	Voltage	humidité de l'air
	(°C)	(°C)	(°C)	(°C)	(°C)	(°C)	Lecture	Lecture
2390	17.1	19	45.85	45.13	19.23	19.23	1709	426
2400	17.34	19.23	46.33	45.37	19.23	19.71	1709	427
2410	17.1	19	46.09	45.13	19.23	19.47	1715	427
2420	17.34	19	46.33	45.13	19.23	19.47	1712	427
2430	17.1	19	46.09	45.37	19.23	19.47	1712	427
2440	17.34	19.23	46.09	45.37	19.23	19.47	1708	427
2450	17.34	19.23	46.09	45.37	19.23	19.47	1714	427
2460	16.86	18.76	45.85	45.13	19	19.23	1713	427
2470	17.1	19	46.09	44.9	19	19.23	1711	427
2480	17.34	19	46.33	45.13	19	19.23	1707	428
2490	17.1	19	46.09	45.13	19	19.47	1715	428
2500	17.1	19	46.09	45.13	19.23	19.47	1715	428
2510	16.86	19	46.09	45.13	19.23	19.47	1715	428
2520	16.86	19	46.09	45.37	19.23	19.47	1714	428
2530	17.1	19	46.09	45.13	19	19.23	1713	428
2540	17.1	19	46.33	45.37	19	19.47	1714	429
2550	17.34	19	46.33	45.37	19	19.47	1708	429
2560	17.34	19	45.85	45.37	19.23	19.23	1714	429
2570	17.1	19	46.33	45.37	19	19.23	1713	429
2580	17.1	19	46.09	45.13	19	19.23	1715	429
2590	17.34	19	46.33	45.37	19.23	19.47	1714	430
2600	17.1	19	45.85	45.61	19	19.47	1713	430
2610	17.1	19.23	46.33	45.61	19.23	19.47	1715	430
2620	16.86	19	46.09	45.37	19	19.23	1715	430
2630	17.34	19.23	46.33	45.37	19.23	19.47	1712	430
2640	17.34	19.23	46.33	45.61	19.23	19.47	1712	431
2650	17.1	19	46.09	45.37	19	19.47	1711	431
2660	17.1	19	46.33	45.13	19.23	19.47	1711	431
2670	17.1	19	46.33	45.37	19	19.47	1708	431
2680	17.1	19	46.33	45.37	19.23	19.47	1711	431
2690	17.1	19	46.33	45.37	19.23	19.47	1713	431
2700	16.86	19	45.85	45.13	19.23	19.23	1715	431
r/R = 0								
2710	16.86	19	45.85	44.9	19.23	19.23	1712	431
2720	16.86	19	45.61	44.9	19	19.23	1711	432
2730	17.1	19	45.61	44.66	19.23	19.47	1709	432
2740	16.86	19.23	45.37	44.9	19.23	19.47	1714	432
2750	16.86	19	45.13	44.42	19	19.23	1711	432
2760	17.1	19	45.13	44.42	19.23	19.23	1713	433
2770	17.1	19	45.13	44.42	19.23	19.23	1712	433
2780	17.34	19	45.13	44.42	19.23	19.47	1714	433

hrs(sec.)	T0	T1	T2	T3	T4	T5	Voltage	humidité de l'air
	(°C)	(°C)	(°C)	(°C)	(°C)	(°C)	Lecture	Lecture
2790	16.86	19	44.9	44.42	19	19.23	1713	433
2800	17.1	19	44.66	44.42	19	19.23	1709	433
2810	17.1	19	44.66	44.18	19	19.23	1706	433
2820	16.63	18.76	44.42	44.18	18.76	19	1715	433
2830	16.86	19	45.13	44.18	19.23	19.23	1714	434
2840	16.86	19	45.13	44.42	19.23	19.23	1716	433
2850	17.1	19	44.9	44.42	19	19.23	1711	432
2860	17.1	19	45.13	44.42	19	19.23	1709	430
2870	16.86	19	44.9	44.18	19	19.23	1713	427
2880	17.34	19	45.13	44.18	19.23	19.23	1711	426
2890	17.1	19.23	44.9	44.18	19.23	19.47	1709	424
2900	17.34	19.23	45.13	44.42	19.23	19.23	1708	424
2910	17.1	19.23	45.13	44.18	19.47	19.47	1707	422
2920	17.1	19.23	45.13	44.18	19.23	19.23	1707	422
2930	17.1	19	44.66	43.94	19.23	19.23	1709	421
2940	16.86	19	44.66	43.94	19	19.23	1708	420
2950	17.1	19.23	44.66	43.94	19.23	19.23	1704	420
2960	17.34	19.23	44.9	43.94	19.23	19.23	1709	420
2970	17.34	19.23	44.9	44.18	19.47	19.47	1706	420
2980	17.34	19.23	44.9	44.18	19.47	19.47	1704	419
2990	17.34	19.23	44.66	43.94	19.23	19.23	1703	419
3000	17.1	19	44.18	43.7	19	19.23	1707	419
3010	17.1	19	44.66	43.47	19	19	1703	419
3020	17.34	19	44.18	43.47	19	19.23	1703	419
3030	17.1	19	44.42	43.7	19.23	19.23	1707	420
3040	17.1	19	44.42	43.7	19	19.23	1708	420
3050	17.1	19	44.18	43.7	19.23	19.23	1705	420
3060	17.1	19	44.42	43.47	19	19.23	1702	420
3070	17.1	19	44.18	43.7	19.23	19.23	1705	421
3080	17.1	19	43.94	43.7	19.23	19.47	1708	422
3090	16.63	19.23	44.18	43.47	19.23	19.23	1706	422
3100	16.63	19	43.94	43.47	19.23	19.23	1709	422
3110	16.86	19	44.18	43.47	19	19.23	1715	423
3120	16.63	18.76	44.18	43.47	19	19.23	1710	423
3130	16.86	19	44.18	43.47	19.23	19.23	1710	423
3140	17.1	19	44.18	43.47	19	19.23	1709	424
3150	17.34	19.23	44.66	43.47	19.23	19.23	1705	424
3160	17.1	19	43.94	43.47	19	19	1708	424
3170	17.1	19	43.94	43.47	19.23	19.23	1705	425
3180	16.86	19	43.94	43.47	19	19.23	1709	425
3190	17.1	19	44.18	43.47	19	19.23	1702	425
3200	17.1	19	44.42	43.7	19.23	19.23	1703	425

Voltage (volts)	Hum. rel. (%)	P sat. (kPa)	Hum. abs. (kg eau/kg air sec)	Puissance (watts)	h moyen (W/m2°C)
r/R = 0.823					
115.18162	4.174	2.163332895	0.0005548	8.63724322	1091.189962
115.05254	4.174	2.163332895	0.0005548	8.617895157	587.6367148
114.85892	4.174	2.131104361	0.000546528	8.588913739	425.2136419
115.18162	4.233	2.163332895	0.00056265	8.63724322	329.5511835
114.988	4.174	2.163332895	0.0005548	8.60822926	275.3161886
115.05254	4.233	2.163332895	0.00056265	8.617895157	240.4043897
115.24616	4.233	2.163332895	0.00056265	8.646925387	217.757703
115.05254	4.292	2.163332895	0.000570499	8.617895157	197.7925858
115.05254	4.292	2.131104361	0.000561992	8.617895157	185.4548149
114.92346	4.292	2.131104361	0.000561992	8.598568788	175.0729328
115.11708	4.292	2.163332895	0.000570499	8.627566476	165.8415305
115.05254	4.292	2.131104361	0.000561992	8.617895157	159.7426876
115.05254	4.292	2.09930403	0.000553599	8.617895157	152.9060108
115.11708	4.351	2.131104361	0.000569725	8.627566476	148.5886849
114.988	4.351	2.131104361	0.000569725	8.60822926	144.6698368
114.85892	4.41	2.131104361	0.000577458	8.588913739	142.0467295
112.92272	4.41	2.163332895	0.000586199	8.301784305	133.5594825
114.92346	4.41	2.131104361	0.000577458	8.598568788	136.2021885
115.05254	4.41	2.131104361	0.000577458	8.617895157	133.9493268
114.92346	4.41	2.131104361	0.000577458	8.598568788	131.6578883
114.92346	4.469	2.131104361	0.00058519	8.598568788	130.2230902
114.85892	4.469	2.131104361	0.00058519	8.588913739	128.1879879
114.79438	4.528	2.163332895	0.000601899	8.579264114	127.5808107
114.92346	4.528	2.163332895	0.000601899	8.598568788	127.4261689
114.85892	4.587	2.195994635	0.000618965	8.588913739	126.3720233
114.79438	4.587	2.131104361	0.000600657	8.579264114	125.3515
114.988	4.587	2.131104361	0.000600657	8.60822926	125.3108014
114.72984	4.587	2.131104361	0.000600657	8.569619913	123.4555563
114.60076	4.587	2.131104361	0.000600657	8.550347782	123.1779184
114.988	4.646	2.163332895	0.0006176	8.60822926	122.7216604
114.6653	4.646	2.131104361	0.00060839	8.559981135	120.7773583
114.79438	4.646	2.163332895	0.0006176	8.579264114	121.466305
115.18162	4.646	2.131104361	0.00060839	8.63724322	121.4506713
115.3107	4.705	2.131104361	0.000616124	8.656612978	121.7403842
114.85892	4.705	2.163332895	0.000625451	8.588913739	120.3765324
114.92346	4.646	2.163332895	0.0006176	8.598568788	120.9240924
114.6653	4.528	2.163332895	0.000601899	8.559981135	119.9710322
115.05254	4.41	2.163332895	0.000586199	8.617895157	119.5599446
114.72984	4.292	2.163332895	0.000570499	8.569619913	119.6980614

Voltage (volts)	Hum. rel. (%)	P sat. (kPa)	Hum. abs. (kg eau/kg air sec)	Puissance (watts)	h moyen (W/m2°C)
114.85892	4.174	2.163332895	0.0005548	8.588913739	119.5613415
114.85892	4.115	2.163332895	0.000546951	8.588913739	119.1578724
115.18162	4.056	2.163332895	0.000539102	8.63724322	120.6426048
115.24616	3.997	2.163332895	0.000531254	8.646925387	121.1895853
115.18162	3.997	2.163332895	0.000531254	8.63724322	119.8452202
115.24616	3.938	2.163332895	0.000523405	8.646925387	119.5592321
115.11708	3.879	2.163332895	0.000515557	8.627566476	118.5110088
115.11708	3.879	2.163332895	0.000515557	8.627566476	119.6941192
115.3107	3.879	2.163332895	0.000515557	8.656612978	119.7099559
115.11708	3.82	2.163332895	0.000507709	8.627566476	118.5110088
115.11708	3.82	2.131104361	0.000500139	8.627566476	118.8917005
115.3107	3.82	2.163332895	0.000507709	8.656612978	118.9100008
115.37524	3.82	2.163332895	0.000507709	8.666305993	119.0431471
115.43978	3.82	2.163332895	0.000507709	8.676004431	119.9781151
115.24616	3.82	2.163332895	0.000507709	8.646925387	118.3813904
115.3107	3.879	2.163332895	0.000515557	8.656612978	119.3086375
115.37524	3.879	2.131104361	0.00050787	8.666305993	119.0431471
115.3107	3.879	2.195994635	0.000523347	8.656612978	119.3086375
115.24616	3.879	2.195994635	0.000523347	8.646925387	118.3813904
115.43978	3.938	2.163332895	0.000523405	8.676004431	118.7794993
115.37524	3.938	2.163332895	0.000523405	8.666305993	119.0431471
115.18162	3.997	2.131104361	0.000523333	8.63724322	119.828369
r/R = 0.588					
115.05254	3.997	2.163332895	0.000531254	8.617895157	119.1578372
115.24616	4.056	2.163332895	0.000539102	8.646925387	120.7778427
115.43978	4.056	2.163332895	0.000539102	8.676004431	121.5971379
115.37524	4.056	2.163332895	0.000539102	8.666305993	122.2950409
115.3107	4.056	2.163332895	0.000539102	8.656612978	122.5790091
115.3107	4.115	2.195994635	0.000555217	8.656612978	123.840878
115.18162	4.115	2.195994635	0.000555217	8.63724322	123.1352927
115.3107	4.115	2.195994635	0.000555217	8.656612978	124.7087948
115.69794	4.174	2.195994635	0.000563184	8.714852422	125.5478032
115.56886	4.174	2.195994635	0.000563184	8.695417579	125.7083234
115.69794	4.174	2.22770665	0.000571325	8.714852422	125.1093997
115.56886	4.174	2.195994635	0.000563184	8.695417579	126.1519346
115.43978	4.233	2.195994635	0.000571152	8.676004431	126.3160471
115.43978	4.233	2.22770665	0.000579408	8.676004431	126.3160471
115.56886	4.233	2.195994635	0.000571152	8.695417579	127.5017547
115.37524	4.233	2.195994635	0.000571152	8.666305993	126.1748452
115.3107	4.233	2.195994635	0.000571152	8.656612978	126.4816431
115.50432	4.292	2.22770665	0.000587491	8.685708293	127.815259

Voltage (volts)	Hum. rel. (%)	P sat. (kPa)	Hum. abs. (kg eau/kg air sec)	Puissance (watts)	h moyen (W/m2°C)
115.37524	4.292	2.195994635	0.00057912	8.666305993	127.0748887
115.3107	4.292	2.195994635	0.00057912	8.656612978	127.3871045
115.24616	4.292	2.195994635	0.00057912	8.646925387	126.3400978
115.50432	4.292	2.163332895	0.000570499	8.685708293	128.2552098
115.50432	4.351	2.195994635	0.000587089	8.685708293	126.9067543
115.50432	4.351	2.195994635	0.000587089	8.685708293	127.3593865
115.37524	4.351	2.195994635	0.000587089	8.666305993	127.987865
115.56886	4.351	2.195994635	0.000587089	8.695417579	127.5017547
115.69794	4.41	2.195994635	0.000595057	8.714852422	128.7048202
115.24616	4.351	2.195994635	0.000587089	8.646925387	127.6825323
115.50432	4.41	2.195994635	0.000595057	8.685708293	127.3593865
115.69794	4.41	2.195994635	0.000595057	8.714852422	127.7867297
115.50432	4.41	2.195994635	0.000595057	8.685708293	128.2744068
115.50432	4.41	2.195994635	0.000595057	8.685708293	127.815259
115.43978	4.41	2.22770665	0.000603659	8.676004431	127.6343896
115.6334	4.41	2.195994635	0.000595057	8.705132289	128.1010944
115.50432	4.469	2.195994635	0.000603026	8.685708293	127.815259
115.3107	4.469	2.195994635	0.000603026	8.656612978	127.3871045
115.18162	4.469	2.195994635	0.000603026	8.63724322	126.1986318
115.3107	4.469	2.22770665	0.000611743	8.656612978	126.4816431
115.05254	4.469	2.22770665	0.000611743	8.617895157	127.2729122
115.24616	4.469	2.195994635	0.000603026	8.646925387	126.790709
115.3107	4.469	2.22770665	0.000611743	8.656612978	126.932759
115.37524	4.528	2.22770665	0.000619827	8.666305993	127.5297428
115.37524	4.528	2.195994635	0.000610995	8.666305993	127.987865
115.3107	4.528	2.195994635	0.000610995	8.656612978	126.932759
115.05254	4.528	2.195994635	0.000610995	8.617895157	126.8173492
115.24616	4.528	2.195994635	0.000610995	8.646925387	127.6825323
115.24616	4.587	2.22770665	0.000627912	8.646925387	126.3400978
115.18162	4.587	2.22770665	0.000627912	8.63724322	127.1020672
115.3107	4.587	2.195994635	0.000618965	8.656612978	127.8447142
115.3107	4.587	2.195994635	0.000618965	8.656612978	127.8447142
r/R = 0.412					
115.50432	4.587	2.195994635	0.000618965	8.685708293	129.1831944
115.24616	4.587	2.195994635	0.000618965	8.646925387	129.9976658
115.3107	4.587	2.22770665	0.000627912	8.656612978	130.1433088
115.3107	4.646	2.195994635	0.000626934	8.656612978	130.620972
114.92346	4.646	2.195994635	0.000626934	8.598568788	130.7045806
115.18162	4.646	2.195994635	0.000626934	8.63724322	132.2705821
115.43978	4.646	2.195994635	0.000626934	8.676004431	132.3301671
115.18162	4.646	2.195994635	0.000626934	8.63724322	131.2924604

Voltage (volts)	Hum. rel. (%)	P sat. (kPa)	Hum. abs. (kg eau/kg air sec)	Puissance (watts)	h moyen (W/m2°C)
115.43978	4.646	2.195994635	0.000626934	8.676004431	133.8405021
115.43978	4.587	2.163332895	0.000609749	8.676004431	133.861431
115.24616	4.528	2.163332895	0.000601899	8.646925387	132.9139555
115.11708	4.41	2.195994635	0.000595057	8.627566476	134.1207777
115.18162	4.233	2.195994635	0.000571152	8.63724322	134.7595447
115.24616	4.174	2.163332895	0.0005548	8.646925387	133.9153478
115.3107	4.115	2.195994635	0.000555217	8.656612978	133.5622417
115.24616	4.056	2.195994635	0.000547249	8.646925387	133.9153478
115.50432	3.997	2.22770665	0.000547076	8.685708293	135.0246276
115.18162	3.938	2.195994635	0.000531314	8.63724322	134.2712085
115.37524	3.938	2.195994635	0.000531314	8.666305993	135.2129864
115.24616	3.879	2.195994635	0.000523347	8.646925387	135.4245525
115.37524	3.879	2.195994635	0.000523347	8.666305993	135.7280835
115.05254	3.82	2.195994635	0.000515381	8.617895157	132.9648673
115.11708	3.82	2.22770665	0.000522829	8.627566476	135.1213612
115.3107	3.82	2.195994635	0.000515381	8.656612978	135.0831149
115.3107	3.82	2.22770665	0.000522829	8.656612978	134.5511241
115.3107	3.82	2.22770665	0.000522829	8.656612978	135.0831149
115.37524	3.82	2.195994635	0.000515381	8.666305993	136.2471201
115.24616	3.82	2.22770665	0.000522829	8.646925387	134.9319438
115.37524	3.82	2.22770665	0.000522829	8.666305993	136.2471201
115.18162	3.879	2.22770665	0.000530911	8.63724322	135.7902104
115.3107	3.879	2.22770665	0.000530911	8.656612978	136.0947316
115.11708	3.879	2.22770665	0.000530911	8.627566476	135.6380777
115.05254	3.938	2.22770665	0.000538994	8.617895157	134.9698931
115.11708	3.997	2.195994635	0.000539282	8.627566476	136.6834579
115.18162	3.997	2.195994635	0.000539282	8.63724322	136.311478
115.37524	3.997	2.195994635	0.000539282	8.666305993	136.7701417
115.37524	4.056	2.22770665	0.000555159	8.666305993	137.2971943
115.18162	4.115	2.22770665	0.000563242	8.63724322	135.2729144
115.11708	4.115	2.22770665	0.000563242	8.627566476	135.1213612
115.18162	4.115	2.22770665	0.000563242	8.63724322	135.2729144
114.988	4.174	2.22770665	0.000571325	8.60822926	134.8185098
114.6653	4.174	2.22770665	0.000571325	8.559981135	133.5540902
115.11708	4.174	2.22770665	0.000571325	8.627566476	134.5872847
115.24616	4.174	2.261231432	0.000579931	8.646925387	134.8892776
115.24616	4.174	2.22770665	0.000571325	8.646925387	135.4245525
115.24616	4.233	2.22770665	0.000579408	8.646925387	135.4030599
115.3107	4.233	2.22770665	0.000579408	8.656612978	136.5734787
115.3107	4.292	2.261231432	0.000596341	8.656612978	135.5547589
115.37524	4.292	2.22770665	0.000587491	8.666305993	135.7065427
115.3107	4.292	2.22770665	0.000587491	8.656612978	135.5547589

Voltage (volts)	Hum. rel. (%)	P sat. (kPa)	Hum. abs. (kg eau/kg air sec)	Puissance (watts)	h moyen (W/m2°C)
r/R = 0.235					
115.05254	4.292	2.22770665	0.000587491	8.617895157	135.4860303
115.05254	4.292	2.22770665	0.000587491	8.617895157	138.1046494
115.37524	4.292	2.195994635	0.00057912	8.666305993	141.0801725
115.37524	4.292	2.22770665	0.000587491	8.666305993	141.6410346
115.24616	4.351	2.195994635	0.000587089	8.646925387	141.8647623
114.988	4.351	2.195994635	0.000587089	8.60822926	143.5208874
115.3107	4.351	2.22770665	0.000595575	8.656612978	146.0801326
115.11708	4.351	2.22770665	0.000595575	8.627566476	146.1900354
115.50432	4.41	2.22770665	0.000603659	8.685708293	147.7843269
115.24616	4.41	2.261231432	0.000612752	8.646925387	148.300831
115.50432	4.41	2.261231432	0.000612752	8.685708293	149.5900352
115.18162	4.41	2.22770665	0.000603659	8.63724322	148.8072919
115.24616	4.41	2.22770665	0.000603659	8.646925387	150.1803697
115.37524	4.41	2.195994635	0.000595057	8.666305993	149.9363363
115.3107	4.41	2.22770665	0.000603659	8.656612978	151.0131781
115.24616	4.41	2.195994635	0.000595057	8.646925387	150.20681
115.50432	4.469	2.195994635	0.000603026	8.685708293	151.5207411
115.43978	4.469	2.22770665	0.000611743	8.676004431	151.9964224
115.50432	4.469	2.22770665	0.000611743	8.685708293	150.8805126
115.43978	4.469	2.22770665	0.000611743	8.676004431	150.7384841
115.37524	4.469	2.22770665	0.000611743	8.666305993	150.5699816
115.56886	4.528	2.261231432	0.000629165	8.695417579	152.9339229
115.11708	4.528	2.22770665	0.000619827	8.627566476	152.3925127
115.37524	4.528	2.22770665	0.000619827	8.666305993	151.8265138
115.37524	4.528	2.22770665	0.000619827	8.666305993	150.5434729
115.3107	4.528	2.22770665	0.000619827	8.656612978	151.6567002
115.24616	4.587	2.22770665	0.000627912	8.646925387	152.0810482
115.50432	4.587	2.22770665	0.000627912	8.685708293	152.1124089
115.37524	4.587	2.195994635	0.000618965	8.666305993	151.8265138
115.43978	4.587	2.22770665	0.000627912	8.676004431	151.9964224
115.11708	4.587	2.22770665	0.000627912	8.627566476	151.120997
114.988	4.646	2.22770665	0.000635997	8.60822926	152.0509509
115.37524	4.646	2.261231432	0.000645578	8.666305993	151.7995608
115.50432	4.646	2.22770665	0.000635997	8.685708293	152.7631572
115.3107	4.646	2.22770665	0.000635997	8.656612978	150.9864832
115.24616	4.646	2.22770665	0.000635997	8.646925387	151.4869816
115.37524	4.646	2.22770665	0.000635997	8.666305993	151.8265138
115.37524	4.528	2.22770665	0.000619827	8.666305993	152.4762706
115.37524	4.41	2.22770665	0.000603659	8.666305993	151.1822712
115.37524	4.292	2.22770665	0.000587491	8.666305993	151.1822712
115.37524	4.174	2.22770665	0.000571325	8.666305993	151.8265138

Voltage (volts)	Hum. rel. (%)	P sat. (kPa)	Hum. abs. (kg eau/kg air sec)	Puissance (watts)	h moyen (W/m2°C)
114.988	4.115	2.22770665	0.000563242	8.60822926	150.1691322
114.988	3.997	2.22770665	0.000547076	8.60822926	149.5609459
115.24616	3.938	2.195994635	0.000531314	8.646925387	152.0810482
115.43978	3.938	2.261231432	0.000547112	8.676004431	153.2480937
115.3107	3.82	2.22770665	0.000522829	8.656612978	152.3057303
115.37524	3.82	2.22770665	0.000522829	8.666305993	152.4762706
115.43978	3.82	2.22770665	0.000522829	8.676004431	151.3514588
115.37524	3.761	2.22770665	0.000514748	8.666305993	152.4490864
115.3107	3.761	2.195994635	0.000507414	8.656612978	151.6567002
115.3107	3.761	2.22770665	0.000514748	8.656612978	151.6297773
115.56886	3.761	2.22770665	0.000514748	8.695417579	152.9884642
115.56886	3.761	2.22770665	0.000514748	8.695417579	153.5909966
115.24616	3.761	2.261231432	0.000522501	8.646925387	152.7344577
115.43978	3.761	2.261231432	0.000522501	8.676004431	153.2480937
115.56886	3.761	2.22770665	0.000514748	8.695417579	152.9884642
115.56886	3.761	2.261231432	0.000522501	8.695417579	152.9339229
115.3107	3.82	2.22770665	0.000522829	8.656612978	152.9603395
115.37524	3.82	2.22770665	0.000522829	8.666305993	152.4762706
115.11708	3.82	2.22770665	0.000522829	8.627566476	151.120997
r/R = 0.118					
115.37524	3.879	2.22770665	0.000530911	8.666305993	153.7926126
115.43978	3.879	2.22770665	0.000530911	8.676004431	154.6042715
115.50432	3.938	2.261231432	0.000547112	8.685708293	156.1306817
115.43978	3.938	2.261231432	0.000547112	8.676004431	158.6735591
115.6334	3.997	2.261231432	0.000555316	8.705132289	157.8022851
115.3107	3.997	2.261231432	0.000555316	8.656612978	158.318913
115.3107	3.997	2.22770665	0.000547076	8.656612978	157.6759342
115.50432	4.056	2.261231432	0.000563521	8.685708293	159.5311451
115.6334	4.056	2.22770665	0.000555159	8.705132289	161.3294211
115.56886	4.056	2.261231432	0.000563521	8.695417579	159.0580844
115.50432	4.056	2.261231432	0.000563521	8.685708293	160.9694425
115.50432	4.115	2.261231432	0.000571726	8.685708293	160.9694425
115.56886	4.115	2.261231432	0.000571726	8.695417579	161.8791146
115.69794	4.115	2.261231432	0.000571726	8.714852422	161.5095612
115.56886	4.115	2.261231432	0.000571726	8.695417579	160.4261981
115.24616	4.115	2.261231432	0.000571726	8.646925387	160.9763548
115.6334	4.174	2.22770665	0.000571325	8.705132289	162.0599694
115.56886	4.174	2.261231432	0.000579931	8.695417579	162.6154866
115.56886	4.174	2.22770665	0.000571325	8.695417579	163.3585886
115.56886	4.233	2.295204509	0.00059698	8.695417579	161.1493815
115.9561	4.233	2.261231432	0.000588136	8.753787192	163.7070734

Voltage (volts)	Hum. rel. (%)	P sat. (kPa)	Hum. abs. (kg eau/kg air sec)	Puissance (watts)	h moyen (W/m2°C)
115.76248	4.233	2.261231432	0.000588136	8.724577979	162.4219821
115.76248	4.233	2.261231432	0.000588136	8.724577979	162.4219821
115.50432	4.233	2.261231432	0.000588136	8.685708293	161.6983607
115.89156	4.233	2.261231432	0.000588136	8.744045364	162.7843986
115.82702	4.233	2.22770665	0.000579408	8.73430896	162.6645227
115.69794	4.233	2.22770665	0.000579408	8.714852422	162.2715426
115.43978	4.292	2.22770665	0.000587491	8.676004431	160.1279183
115.9561	4.292	2.261231432	0.000596341	8.753787192	162.292093
115.9561	4.292	2.261231432	0.000596341	8.753787192	163.7070734
115.9561	4.292	2.261231432	0.000596341	8.753787192	163.7070734
115.89156	4.292	2.261231432	0.000596341	8.744045364	162.7843986
115.82702	4.292	2.22770665	0.000587491	8.73430896	161.9309736
115.89156	4.351	2.261231432	0.000604547	8.744045364	160.6624418
115.50432	4.351	2.261231432	0.000604547	8.685708293	159.5905608
115.89156	4.351	2.22770665	0.000595575	8.744045364	163.5248887
115.82702	4.351	2.22770665	0.000595575	8.73430896	160.4835459
115.9561	4.351	2.22770665	0.000595575	8.753787192	162.292093
115.89156	4.41	2.261231432	0.000612752	8.744045364	162.0505847
115.82702	4.41	2.261231432	0.000612752	8.73430896	161.2040107
115.9561	4.41	2.261231432	0.000612752	8.753787192	161.5030889
115.9561	4.41	2.22770665	0.000603659	8.753787192	161.563509
115.76248	4.41	2.261231432	0.000612752	8.724577979	161.6898019
115.76248	4.469	2.261231432	0.000620958	8.724577979	160.9641932
115.69794	4.469	2.261231432	0.000620958	8.714852422	160.8449128
115.69794	4.469	2.261231432	0.000620958	8.714852422	162.2409253
115.50432	4.469	2.261231432	0.000620958	8.685708293	159.5905608
115.69794	4.469	2.261231432	0.000620958	8.714852422	161.5095612
115.82702	4.469	2.261231432	0.000620958	8.73430896	161.870143
115.9561	4.469	2.22770665	0.000611743	8.753787192	164.4551636
r/R = 0					
115.76248	4.469	2.22770665	0.000611743	8.724577979	164.6273676
115.69794	4.528	2.22770665	0.000619827	8.714852422	163.7548855
115.56886	4.528	2.261231432	0.000629165	8.695417579	165.5972413
115.89156	4.528	2.261231432	0.000629165	8.744045364	166.5233184
115.69794	4.528	2.22770665	0.000619827	8.714852422	166.8044431
115.82702	4.587	2.22770665	0.000627912	8.73430896	168.6820594
115.76248	4.587	2.22770665	0.000627912	8.724577979	168.494129
115.89156	4.587	2.261231432	0.000637371	8.744045364	168.8700945
115.82702	4.587	2.22770665	0.000627912	8.73430896	167.9260798
115.56886	4.587	2.22770665	0.000627912	8.695417579	167.9638425
115.37524	4.587	2.22770665	0.000627912	8.666305993	168.1917635

Voltage (volts)	Hum. rel. (%)	P sat. (kPa)	Hum. abs. (kg eau/kg air sec)	Puissance (watts)	h moyen (W/m2°C)
115.9561	4.587	2.195994635	0.000618965	8.753787192	169.0913311
115.89156	4.646	2.22770665	0.000635997	8.744045364	169.6671215
116.02064	4.587	2.22770665	0.000627912	8.763534444	169.2464789
115.69794	4.528	2.22770665	0.000619827	8.714852422	167.5520078
115.56886	4.41	2.22770665	0.000603659	8.695417579	166.4324553
115.82702	4.233	2.22770665	0.000579408	8.73430896	168.7150825
115.69794	4.174	2.22770665	0.000571325	8.714852422	169.1006694
115.56886	4.056	2.261231432	0.000563521	8.695417579	169.4901832
115.50432	4.056	2.22770665	0.000555159	8.685708293	167.743455
115.43978	3.938	2.261231432	0.000547112	8.676004431	169.9511319
115.43978	3.938	2.22770665	0.000538994	8.676004431	168.3468734
115.50432	3.82	2.22770665	0.000522829	8.685708293	169.3678481
115.24616	3.82	2.22770665	0.000522829	8.646925387	170.1584923
115.56886	3.82	2.22770665	0.000522829	8.695417579	170.2975997
115.37524	3.82	2.261231432	0.000530704	8.666305993	170.5398735
115.24616	3.761	2.261231432	0.000522501	8.646925387	170.1584923
115.18162	3.761	2.22770665	0.000514748	8.63724322	169.9679618
115.43978	3.761	2.22770665	0.000514748	8.676004431	171.6206598
115.18162	3.761	2.195994635	0.000507414	8.63724322	170.0018673
115.18162	3.761	2.22770665	0.000514748	8.63724322	171.6453899
115.43978	3.82	2.22770665	0.000522829	8.676004431	172.3809608
115.50432	3.82	2.22770665	0.000522829	8.685708293	170.9898866
115.3107	3.82	2.22770665	0.000522829	8.656612978	172.8309461
115.11708	3.82	2.22770665	0.000522829	8.627566476	170.6282974
115.3107	3.879	2.22770665	0.000530911	8.656612978	172.8309461
115.50432	3.938	2.261231432	0.000547112	8.685708293	174.2580951
115.37524	3.938	2.22770665	0.000538994	8.666305993	173.8334877
115.56886	3.938	2.22770665	0.000538994	8.695417579	175.2725858
115.9561	3.997	2.22770665	0.000547076	8.753787192	173.9614339
115.6334	3.997	2.22770665	0.000547076	8.705132289	172.9945293
115.6334	3.997	2.22770665	0.000547076	8.705132289	174.6122867
115.56886	4.056	2.22770665	0.000555159	8.695417579	172.8014718
115.3107	4.056	2.22770665	0.000555159	8.656612978	171.96105
115.50432	4.056	2.195994635	0.000547249	8.685708293	173.4469362
115.3107	4.115	2.22770665	0.000563242	8.656612978	174.4904056
115.56886	4.115	2.22770665	0.000563242	8.695417579	173.6408232
115.11708	4.115	2.22770665	0.000563242	8.627566476	171.4530868
115.18162	4.115	2.22770665	0.000563242	8.63724322	171.6108257

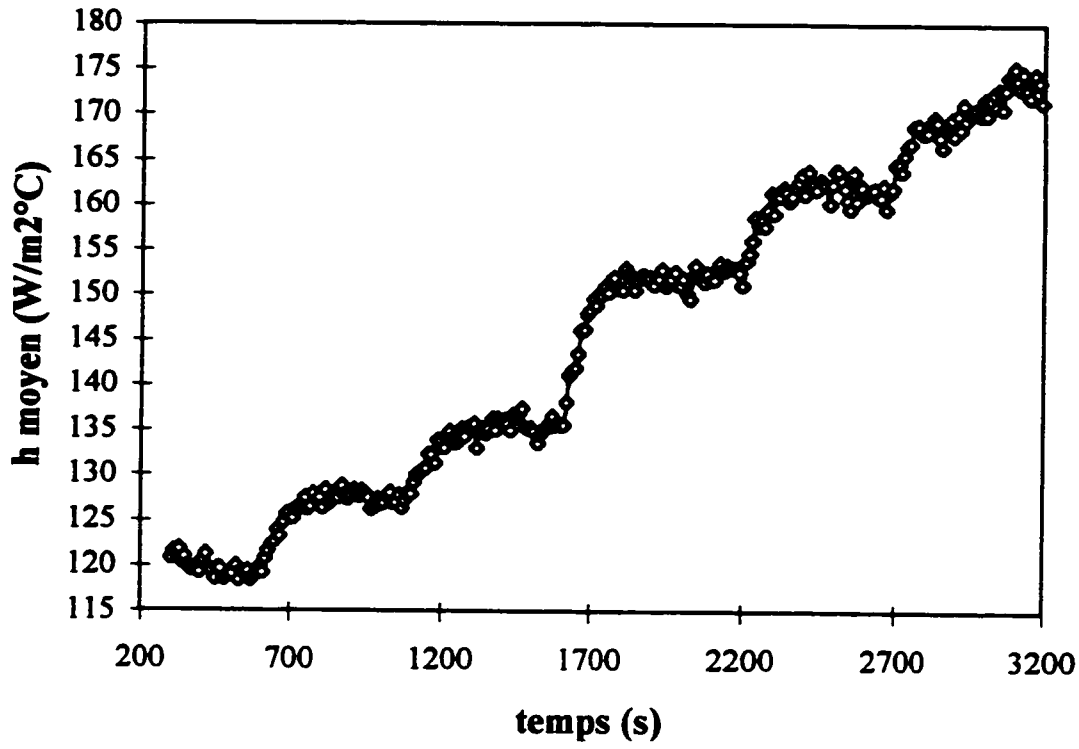

Figure A.2 Effet de la position radiale sur h_e pour des particules de polyéthylène.
$U/U_{ms} = 1.3$, $z = 0.21$ m, $H = 0.27$ m, $D_i = 0.019$ m.

A.4.3 Résultats

Le tableau A.1 présente les valeurs de h_s provenant du graphe A.2 lorsque le régime permanent est atteint pour chaque position radiale de la sonde.

Tableau A.1 Effet de la position radiale de la sonde sur h_s pour des particules de polyéthylène. H = 0.27 m, z = 0.21 m, U/U_{ms} = 1.3.

r/R	h_s
0	118
0.118	127
0.235	135
0.412	153
0.588	162
0.823	171

- Par essais répétés, la précision sur les valeurs de h_s est estimée à 2 %.

- L'exactitude de la valeur de h_s est reliée à la perte de chaleur par conduction axiale. La chaleur maximale transférée par conduction axiale à travers le bouchon de Téflon est estimée de la façon suivante :

$$q_{axiale\,max} = k * A1 * (\Delta T_{max}) / \Delta X = 0.085 \text{ W}$$

où $k = 0.25$ W/m°C

$A1 = \pi * (D_t)^2/4 = \pi * (0.0127)^2/4 = 0.000127$ m^2

$\Delta T_{max} = (T_s - T_b) = 53 - 19 = 34$°C et $\Delta X = 0.0127$ m.

La perte par conduction axiale est donc de l'ordre de (0.085 W)/(8.6 W)*100 = 1 %.

IMAGE EVALUATION TEST TARGET (QA-3)

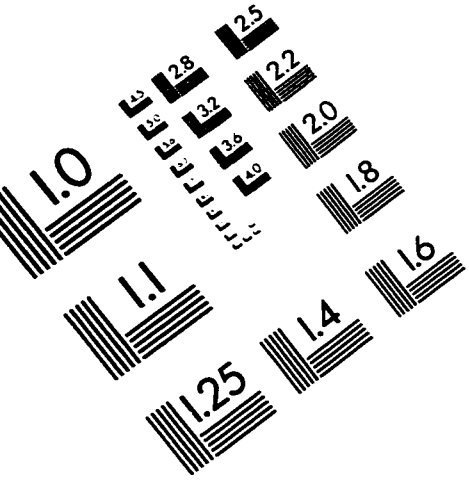

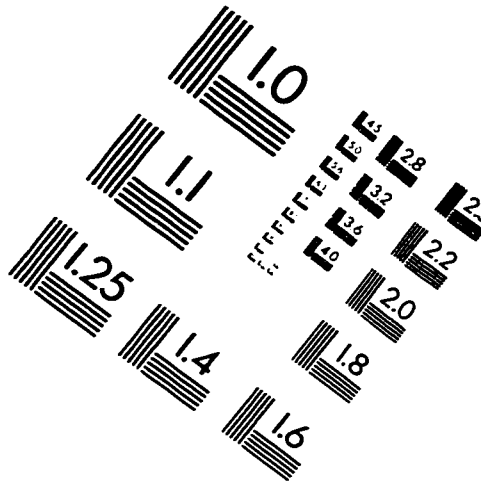

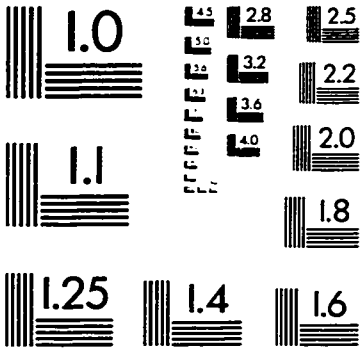

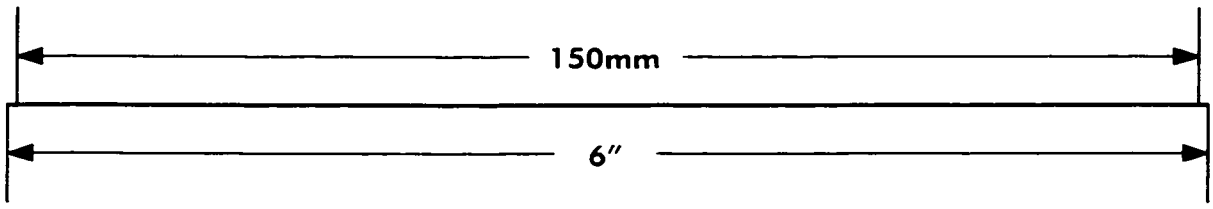

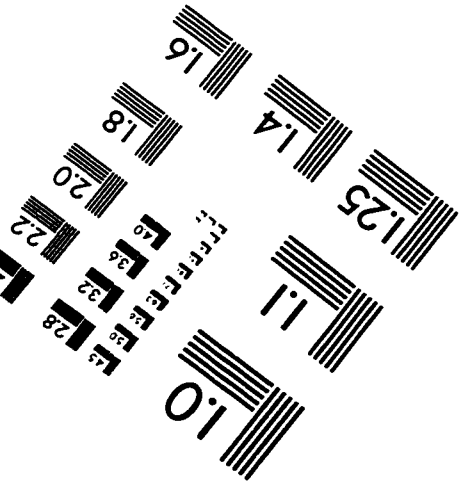

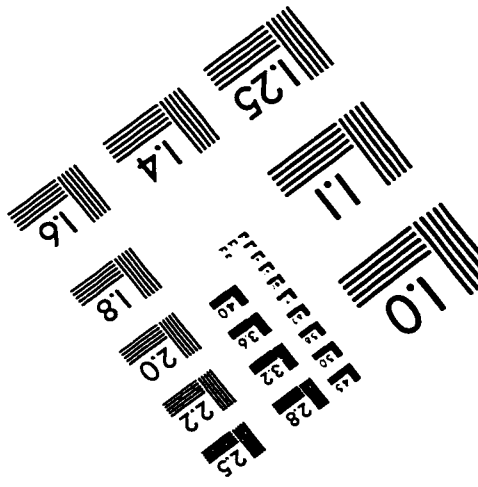

APPLIED IMAGE, Inc
1653 East Main Street
Rochester, NY 14609 USA
Phone: 716/482-0300
Fax: 716/288-5989